ACCURATE AND COST EFFICIENT OBJECT LOCALIZATION USING PASSIVE UHF RFID

by

JAE SUNG CHOI

Presented to the Faculty of the Graduate School of

The University of Texas at Arlington in Partial Fulfillment

of the Requirements

for the Degree of

DOCTOR OF PHILOSOPHY

THE UNIVERSITY OF TEXAS AT ARLINGTON

May 2011

ACKNOWLEDGEMENTS

First and foremost, I would like to express my sincere gratitude towards Dr. Ramez Elmasri and Dr. Daniel W. Engels for giving me priceless guidance and invigoration. Without their patience and continuous supports, this dissertation would not have been completed.

I am extremely thankful to the members of my dissertation committee. I give deep appreciation to Dr. Leonidas Fegaras, Dr. Gergely Zaruba and Prof. David Levine for donating their precious time to ameliorate my dissertation. Also, I would like to thank Dr. Mingyu Lu for assistance in this research.

I would like to express my deep gratitude to my parents, Mr. Jin Seung Choi and Mrs. Jung Soon Son, and my elder brother, Eun Young Choi who have encouraged and supported me. Without their devotion, I could not completely finish my Ph.D program.

Last but not the least, I would like to give my best love and thank to my wife, Haw Jeong Chang, and my lovely daughters, Ally Choi and Emily N. Choi. Without their unconditional and endless love, my work would not have been possible. I dedicate this work to my family.

April 7, 2011

ABSTRACT

ACCURATE AND COST EFFICIENT OBJECT LOCALIZATION USING PASSIVE UHF RFID

Jae Sung Choi, PhD

The University of Texas at Arlington, 2011

Supervising Professors: Ramez Elmasri, Daniel W. Engels

In a smart environment, accurate locations of objects are a fundamental and critical issue. To achieve this goal, we present several methods based on passive far-field UHF RFID technologies, which can satisfy accuracy, robustness and reliability, cost efficiency, simplicity, compatibility, and scalability. Our research overcomes several negative characteristics of the use of cost efficient passive UHF RFID. Our research has several important contributions.

First, we study the causes of the problems of using passive UHF RFID in localization, with detailed empirical results, and then, present the impacts of the causes on existing localization techniques such as KNN.

Second, we present a new model of backscattered signal strength for passive far-field UHF RFID system under tag-to-tag interference. We propose a method to estimate power variations due to tag interference, based on a tag-to-tag distance and angle using a second order under-damped system. We present a novel localization algorithm to estimate target object location using our Tag-to-tag Interference Model (LMTI). According to the empirical results, LMTI improves accuracy be over 200% compared with RSSI based KNN algorithm when

objects are empty boxes, and 127% improvement when objects are the print cartridges contained in aluminum foil bags.

Third, we present another approach to achieve accurate localization. Localization using Detection of Tag Interference (LDTI) algorithm, which detects the tag interference on a map of reference tags to estimate target location. To avoid selection of spatially non-adjacent reference tags, we also present the most interfered reference group finding algorithm, which considers spatial relations between reference tags. LDTI based smart shelf performs on average 0.0948m estimation error for 9 empty cardboard boxes, and average 0.1831m estimation error for 9 print cartridge containers, which is a 71% accuracy improvement compared to the KNN algorithm.

Finally, we present a novel Vision and passive UHF RFID integrated Localization (VRL) system on smart shelf application to improve performance under harsh conditions. VRL performs on average 0.079m estimation error for 10 print cartridge containers, which is a 61% accuracy improvement compared to the LDTI algorithm under low False Negative Reference (FNR) interrogation conditions. Moreover, it shows 555% computation overhead reduction compared a homogeneous vision system. In high FNR conditions, VRL system achieves over 620% increased accuracy compared to LDTI, and 437% reduced computation time compared to a pure vision based localization system.

TABLE OF CONTENTS

LIST OF ILLUSTRATIONS

Figure Page

LIST OF TABLES

CHAPTER 1

INTRODUCTION

In this chapter, we first introduce to RFID and discuss the problem statement and the challenges for the given problem. Then we describe our contributions and the structure of this dissertation.

1.1 Introduction to Passive UHF RFID based Localization

Radio Frequency Identification (RFID) used for Automated Identification and Data Capture (AIDC). RIFD technology allows indentifying objects using a wireless channel under non-Line-of-Sight condition and it may interrogate over 1000 objects per second [1]. Due to remote identification and fast interrogation capacities, RFID technologies are widely adopted by many industries, and RFID based AIDC system is promising in the industries to replace Bar-code based AIDC system [2] which can identify objects with Line-of-Sight condition and performs longer identification time than RIFD system.

An RFID system provides a cost efficient and simple method to identify objects. An RFID tag is attached to the object and communicates with a reader for detection of the presence and identification of the tagged object. Depending on the type of communication and existence of a built-in power source in a tag, the RFID systems are generally classified to active, semi-passive, and passive system. In an active RFID system, a tag actively generates a signal using its own power source and often communicates to a reader based on the tag's transmission schedule. A semi-passive RFID tag communicates passively with a reader using on-tag power for its logical operations. In contrast with the active and semi-passive systems, a passive RFID tag does not contain a power source itself and the tag communicates with a passive RIFD reader using passive communication such as backscattered communication.

Since gathering spatial information of objects often provides a number of extended functions in RFID based applications, many different localization systems have been developed in recent years using passive or active RFID systems [3-14]. According to [15], the Real Time Locating System (RTLS) can be defined as follows:

"Combination of hardware and software that is used to continuously determine and provide the real time position of assets and resources equipped with devices designed to operate with the system."

In location-sensing systems, determining and estimating the physical location of object of interest in an interrogating area is primary goal. Using active or passive RFID system, real time locating systems are already commercially applied to emergency rescuing [3], patient tracking [4], asset or livestock tracking [5], [6], and may be applied to other areas. Moreover, GPS [16], ultra-sound [17], WI-FI [18], and UWB [18] utilize actual communication for positioning after at long range. GPS is not suitable in an indoor situation because signals from satellites are blocked by building structure. For indoor environments, ultra-sound, WI-FI, and UWB based localization systems have been researched. However, for higher accuracy, these systems are expensive to implement in a large monitoring areas. Additionally, if the signal transmitter and receiver run with built-in power sources, the maintenance costs are increased to replace the power source. Passive UHF RFID based localization overcomes the drawback of conventional indoor localization systems such as high cost of installation and maintenance because of the relatively cheap cost, the absence of a power source, and light weight of the passive RFID tag.

1.2 Overview of Research

1.2.1. Problem Statement

In a smart environment, real time object spatial information is fundamental and critical issue. To collect and estimate object spatial information, a certain type of localization system is implemented in a monitoring area, and the localization system periodically or continuously

observes. In order to carry out maximal efficiency and performance, the localization system must satisfy the following criteria:

1) **Accuracy**
2) **Robustness and Reliability**
3) **Cost Efficiency**
4) **Simplicity**
5) **Compatibility**
6) **Scalability**

First, the first and foremost issue on localization system is accuracy. The localization performs for accurate estimation of object location sensing. Using the accurately estimated object spatial information, the system users meet their needs for high level application.

Second, the localization system has to perform precisely under practical and harsh condition. Thus, the system must carry out robust and reliable performance against many environmental factors. Relatively, the localization system should overcome a gap between theoretical and practical output.

Third, the localization system has to be designed and implemented under consideration of cost efficiency. Depending on the number of objects of interest and priority, the requirement and available localizing technology can be varied. For example, warehousing manager may not apply over $100 wireless sensor devices for each $10 valued asset for inventory localization system.

Fourth, the localization system should be implemented simply in the monitoring area. Thus, better localization system should be applied and implemented to a certain application with less intervention of human being and change of current infrastructures.

Fifth, the localization system should solve the integration process with existing system. The accumulated data from the existing system should integrate to localization system for maximized efficiency. For example, many supply chain management applications adopt

Electronic Product Code (EPC) [1] system to identify assets. Where the computer vision based localization system is applied to the asset management application, the system can integrate existing data such as asset IDs from EPC system to improve localization results. However, the integration process may be expensive and complicate. Thus, the localization system should provide a way to decrease complicity of the integration process and increase re-use of existing data.

Sixth, the localization system should be easily expanded for large monitoring area with constant performance. Depending on the requirement of application, the localization system can be expanded to larger area, and the expanding process should consider simple and easy construction of system infrastructures.

In order to satisfy the given criteria, we apply passive far-field UHF RFID to localization system in this dissertation. We define the thesis statement to 'Accurate Localization can be achieved using passive UHF RFID with low cost'.

1.2.2. Importance and Possible Applications

Passive far-field UHF RFID based localization system can improve performances of many industrial applications such as, supply chain management system, surveillance system, healthcare, and pharmaceuticals, and smart library.

1.2.2.1 Supply chain management

Automation of asset tracking is an important topic of interest in the supply chain [6], [20], [21]. The major benefits of RFID based asset tracking and inventory control can be reduction of labor, fast process of inventory management, and high visibility of individual items. The US Department of Defense, and many retailers such as Walmart, and Target have implemented passive UHF RFID system since 2003, and the passive UHF RFID based localization can improve asset management with high cost efficiency, simplicity, and compatibility.

1.2.2.2 Surveillance system

Most of current security and surveillance architectures [22] are based on vision system such as camera, and the homogeneous vision based surveillance system has several drawbacks such as the difficult identification of detected object, high computation overload and processing time, and requirements of huge storage space for the captured multimedia data. Using passive UHF RFID based localization, surveillance system can achieve the improvement of automation and object identification, and the decrease of computation time.

1.2.2.3 Healthcare

Spatial information of single or multiple persons is one of most important factors to check the targeted person's condition in a pervasive healthcare monitoring system [4]. In the healthcare monitoring area, the system has to keep tracking the person's location, because, depended on the location, a body condition of a body sensor worn person might be changed, and the system might falsely warn to a medical institution. Therefore accurate location person's information is a momentous factor to make a correct decision of need of emergency aid. Moreover, visibility of hospital equipments and medical supplies are one of main issue in the healthcare industry to prepare fast uses and prevent misuse of products to patients. Using RFID localization can aid to the healthcare monitoring system to carry out accurate and reliable personnel and other medical properties tracking and identifying.

1.2.2.4 Pharmaceuticals

Identification and localization of pharmaceutical drugs are critical and mandatory requirements in the pharmaceutical industry [19]. The pharmaceutical systems can adopt RFID system to provide anti-counterfeit, drug usability, and efficient and secure pharmaceutical supply chain. Item-level or box level pharmaceutical tracking and localizing is very expensive, and it demands time-consuming process. If the pharmaceutical management system applies passive UHF RFID based item level localization, the system can significantly improve efficiency and security of the pharmaceutical supply chain with low implementation and maintenance cost.

1.2.2.5 Smart library

Smart library is one of possible applications using passive far-field UHF RFID based localization. For smart library, a few applications are published in a decade using Wireless LAN [23] and passive near-field RFID system [24]. The major benefits of smart library are automated book inventory management in real time, and reduction of librarian's workloads. However, Wireless LAN or Active RF device based localization system cannot be applied to location sensing of individual books due to cost problem, and passive near-field RFID based smart library system requires high cost for implementation of infrastructure due to low read range of near-field RFID. To overcome the cost problem, passive far-field UHF RFID book localization system can be useful for the smart library system

1.2.3. Challenges

For maximal performance of passive far-field UHF RFID based localization, we encounter several major challenges which are huddles of localization system. First we have to investigate the causes of low accurate location estimation in standard passive far-field UHF RFID. Second, the localization system requires accurate and cost efficient localization algorithms which are suitable for passive UHF RFID based location sensing system, because most of existing RFID based localization systems focus on the active RFID based applications, and their algorithms shows low performances on passive far-field UHF RFID under practical condition. Third, the localization system has to provide robust and reliable localization algorithms, because, wireless communication using weak RF signal between RFID reader antenna and RFID tag can be influenced by environmental factors, such as background noise, humidity, pressure, and temperature, and affects to the performance of the system. Moreover, related on implementation cost, there is a coarse RFID reader and reader antenna deployment, and it can reduce accuracy of object localizing.

1.2.4. Contribution

First, we investigate causes of unreliable and inaccurate passive RFID based localization with actual examination. We study about impacts of the variation of uniform tags, tag posture, the material of tagged object, the strong-weak tag problem and the tag-to-tag interference under various conditions such as an anechoic chamber room and an ordinary office environment, and describe their influences on an existing localization algorithm.

Second, this dissertation presents a new model of backscattered signal strength for passive far-field UHF RFID system under tag-to-tag interference, and proposed a method to estimate variations of excess power volume by the interference depended on a tag-to-tag distance and angle using the second order under-damped system.

Third, we presented a novel localization algorithm to estimate target object location using the presented Tag-to-tag Interference Model to tackle the major problem of lack of accuracy in passive far-field UHF RFID based localization system.

Fourth, this dissertation presents another novel localization algorithm with lack of prior information, Localization using Detection of Tag Interference (LDTI), in order to achieve maximal accuracy using a single reader and reader antenna. Moreover, for maximum performance of LDTI, we propose the most interfered reference group finding algorithm, which considers spatial relations between reference tags.

Finally, we present computer vision and passive RFID integrated localization system (VRL) to achieve robustness and reliability under a coarse RFID reader deployment. Using RFID system, the proposed VRL overcomes drawbacks of a homogeneous vision based localization system, such as identification problem and computation overload.

1.3 Outline of Dissertation

The rest of this dissertation is organized as follows: In Chapter 2, we overview the backgrounds of RFID systems, RF based localization techniques, and the related work. Chapter 3 describes the limitation of RSSI based exiting location sensing techniques with passive UHF RFID system

in practice with empirically analysis. Chapter 4 describes the model of tag-to-tag interference, and the model based localization system. Chapter 5 describes a novel localization technique using detection of reference tag interference. Chapter 6 describes sensor fusion as integration between passive RFID system and computer vision to achieve maximal accuracy of object localization with less overload compared with homogeneous computer vision based localization. We present our conclusion of this dissertation in Chapter 7.

CHAPTER 2

OVERVIEW OF LOCALIZATION USING RFID

In this chapter, we overview the backgrounds that are important to understand this dissertation. First, we briefly describe about localization methods. Second, we describe the background of RFID system, and then, finally, we describe the related RFID based localization system.

2.1 Localization Methods

The purpose of object localization is to estimate the absolute or relative location information of the objects of interest with given observations of input and spatial relation between the object and known references (or an object detector) by the localization system. The input from the object means any type of signal such as Radio Frequency, (ultra-)sound, image, Infra-Red, and vibration, and the spatial relation refers the distance, angle, and relative nearness between the signal sender and receiver.

2.1.1. Measurement for Localization

2.1.1.1 TOA

The Object localization system can measure signal traveling time between the source and receiver on a channel. This type of measurement is called Time of Arrival (TOA), and the system has to pre-define the velocity of the signal on the channel. If there are multiple signal receivers, which measures same signal, at various points, the localization system can use a variation of TOA, TDOA, which stands for Time Difference of Arrival. TDOA measurement considers different signal travel time from the single source to various receiver locations.

TOA and TDOA measurement based localization system shows more robust performance against impact of environmental factors. For example, between two RF devices, the measured time of arrival denotes the time of first signal detection, and the signal might

travel on the direct or the shortest path. Thus, TOA has less influence from the multi-path environment.

However, TOA has several disadvantages. First, accurate time synchronization between the source and receiver is required for precise time measurement and accurate localization. Second, the cost of TOA measurement is high due to the device must have timing circuits.

Satellite system as Global Positioning System (GPS) [16] is the most popular localization technology which uses time measurement. GPS can estimate GPS receiver's location using computation of the TOA of signals from 24 satellites. GPS is not suitable in an indoor situation, and typical localization error is 3-4 meter under line of sight from satellites in the outdoor situation.

Other examples of TOA based localization systems are Active BAT [25] and Cricket [17] location systems. Ultrasound signal is emitted from a object, and the localization system can estimate the source location using calculations of time of signal flight to multiple receivers.

Ultra-Wide Band (UWB) based active RFID using IEEE 802.15.3 is a good example of recent TOA based localization system. According to [18], UWB shows robustness with interference of signals, and it requires around 150mW for communication within 30 m of transmitting range. One of remarkable aspects of UWB is possibility of measurement of Time of Arrival of signal between the signal sender and receiver. This feature is very important for accurate localization system.

2.1.1.2 AOA

The other type of signal measurement is Angle of Arrival (AOA), which considers the direction of signal propagation. For precise measurement of signal arrival angle, the receiver contains a multiple signal receiving array or spinnable device. However, if the signal can be reflected by surrounding, AOA measurement shows less accuracy than TOA. Thus, AOA is more suitable outdoor environments as open space, than indoor environments.

Existing cellular phone based localization system [26] employs AOA measurement. The cell tower uses directional antenna arrays, and each element of antenna arrays divides tower's coverage.

2.1.1.3 Signal strength

The signal strength is one of most common measurement parameters. The signal strength has close relationship with distance between the sender and receiver. A certain type of signal such as RF, ultrasound, and vibration, can be attenuated on the media, and the localization system can estimate spatial information using the degree of signal attenuation. For example, in wireless communication, the receiver antenna measured signal strength from the RF source has related on distance between two devices as following [27]:

$$\text{Singal Strength} \propto \frac{1}{d^n} \tag{2.1}$$

where d denotes the distance between signal source and receiver, and n denotes the path loss exponent. Signal strength measurement based localization system has two main advantages such as cost efficiency and simple implementation, because the system does not need to install extra device.

However, signal strength measurements in practical condition are easily influenced by environmental factors and channel condition. Thus, many of signal strength measurement based localization systems build a map which correspond signal strength values and location information, during the site survey or the training phase, which is a time-consuming procedure. The performance of localization system is highly related on the prepared signal strength map. Moreover, if the monitoring area experiences significant changes, the system has to re-construct the map for further accurate location sensing.

Cellular technique based location sensing and tracking uses commonly in USA with GSM network infrastructure (E911). In [28], SkyLoc is presented. SkyLoc is a GSM

fingerprinting-based localization system with RSSI. With the use of mobile phone, the system identifies where the mobile phone user in the building as the current floor.

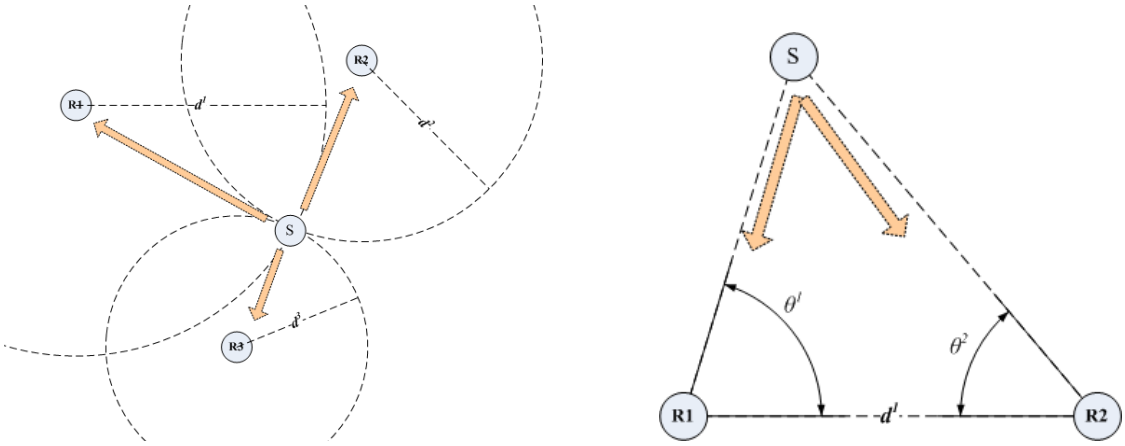

(a) (b)

Figure 2.1 Examples of trilateration and triangulation in 2D space. (a) Trilateration localizing technique. (b) Triangulation localizing technique

2.1.2. Localization Algorithms

2.1.2.1 Range based approach

Using the signal measurement such as TOA, AOA, or Signal Strength, range based localization techniques estimate the location of signal source.

2.1.2.1.2 Trilateration

Trilateration is the process of distance based lateration to find a point from the pre-measured distances. Trillateration applies the distance information between signal receiver and source. When the localization system knows at least a set of three distances from different receiver, the system can draw three circles, and the radius of a circle is the measured distance, and the center is the known signal receiver's position as shown in Figure 2.1(a). The intersection of three circles will be the expected signal source's location. However, there is one restrictive condition such as the three of signal receivers cannot place in a single straight line for

calculation of trilateration. TOA, TDOA, and signal strength measurements are more suitable for trilateration localization algorithms.

2.1.2.1.2 Triangulation

Triangulation is signal direction (or angle) based localization technique to determine the location of signal source by angle measurement from the more than two different signal receivers. Also it requires one known distance as a triangle's one side as shown in Figure 2.1(b). AOA is best type of signal measurement for triangulation technique.

2.1.2.2 Scene Analysis

Scene analysis technique estimates the location of signal source using pre-observed data set about the monitoring scene. The most well know scene analysis based location sensing technique is fingerprinting [29]. The system compares current received signal measurement and priory observed measurements from known locations. Then the system estimate the source location with most closed fingerprints. However, this approach requires extra information server to maintain pre-observation. Another approach of scene analysis employs a matching process between current signal measurement from the source and measurements from deployed reference devices, and then the most similar signal measurement sent references' location information are used to estimate source location. K-Nearest Neighbor [8], [13] algorithm is well known online signal measurement based scene analysis technique. The signal strength is the most common measurement for scene analysis technique.

2.1.2.3 Proximity

Proximity technique provides object location using signal detected (or the most strong signal detected) receiver location information. Thus, the proximity technique guarantees the most simple and easy implementation for object localization. RFID, pressure sensor, or Infra-Red based localization systems widely adopt proximity approach. However, depending on the signal propagation range, the accuracy of proximity approaches is varied.

2.2 RFID Concepts

2.2.1. RFID system

2.2.1.1 Components

The primary components of an RFID system are an interrogator, tags, and a middleware as shown in Figure 2.2. The main purpose of the interrogator is requesting of identification of each tag in the reading area, also we call the interrogator to a reader. RFID reader and reader antennas locate at fixed positions for the stationary RFID system, and some applications use mobile reader and antenna. The reader and the reader antenna periodically or continuously send queries and receive responses from the tags. Other possible capacities of RFID reader are a report of tag interrogation time and received signal strength for further service. The tag responds to the reader by sending its unique ID through a wireless channel. Due to the use of wireless channel, RFID can provide object identification under non-Line-of-Sight condition. The reader is controlled by the linked middleware, and the reader sends the tag interrogation information to the middleware. Depending on the RFID application, the middleware runs various utilities for satisfactions of application users.

Depending on the existence of a built-in power source and type of communication, the tag can be classified as passive, semi-active, and active. In the passive RFID system, the tag can communicate with the reader with the use of the backscattered coupling or the inductive coupling mechanism. In Ultra High Frequency (UHF) RFID system, the backscattering method is used from the tags to the reader. By contrast, an active RFID tag is operated by a built-in power source, and the tag can communicate using lower transmission power with the reader or other active tag with longer range compared to the passive tag.

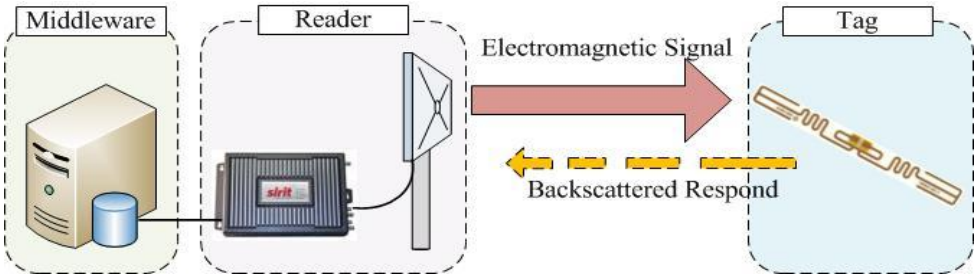

Figure 2.2 Essential components and backscattered communication scheme of passive far-field UHF RIFD system.

2.2.1.2 Category of RFID tags

Depending on the type of communication and existence of a built-in power source in a tag, the RFID systems are generally classified to active, semi-passive, and passive system. In an active RFID system, a tag actively generates a signal using its own power source and often communicates to a reader based on the tag's transmission schedule. A semi-passive RFID tag communicates passively with a reader using on-tag power for its logical operations. In contrast with the active and semi-passive systems, a passive RFID tag does not contain a power source itself and the tag communicates with a passive RIFD reader using passive communication such as backscattered communication.

2.2.1.3 Passive RFID

A passive UHF RFID system consists of four essential components: reader, reader antenna, RFID tags, and middleware. The RFID tag contains an IC chip and an attached antenna. The tag is attached to an object of interest. The reader is an interrogator, and talks to the tag for identification of the tag (and the tagged object) in the monitoring area. The reader antenna, which cables to the reader, emits RF signal and power, and receives the signal from the tag. Because a tag does not contain a power source, the tag powers up from a RFID reader's transmitted a continuous RF wave (CW). When the tag harvests enough power, the tag responds to the reader using the backscatter coupling manner as described in Figure 2.2. The middleware collects identification data from connected multiple readers and associates the gathered data with the objects of interest.

The interrogating range of the RFID reader is generally limited by how far the reader antenna delivers the RF power to the tag for its successful modulating backscattered signal. Theoretically, using Friis equation [2], the tag received power from the reader antenna is calculated by the transmission power from the reader, and the gain of the reader antenna as follows:

$$P_{tag}^{RX} = \frac{P^{TX} G_{ant} G_{tag} \lambda^2}{(4\pi)^2 d^2} \tag{2.2}$$

where P^{TX} is the transmitted power from the reader, G_{ant} is the gain of the reader antenna, G_{tag} is the gain of the tag antenna, and λ is the wavelength.

Equation (2.2) is commonly used in the 'RF-sender to RF-receiver system' as in Active RFID systems and Wireless Sensor Networks (WSN). The received signal strength indicator (RSSI) can be directly measured by the receiver, and the sender reports the transmission power to the receiver, and then the receiver can measure the distance between two devices in WSN based localization. On the other hand, in the passive UHF RFID system, the passive tag cannot measure strength of the incoming power. The reader's transmitted power arrives at the tag antenna, and then, a portion of the power is reflected by the tag to the reader's antenna using backscattering schemes. The backscatter transmission loss rate is the ratio of the incoming power and the backscattering power at the tag side. The tag needs to gather the power to turn on the IC chip and the minimum strength of power needed is called tag sensitivity. A tag responding range is relative to reader antenna sensitivity and the strength of backscattered signal. The sensitivity of a reader antenna is the minimum strength of signal from the tag to detect and identify. If the antenna has better sensitivity, the system will have longer the communication (interrogation) range. And, the reflected power from the tag is given by,

$$P_{tag}^{TX} = P_{tag}^{RX} L \tag{2.3}$$

where L denotes a backscatter transmission loss ratio. Then, the backscattered power from the tag to the reader antenna can be obtained by Friis equation and Equation (2.3) as following:

$$
\begin{aligned}
P_{reader}^{RX} &= \frac{P_{tag}^{TX} G_{tag} G_{reader} \lambda^2}{(4\pi)^2 d^2} \\
&= \frac{P_{tag}^{RX} L G_{tag} G_{reader} \lambda^2}{(4\pi)^2 d^2} \\
&= \left(\frac{P_{reader}^{TX} G_{reader} G_{tag} \lambda^2}{(4\pi)^2 d^2} \right) \left(\frac{L G_{tag} G_{reader} \lambda^2}{(4\pi)^2 d^2} \right) \\
&= \frac{P_{reader}^{TX} L G^2{}_{tag} G^2{}_{reader} \lambda^4}{(4\pi)^4 d^4}
\end{aligned}
\tag{2.4}
$$

In the passive UHF RFID system, the strength of backscattered signal is generally influenced by the amount of gathered power from the reader antenna on the passive tag. In the actual circumstance, the volume of tag received power can vary due to reflection of reader antenna's transmitted power by the floor, walls and existence of object near tag. The transmitted power from the reader can be reflected, and the tag receives the power from the direct beam and the additional reflected waves, which also contain the power. According to [2], the reflection by the floor and single wall can increase the tag received power about 4 dB higher than non-reflection circumstance as in an anechoic chamber. Moreover, the added volume of reflected power can differ depending on the tag location.

2.3 RFID based Object Localization

2.3.1. Active RFID based Localization system

Two features of active tag are built-in power source and active communication method. Active RFID system overcomes the limitation of passive RFID system such as limitations of reading range and communication. Therefore, active RFID based localization systems have been researched in many applications [3-11].

The earliest RFID based localization system is SpotON [7] which investigates ad-hoc location sensing using RSSI based distance estimation. LANDMARC [8] is the most common active RFID based localization system. The main concepts of LANDMARC are estimation of distance between a reader and tag with the use of pre-measured RSSI for each reference tags and KNN. There are several variations of LANDMARC such as [9] and [10]. In [9], the authors applied LANDMARC idea on regional localization instead of coordinates. In [10], the authors research how to reduce the computational overhead with higher locating accuracy than LANDMARC. In VIRE [11], the system introduces an idea of virtual reference tags and the RSSI value of the virtual reference tags can be calculated by linear interpolation algorithm. Moreover, the authors address the elimination of unlikely positions of tagged objects to reduce estimation error.

2.3.2. Passive RFID based Localization system

Cost efficiency is the most important advantage of the passive RFID based localization system compared to the active RFID based system for localization of large numbers of targeted objects. However, as is well known, because the passive RFID mainly employees backscattering communication, the communication range between the tag and the reader's antenna is very limited. Moreover, accuracy of the localization depends on environmental factors.

Depending on the mobility of passive RFID reader, the localization systems can be classified to the mobile RFID reader localization and the fixed RFID reader localization. Hahnel et al [12] propose the earliest passive RFID based localization system for location sensing of mobile robots, which equip passive RFID antennas and a laser-scanner, in an indoor condition. On the other hand, the localization system using fixed RFID readers finds physical position of a passive tag attached object in the interrogating area. For example, Chattopadhyay at el. [13] propose passive UHF RFID based indoor localization system using a neural network and KNN algorithms to predict the location of a tag of interest.

2.3.3. Hybrid RFID based localization system

For increase of accuracy of location sensing, there are several hybrid RFID based localization systems such as the combination of passive RFID and camera [14], [30], [31], and the combination of RFID and GPS technologies [32] for construction materials' localization and tracking.

Ferret [14] uses a mobile RFID reader equipped with cameras. The image recordable RFID reader services better location information for indentified objects. With the use of mobile camera for one targeted object, the possible physical location is narrowed based on multiple images which record various times for the object. Sherlock [30] uses a fixed RFID reader in the monitoring area. In a smart space such as office and home, the Sherlock system focuses on localization of a human being who has a passive RFID tag. One of the features is the reader's antenna sweeps the monitoring area by various panning, tilting, and power leveling to detect an object. Then the location of the identified object is estimated by steerable camera. The accuracy of localization is increased by fusing multiple results from multiple antennas and iterations in Sherlock. Kamol et al. [31] proposed RFID based object localization system using ceiling cameras with particle filter. In this application, the mobile robot is equipped with Bluetooth RFID antennas. The Bluetooth RFID antennas transmit the identification result to the reader. For the localization of each object, the RFID system estimates rough location of the objects, then, the camera system recognizes the accurate location.

In [33], there is integration of RFID and inertial sensors such as accelerometer and gyroscope for moving object tracking in indoor environment. The accelerometer counts walker's steps, and the system can calculate approximate walker's location with known step length and the number of steps as dead-reckoning technique [34]. The walker, who brings RFID tag, passes near fixed RFID reader, the system can adjust the location of walker.

CHAPTER 3

LIMITATIONS OF PASSIVE FAR-FIELD UHF RIFD BASED LOCALIZATION

In this chapter, we present causes of variation performances for passive UHF RFID tag with empirical results in two different environments such as a practical condition and an anechoic chamber. I study the critical causes of RSSI ambiguity such as environmental factors, tag-to-tag interference, posture of tag, discrepancy of uniform tag, and material of tagged object with empirical results. Moreover, I practically evaluate ambiguous RSSI mapping to spatial information on passive RFID based localization system.

The rest of this chapter is organized as follows: In Chapter 3.1, we present causes of variation of passive UHF RFID system performances with empirical results. We test influences of the ambiguity on the RSSI fingerprinting based localization in Chapter 3.2. we present conclusions in Chapter 3.3.

3.1 Variations in Performance of Passive UHF RFID System

3.1.1. Difference between theoretically and practically measured RSSI

Interrogating range of the RFID reader is generally limited by how far the reader antenna delivers the RF power to the tag for its successful modulating backscattered signal. Theoretically, using Friis equation, the tag received power, P_{tag}^{RX}, from the reader antenna is calculated by the transmission power from the reader, and the gain of the reader antenna, and the reader operating frequency. In [35], the authors well define modification of Friis transmission equation as Equation (2.2) in the logarithmic scale as follows:

$$P_{tag}^{RX} = P_{reader}^{TX} + G_{reader} + G_{tag} - 20log_{10}\left(\frac{4\pi}{\lambda}\right) - 20\,log_{10}(d) \quad (3.1)$$

where P_{reader}^{TX} is the transmitted power from the reader, G_{reader} is the gain of the reader antenna, G_{tag} is the gain of the tag antenna, d denotes the reader antenna to the tag distance, and λ is the wavelength.

The tag needs to gather the power to turn on the IC chip and the minimum strength of power needed is called tag sensitivity. A tag responding range is relative to reader antenna sensitivity and the strength of backscattered signal. The sensitivity of a reader antenna is the minimum strength of signal from the tag to detect and identify. If the antenna has better sensitivity, the system will have longer communication (interrogation) range. The strength of backscattered signal, RSSI, is obtained as follow [35]:

$$P_{reader}^{RX} = P_{reader}^{TX} + 2G_{reader} - 20log_{10}\left(\frac{4\pi}{\lambda}\right) - 40\,log_{10}(d) + 10log_{10}\left(\frac{\sigma}{4\pi}\right) \quad (3.2)$$

where σ denotes the radar cross section of passive RFID tag, and the radar cross section of tag can be written by following:

$$\sigma = \frac{G_{tag}^2 \lambda^2 |\rho|^2}{4\pi} \quad (3.3)$$

where ρ denotes the reflection coefficient.

In the passive UHF RFID system, the volume of tag received power can vary due to reflection of reader antenna's transmitted power by the floor, walls and existence of objects near a tag, as known as multipath [36]. The transmitted power from the reader can be reflected, and the tag receives the power from the direct beam and the additional reflected waves, which also contain the power. According to [2], the reflection by the floor and single wall can increase the tag received power about 4dB higher than non-reflection circumstance as in an anechoic chamber. Moreover, the added volume of reflected power can differ depending on the tag

location. Therefore, Equation (3.2) cannot be directly applied to estimate the distance between the antenna and the tag.

As shown in Figure 3.1, multiple distance variables are related on a narrow range of measured RSSI. For example, an RSSI value of -55.8dBm can map to two positions separated by 230cm in a simple linear measurement of 40 positions with 10 cm intervals in one dimensional space. The reader antenna and tags were placed at 90 degrees to one another and at a height of 100cm in a long, unobstructed hallway.

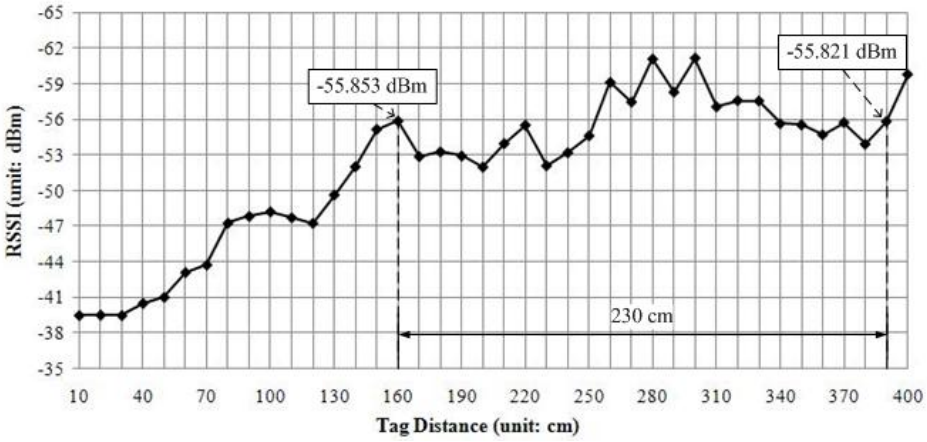

Figure 3.1 Example of ambiguous RSSI mapping to physical location on 400cm 1D space which is covered by a single reader antenna.

For example, Figure 3.2 shows the series of contour graphs from collecting RSSI values in 180cm × 200cm × 400 cm 3D spaces with total 1800 tag points in an office environment. A test frame with 9 × 10 grid cells is built by PVC mount and thin paper sheet and it contains 90 Alien GEN 2 Squiggle tags [37]. Each tag is placed at the center of 20cm × 20cm grid cell. As shown in Figure 3.2 (a), a single circular polarized 6dBi Poynting Patch-A0025 antenna [39] places at the center of the test frame with one meter above the ground and the antenna is cabled to the SIRIT Infinity 510 RFID reader [38]. From 20cm to 400cm of antenna distances with 20cm of interval, the reader measures the RSSI values for 90 tags (a total 40

iterations for 1800 tag points). According to the empirical results, ambiguous RSSI mapping employs higher uncertainty in the higher dimensional space than linear space.

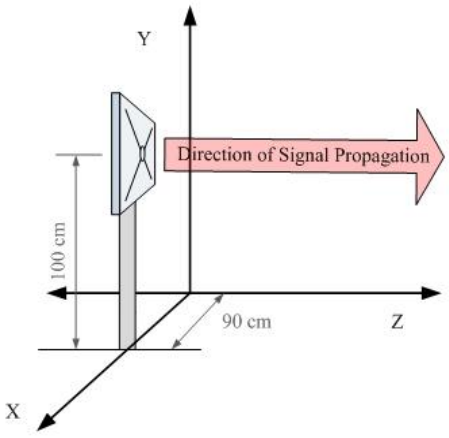

(a)

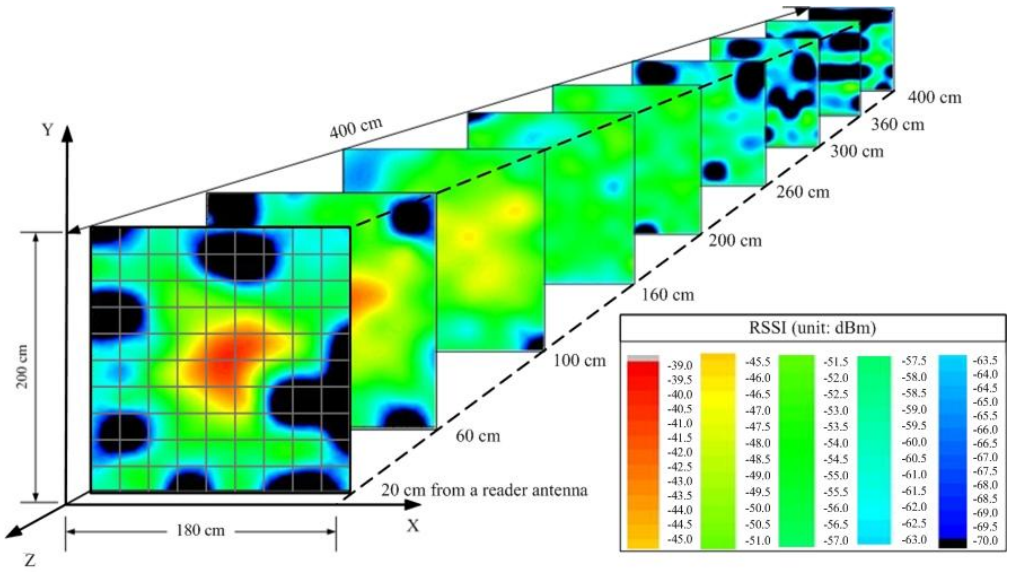

(b)

Figure 3.2 Contour graphs for collecting RSSI values in 180cm × 200cm × 400 cm 3D spaces with total 1800 tag points. (a) Antenna position and RF direction. (b) Series of contour graphs for measured RSSI values.

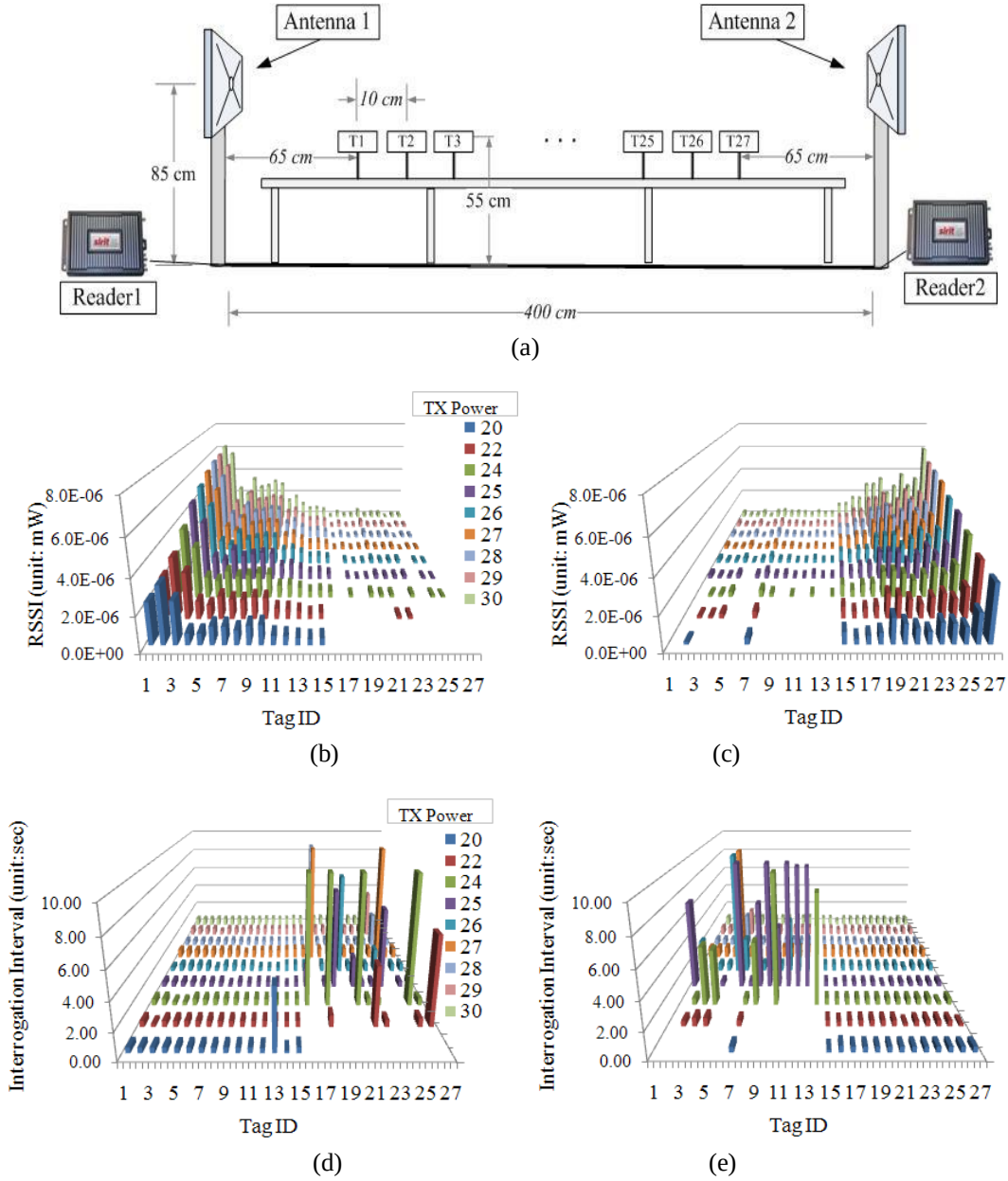

Figure 3.3 Reader performance without reader collision under various TX powers. (a) Test Set-up (b) For Reader Antenna 1 (RA1), the reading range (RR) and RSSI without interference by reader collision. (c) For Reader Antenna 2 (RA2), RR and RSSI without the interference. (d) For RA1, the interrogation intervals for 27 tags without interference by reader collision. (e) For RA2, the interrogation intervals without the interference.

A certain received strength can correspond to more physical positions in 3D space as shown in Figure 3.2 (b). For instance, if the collected RSSI value from a target is between -55dBm to -55.5dBm, 146 points within the total 1800 points are related with 406.448cm of maximal different distance.

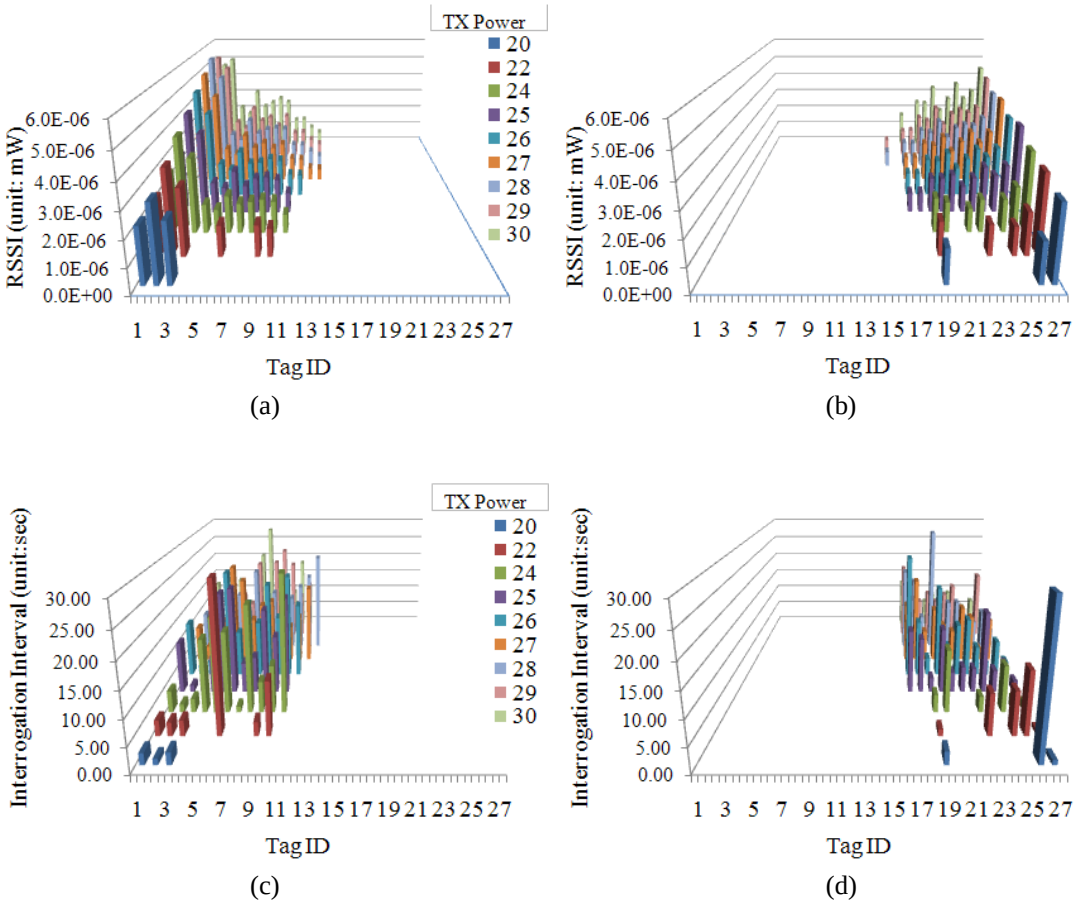

Figure 3.4 Reader performances with occurrence of collision case under same condition as Figure 3.3 (a). (a) For Reader Antenna 1 (RA1), the reading range (RR) and RSSI with interference by reader collision. (b) For Reader Antenna 2 (RA2), RR and RSSI with the interference. (d) For RA1, the interrogation intervals for 27 tags with interference by reader collision. (d) For RA2, the interrogation intervals with the interference.

3.1.2. Interference by Reader Condition

The reader collision problem affects both the read range and interrogation rate. In the passive UHF RFID system, the reader collision problem causes mainly two types of interferences: reader-to-reader frequency interference and multiple reader-to-tag interference [40]. In the multiple reader deployment, when a reader's transmitted signal interferes with performances of other adjacent readers, it is called Reader-to-Reader frequency (RR) interference. Because of signal masking and jamming by RR interference, the readers involved in interference suffer disturbed communication with tags that are placed in the interrogating range of the readers. When a passive RFID tag is located in the overlapped interrogation zones of two readers and multiple readers initiate interrogating operation simultaneously, an identification procedure between the tag and one of readers is interrupted by the other readers. This is called Reader-to-Tag (RT) interference. When the tag harvests enough power from the reader's electromagnetic wave, the tag turns on its IC chip. After the tag receives an interrogation query from the reader, the tag and the reader exchange a number of messages for the interrogation. In the middle of interrogation, the other adjacent readers, which send out the interrogation queries simultaneously, might hear the response and intervene wrongly in the interrogation procedure. Finally, if all the readers fail to identify the tag, this is known as the false negative problem.

Under conditions of Figure 3.3 (a), RT interference employs significant reduction of reading ranges and interrogation rates as shown in Figure 3.3 and Figure 3.4. In a case that RFID system uses a mono-static antenna, which acts as both signal transmitter and receiver, the antenna role is as a signal receiver after transmitting interrogation query to tags. Under the occurrence of interference, the reader antenna (RA1)'s receiving period is interrupted by transmitted signal from the other reader antenna (RA2). Eventually, background noise near RA1 is increased, and RA1's sensitivity is significantly decreased. The strength of backscattered signal from a tag is very weak compared with the reader's transmitted signal. The backscattered

signal is easily masked and jammed by intervening reader signals. For example, in Figure 3.3 (b) and Figure 3.4 (a), the minimum Received Signal Strength Indicators (RSSI) of RA1 is sharply deceased by 98% with 20dBm, and 63% with 30dBm of antennas' transmission power. Moreover, the interrogation intervals for 27 tags is significantly increased under reader collision as shown in the Figure 3.3 (d) and (e), and Figure 3.4 (c) and (d).

Interrogation procedure between a reader and a tag is easily interrupted with high chance by RT interference. Moreover, during a successful interrogation procedure, backscattered signals from the tag are masked and jammed by other intervening reader signals. In Figure 3.5, RA1 can identify 10,126 times for the deployed 27 tags during 200 seconds with 30dBm of transmission power. But, under interference, it can interrogate only 310 times within the same time duration and there is 96.94% of decrease of interrogation rate.

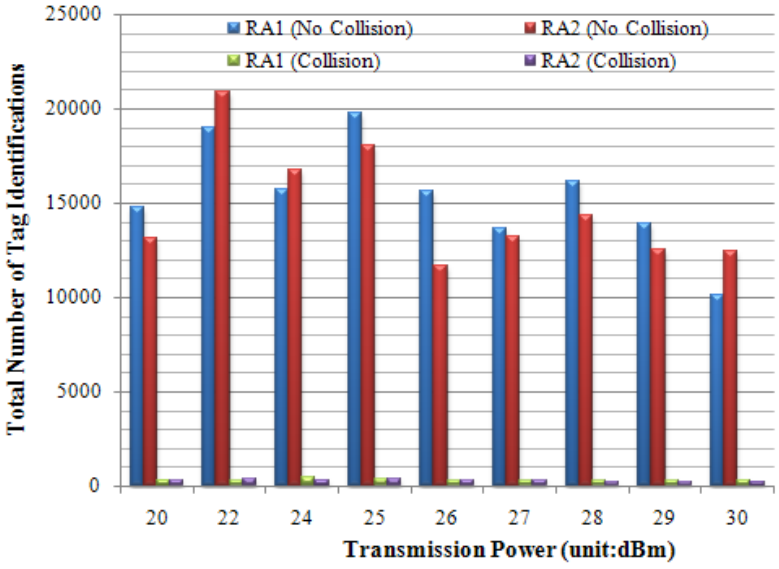

Figure 3.5 Comparison of total number of interrogations for 27 tags within 200 seconds between non reader-to-reader collision case and occurrence of collision case under same condition as Figure 3.3 (a).

The other cause of tag variation is based upon operating frequencies of the reader and reader antenna.

3.1.3. Variations in Performance of Uniform RFID Tags

In an ideal world, all of the same types of passive tags have to perform equally under uniform conditions such as type of reader, distance, and material of tagged object. In practice, passive RFID tags do not behave equally, even if the tags are from the same vendor and same tag model. As an example, we measure and compare the performance of 50 passive RFID tags which are Alien GEN 2 Squiggle tags in an ordinary office environment and an anechoic chamber as shown in Figure 3.6 (a) using the SIRIT Infinity 510 RFID reader and the single circular polarized 6 dBi patch antenna. The distance between the reader antenna and tag is 1.2 meter and both are locate 1.2 meter height from the ground. The antenna's transmission power is 30dBm and operating frequency is fixed as 915MHz. Figure 3.6 (b) illustrates Probability Density Functions (PDF) of the variation of RSSI values for same types of 50 passive tags with over 20,000 samples for each tag under both experimental conditions. Under the office environment, the mean of 50 tags' RSSI values is -47.72dBm and the standard deviation is 0.2821. In the case in the anechoic chamber, the mean of 50 tags' RSSI values is -47.7181dBm and the standard deviation is 0.2829. Moreover, the degree of RSSI variation among the uniform tags is not fixed.

Figure 3.6 (c) illustrates the degree of RSSI variations for 50 reference tags at 11 different locations in the office environment. Depending on the location, the mean and the standard deviation of RSSI values for each position from 50 tags are various. If the standard deviation is high, that means the degree of tag variation is increased. According to the results, when the tags are placed to send stronger response to the reader antenna (as tag positions 1 to 9), the standard deviation is between 0.22545 and 0.27143. On the other hand, for the tags located in position 10 and 11, the RSSI values are weaker and the standard deviation of 50 tags

sharply increased to 0.32187 and 0.52318. This means that the ambiguity of RSSI mapping increases among the tags which receive weaker power from the reader.

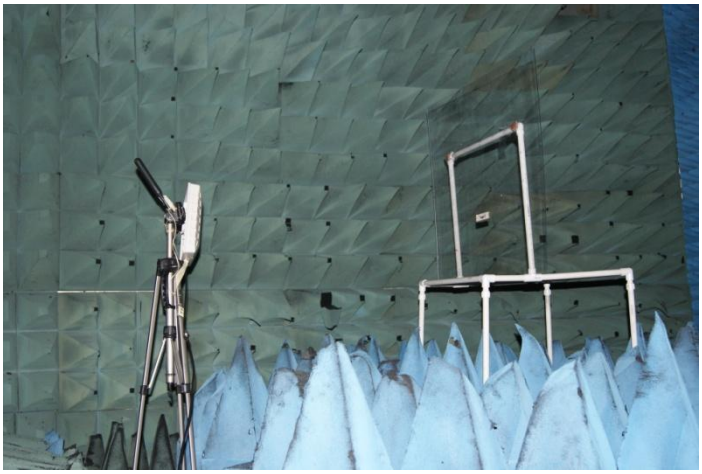

(a)

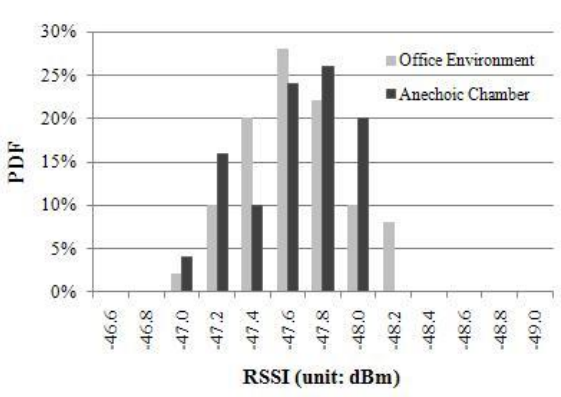

(b)

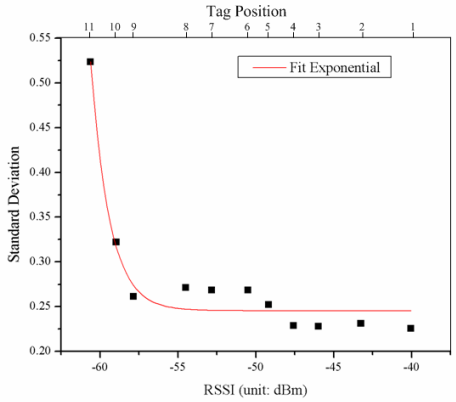

(c)

Figure 3.6 Variations of Uniform RFID Tags. (a) Experiment Setup. (b) RSSI variations among 50 uniform squiggle tags. (c) Degree of variations by tag positions.

3.1.4. Impact of a Tag Posture

In the passive UHF RFID system, the spatial relation between reader antenna and the tag significantly affects RFID system performance. One of well known factors of the spatial relation is the distance between the reader antenna and the tag. In this subsection, we analyze impact of a facing angle (orientation) between the antenna and the tag to RSSI under practical

and ideal condition. Defending on the facing angle, RSC of the tag can be varied with correlation of mismatch of circular polarization, and it relates to RSSI variation at certain physical locations for the tag.

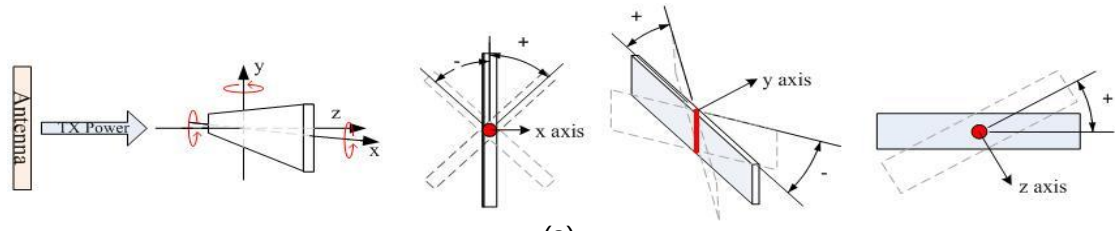

(a)

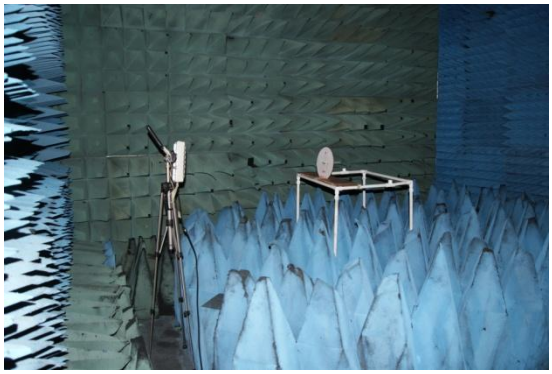

(b)

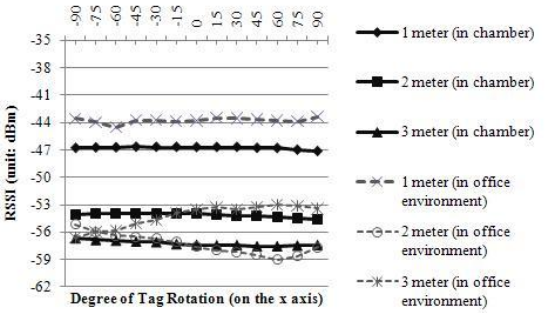

(c)

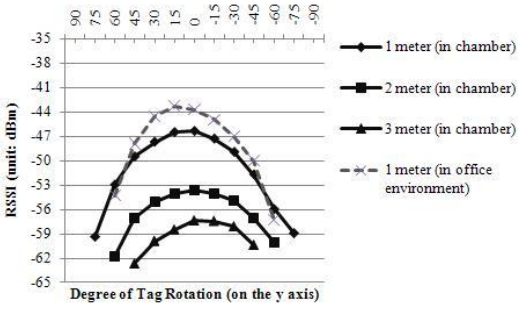

(d)

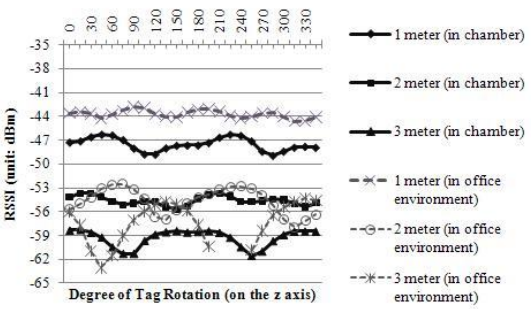

(e)

Figure 3.7 Examples of influcences facing angles of RFID tags to RSSI. (a) Various type of tag orientations depending on the tag posture. (b) Affection of the elevation angle (such as rotation on the x axis in (a)). (c) Impact of the the tag operation by rotation on the y axis in (a). (d) Impact of the tag operation by rotation on the z axis in (a).

Figure 3.7 illustrate the empirical results about various RSSI with three types of different rotation of tags in the office environment and the anechoic chamber. As shown in Figure 3.7 (a) and (b), where the reader antenna locates with fixed height as 1.2 meter and pitch angle, the degree of facing angle is changed by tag rotation on the x, y or z axes. In Figure 3.7 (c), we analyze the relation between RSSI values and the angles of elevation, which rotates on the x axis. According to the results, rotation on the x axis does not remarkably influence to the measured RSSI under various tag distance in the anechoic chamber. In the practical condition as the ordinal office environment, the change of elevation can raise fluctuation in RSSI, and it shows the erratic level of fluctuation depending on the actual tag location. For instance of irregular degrees of RSSI change, when the tag places 2 meter and 3 meter away from the reader antenna with -90° of the elevation, the measured RSSI values are similar due to different volumes of reflected power at each location. Changing the degree of elevation causes fluctuation of RSSI values for both locations in the office environment.

The influence of the polarization mismatch by the tag rotation on the y axis from -90° to +90° causes more noticeable variation of RSSI. As the rotation angle on the y axis continues to increase (or decrease), the RSSI value begins to diminish, and the fluctuation of measured RSSI value shows polynomial decrease as shown in Figure 3.7 (d). The fluctuation of RSSI is similar to a second order polynomial. Under ±75° of rotation angles, the strength difference from 0° is more than 12.48 dB with 1 meter distance between reader antenna and tag in the chamber. Moreover, the range of responsible facial angle (on the y axis) is various depended on physical tag position, which is deeply correlated with the collected power volume at the tag side. When the tag locates near the reader antenna (as 1 meter distance) in the anechoic chamber, the tag responsible rotation range is between -75° to +75°. But if the tag locates at a less power collecting point (as 3 meter distance), the tag responsible rotation range is decreased to ±45°, and it brings out the false negative interrogation case in passive UHF RFID based interrogation area.

Figure 3.7 (e) shows the impact of the tag operation by rotation on the z axis. The change of rotation angle on the z axis employs the wave-like fluctuation of RSSI. The height and wavelength of RSSI fluctuations are various depending on the tag location, which correlates with the volume of harvesting power at the tag. In the anechoic chamber, when the measured RSSI values are strong such as the location with 1 meter distance in the office environment, the height of the wave-like fluctuation is 2.46 dB with shorter wavelength. On the other hand, the fluctuation of RSSI values from the tag with 3 meter distance has over 3.35 dB of height with longer wave length. This pattern is turned up more clearly in the practical condition. When the measured RSSI is strong at the location with 1 meter distance in the office environment, the height of the wave-like fluctuation is 1.3 dB with short wavelength. By contrast, the fluctuation of RSSI value from the tag, which locates with 3 meter distance, has over 8.28 dB of height with long wave length.

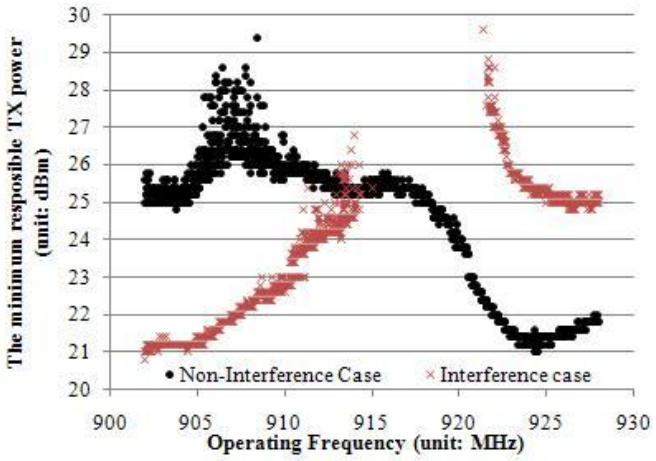

Figure 3.8 Shifting a center of frequency by tag-to-tag interference.

3.1.5. Influence of Tag to Tag Interference

In the passive RFID system, Tag-to-Tag interferences have rarely been researched contrary to Reader-to-Reader interference [40] and Readers-to-Tag interference [41]. In [42], the authors

evaluated the decrease of interrogation range by multiple adjacent tags' interference. According to [43], the adjacent tag affects to change of IC impedance, and it brings substantial decrease of reader's interrogation range. This issue is also related on the tag detuning problem when the tag adhered on the metallic object. In this subsection, we evaluate the tag-to-tag interferences on the RSSI value with detail empirical results.

An appearance of neighbor RFID tag causes the changing center of frequency on an existing tag. Figure 3.8 illustrates the interference of existence of neighbor tag. we measure the minimum responsible reader antenna's transmission power under various reader operating frequencies within the FCC regulation as 902MHz to 928MHhz, when Alien GEN 2 Squiggle tag operates alone at fixed point, where 1 meter distance between the reader antenna and the tag with 1.3 meter height from the ground in the office environment. Interval of the operating frequency is10KHz, and we iterate 50 times per frequency. According to the empirical results, the tag exists alone, as non-interference case, in the monitoring area, the tag can response to reader by higher frequency (as 924MHz) with reader's minimum transmission power (as 20.8dBm). By contrast as the interference case, the reader can successfully interrogate the tag using the lower frequency band as 902MHz with the minimum transmission power, when we place an extra tag vertically 20 cm above the existing tag.

Figure 3.9 illustrates RSSI fluctuations of Tag of Interest (TOI) at the fixed position under interference of a neighbor tag, where the neighbor tag has various positions with small spacing of 5cm intervals, in the anechoic chamber and the hallway. In this evaluation, we focus on the variation of TOI's backscattered signal strength against the interference from the neighbor tag. We analyze the relation between RSSI and a tag to tag distance, which is a distance between two tags' IC chip on the tag, on PVC test-frame in the ideal condition such as the anechoic chamber. We have also use the Alien GEN 2 Squiggle tags in the evaluation. The reader antenna and tag locate 1.2 meter height from the ground. The antenna's transmission power is 30dBm. For the accurate analysis of the tag-to-tag interference to compare with the

non-interference case, we measure RSSI values of TOI only after each change of the tag to tag distance.

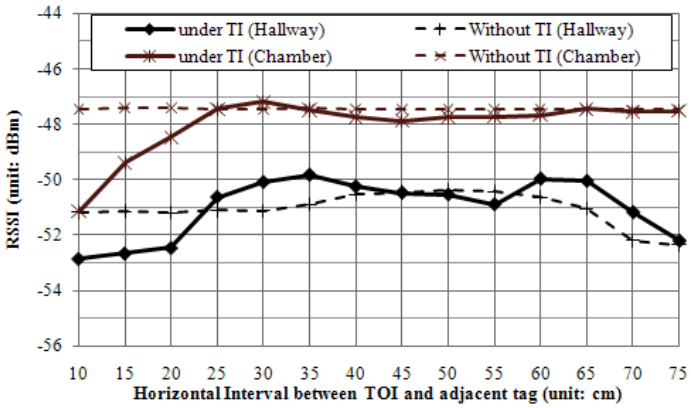

(a)

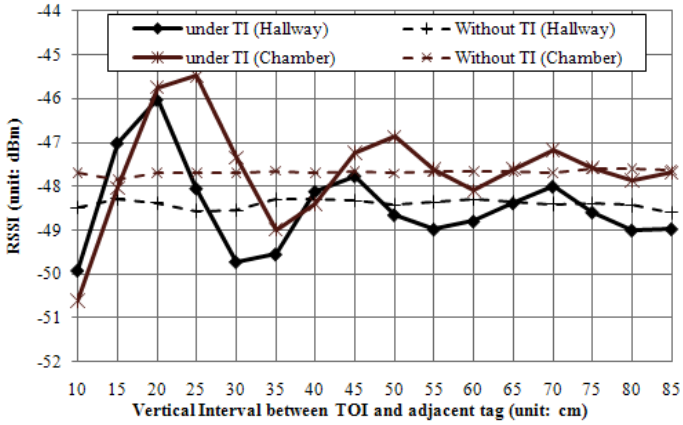

(b)

Figure 3.9 Interferences of adjacent tag under various tag distances. (a) Horizontal Interval case. (b) Vertical Interval case.

Figure 3.9 (a) illustrates the impact of tag-to-tag interference where the neighbor tag vertically locate above the TOI and the reader antenna's operating frequency is fixed to 915MHz. When the distance between the reader antenna and TIO is 100cm, RSSI of TIO is initially -47.66dBm without the neighbor tag's interference, and the volume of RSSI is substantially decreased to -52.83dBm by the existence of the neighbor tag with 5cm vertical interval in the

chamber. And the increase of the distance between the tags causes the variation of RSSI values from the TOI. The interesting observation in this evaluation is that the fluctuation of RSSI variation under the tag-to-tag interference shows a sine wave form with exponential decaying depending on the tag to tag distance.

Figure 3.9 (b) illustrates the impact of tag-to-tag interference where the neighbor tag horizontally locates next to TOI under various operating frequencies. When the reader antenna to tag distance is 100cm, and the neighbor tag places with 10cm of horizontal interval from the TOI, the RSSI from TOI is sharply decrease similar to the vertical interval case. But, increase of tag-to-tag distance increase the RSSI of TOI until the distance is within 30cm. If the tag-to-tag distance is longer than 30cm, the fluctuation of RSSI is in the steady condition such as similar RSSI of TOI under non-interference case. The tag-to-tag interference is observed in the practical condition with similar degree of impact on the TOI's RSSI in both test conditions.

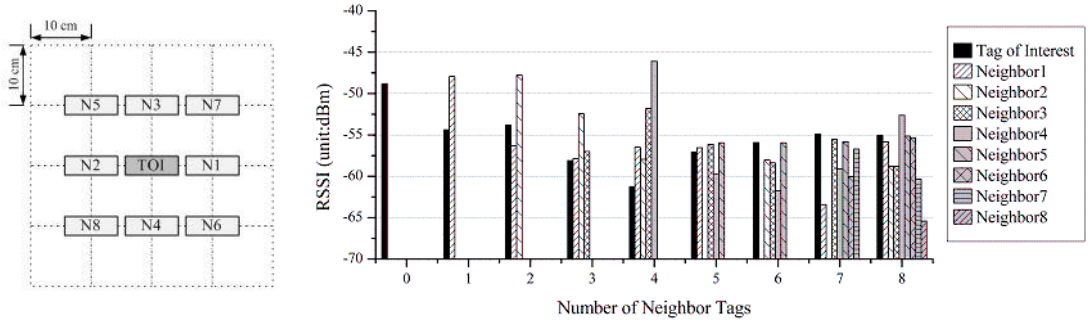

(a) (b)

Figure 3.10 Example of the relation between RSSI and tag population. (a) Deployments of 9 passive UHF tags in 20 cm by 20 cm space. TOI stands for Tag of Interest, and N denotes Neighbor. (b) Variation of RSSI by the number of adjacent tags.

We evaluate the relation between RSSI and tag population in a given area. The strength of backscattered signal varies depending on the number of neighbor tags. We put the tag of interest (TOI) at the center of 20 cm × 20 cm area as shown in Figure 3.10 (a), and the mean of RSSI values is -48.8dBm, which are measured by the antenna with 115cm distance.

When one tag (Neighbor1) places at the left of TOI with the 10 cm horizontal spacing, TOI experiences 5.572 dB of power loss as shown in Figure 3.10 (b). Existence of 4 neighbors causes 8.21 dB of RSSI decrease to TOI. Accordingly, the existence of neighbor tag substantially affects the RSSI value. But, the number of neighbor tags does not directly relate on the level of TOI RSSI value. In the cases of high population (as 5 to 8 neighbors), the means of TOI RSSI values are higher than the case of 4 neighbors.

3.1.6. Strong and Weak Tag Problem

In the ideal world, all of the tags transmit their IDs with the same strength of signal during the tag response period in a PingID procedure. But, in the real world, the strengths of the replies are not the same. If a passive RFID tag is located near the antenna, the signal strength is stronger than the others. On the other hand, since a long distance between the tag and the antenna, and damping and absorbing of a signal under humid environmental conditions can reduce the strength of signal of the tag's reply, there is a high probability of the existence of a weak tag. If one strong tag and multiple normal or weak tags respond simultaneously in the same bin slot, the reader cannot recognize a collision due to a strong signal from the strong tag. Also when one normal strength signal and multiple weak signals arrive at the same bin slot, weak signals might be ignored. The above problem is the strong-weak tag problem, and most of the existing anti-collision algorithms are not concerned with this problem. The strong-weak tag problem affects to probabilistic anti-collision algorithms such as a framed ALOHA and a dynamic framed ALOHA. For example, one of serious disadvantages of ALOHA based anti-collision algorithms is a starvation problem [3]. There is a probability that some of the tags do not have a chance to be identified for a long time. And the strong-weak tag problem increases the probability of starvation of a particular weak tag because the weak tag's signal might be masked by a stronger signal. In the dynamic framed ALOHA algorithms, when the reader changes a frame size based on the numbers of collisions and single replies, the numbers might

be not correct due to masked tags. Therefore, the reader cannot estimate an efficient frame size, and the performance might be decreased.

The bin slot based anti-collision algorithms are robust enough against the strong-weak tag problem. For example, in the basic Bin Slotted Algorithm, the reader always repeats the interrogation procedures with a null value in the [VALUE] field. Even though some of the weaker tags' signals are ignored by stronger tags, the tags' responses can arrive at the reader in further interrogation procedures. Therefore, the strong-weak tag problem does not influence to the identification rate of BSA.

Interestingly, the performance of BSA is increased depending on the portions of strong and weak tags in the interrogation zone. Under the existence of strong and weak tags, the reader can identify a stronger tag's ID earlier than others. Even though one stronger tag and multiple weaker tags transmit signals in a particular bin slot, only the stronger tag can be identified. This characteristic reduces the number of collisions for identifying one tag in BSA. Therefore, the reader can identify all tags with fewer collisions in the interrogation cycle.

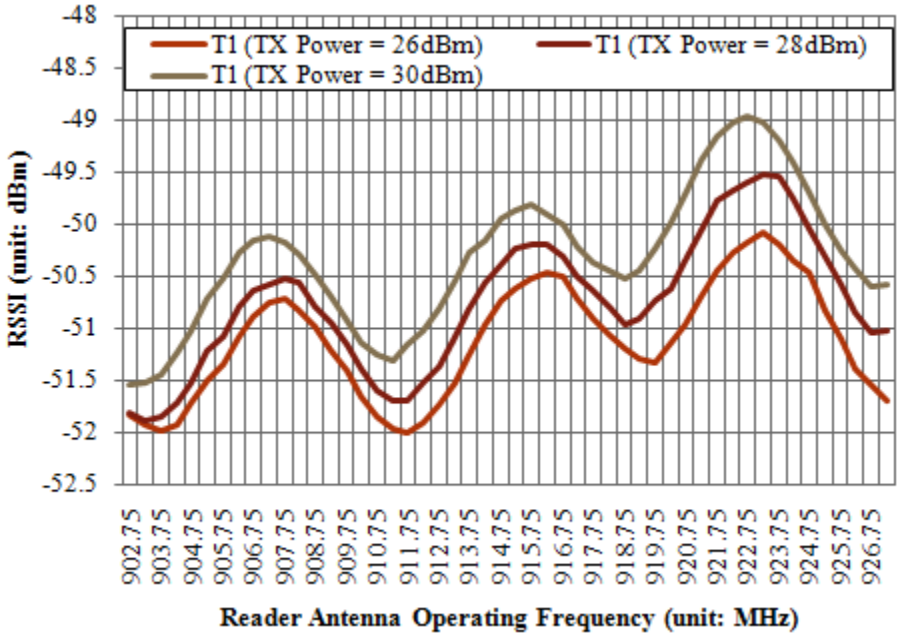

Figure 3.11 Example of tag variations by reader's operating frequencies

3.1.7. Variation of Tag Performance based upon Operating Frequencies

Depending on reader's operating frequency, a tag performs differently under fixed tag conditions such as reader antenna to tag distance, facing angle between reader antenna and tag antenna, and other environmental factors. As shown in Figure 3.11, the change of operating frequency of reader brings out maximally 2.59dB of difference on RSSI values, where the reader antenna to tag distance is set 100cm, and antenna and tag height are 120cm in the chamber.

3.2 Ambiguity caused by Low Performance of existing Passive UHF RFID based Localization

3.2.1. Potential Problem of Fingerprinting technique

Fingerprinting technique [29] finds a target location using a pre-measured data set of information from geometrically known references points, and the collected dataset can be time of signal arrival, received signal strength, and identification rate within a given time duration, and other information. The dataset is stored in the system, and the target location is inferred by comparison between the information from the target and the dataset, when the system detects the target in the monitoring area. The fingerprinting technique consists of two phases: off-line and online. During the off-line phase, the localization system collects RSSI values, which are the fingerprints, from deployed reference tags. Then, in the online phase, which is triggered by detection of the target object within the interrogating area, the system measures the RSSI from the target, and, calculates the Euclidean distances between the target's RSSI and the fingerprints to estimate the target location with the reference tag (or tags) which has the minimum Euclidean distance of RSSI. K-Nearest Neighbor (KNN) [8], [13] is the most common algorithm for the fingerprinting technique in the RFID based localization system. The KNN algorithm gathers the target and the reference information during the on-line phase, and computes the Euclidean distances of the information to figure out k number of the closest references, which have the most similar vectors to the target. Spatially adjacent tags return similar signal strength in theory but there is high chance the far-away tags report similar RSSI in

practice. If the system picks spatially un-adjacent tags as the K-Nearest Neighbors, the accuracy of localization is sharply decreased. Figure 3.12 illustrates the potential problem of KNN technique due to ambiguous RSSI mapping in practical condition. In order to cover the indoor space without consideration of reader collision, we set one reader antenna. The total 9 × 10 reference tags are placed to a 2-dimensional grid with a given interval in the monitoring area, and each reference tag with 20cm of interval from (1, 1) to (9, 10) points and the target tag at point (5.5, 5.5) as shown in Figure 3.12 (a). Figure 3.12 (b) shows frequencies of selected reference tags under a total of 200 iterations of RSSI correction when k value is 3. In theory, the closest reference tags, which place at the points (5, 5), (5, 6), (6, 5), and (6, 6), are estimated for the nearest neighbors, but, in practice, the points (1, 6), (6, 8), and (9, 2) are chosen for the nearest neighbors with over 8 times of frequencies of selection than the actual spatially close references. The RSSI values from the target and reference tags are influenced by the tag variation and the tag-to-tag interference, and the ruined RSSI values are increased the ambiguity of location mapping.

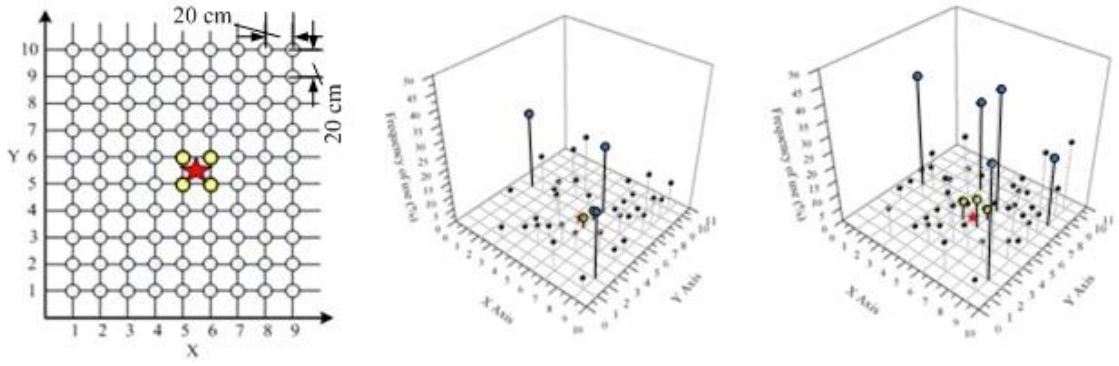

(a) (b) (c)

Figure 3.12 Example of inaccurate selection of the *k*-nearest neighbors in the fingerprinting technology due to the ambiguity problem. (a) Display of the target and reference tags in 2D space (180 cm ×200 cm) (b) Frequency of selected reference tags (*k*=3). (c) Frequency of selected reference tags (*k*=5).

3.2.2. Influence of the Ambiguity under Various Granularities

The granularity of reference tags, as tag population, affects the accuracy of location information. In a monitoring area, low reference granularity as a coarse-grained distribution of reference tags provides faster interrogation of target tag, and less overhead of computation for localization. The drawback of the low granularity is accuracy of estimated result. With the consideration of variation of tag operation and irregular attenuation of signal, wrong selection of reference information might sharply decrease the accuracy of estimated target location in the coarse-grained distribution. On the other hand, high granularity as a fine-grained distribution of reference tags aids higher accuracy estimation. The scenario with dense reference tags increases the required duration of the first identification of the target tag, and rich referral information increases total computation time.

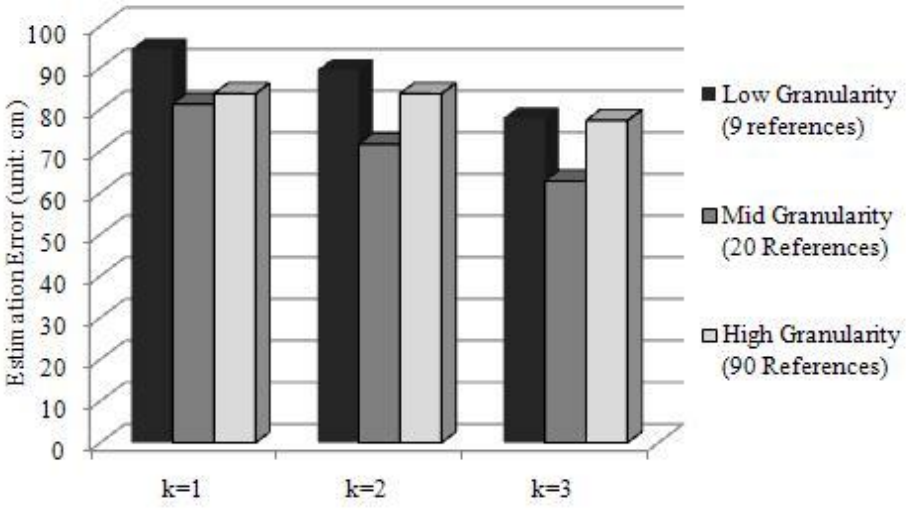

Figure 3.13 Example of relation between the accuracy and the reference tag granularities on k-Nearest Neighbor algorithm based localization system.

Figure 3.13 shows the relation between the accuracy and the reference tag granularities on k-Nearest Neighbor algorithm based localization system [8]. We put total 6 target points in 180cm × 200cm monitoring area under three distinct granularity conditions: low (with 9 reference tags), medium (with 20 reference tags) and high (with 90 reference tags)

granularities. Each reference tag is distributed uniformly in the monitoring area. According to the experimentation results of localization using KNN, the case of medium granularity provides average 17.79% more accurate results than the low granularity under various k values 1 to 3. Ideally, the finest granularity provides the most accurate result, but, in practice, there is high chance to increase ambiguity of selection due to practical issues such as tag-to-tag interference, discrepant performances among tags and influences by the postures of the tags. The localization result under high granularity is worse than the case of medium granularity an average 12.05% of decreased accuracy. Therefore, finding the optimal granularity is one of challenges for accurate and precise performance of the RSSI based localization in the passive UHF RFID system.

3.3 Conclusions

In the RSSI based localization system using passive RFID, the combination of circumstantial factors (such as different volumes of reflected power, and path loss), the characteristics of passive RFID tag (such as the variation of uniform tags, tag posture, and the material of tagged object), and the tag-to-tag interference brings out ambiguous mapping between a physical location and a measured RSSI value in practice. According to the empirical results, the strength of backscattered signal from the tag at a certain physical location can experiences significant power loss by change of tag posture and the type of tagged object. In the worst case, the reader can suffer the illumination of tag as the false negative, even though the tag locates with 1 meter distance from the reader antenna under the Line-Of-Sight condition. Existence of adjacent tag also substantially affects the erratic variation of RSSI from certain location because of tag-to-tag interference. Also we show the minimum distance to avoid tag interference. In Table 3.1, we summarize the causes of ambiguous RSSI and impacts with the empirical results. The ambiguity problem employs incorrect selection of the k-nearest neighbors in the fingerprinting technique to decrease accuracy of localization result. Moreover, we show that the ambiguity problem is influenced by the granularity of deployed references, and the high

granularity condition can cause lower accuracy correlated on increased ambiguity in the real world.

Table 3.1 Causes of RSSI Variation

Cause		Impact	
		Level	Empirical Result
Variation of uniform tag		Low	- 95.44% of 50 tags backscatter signals within 2.09 dB of different RSSI level
Tag posture		High	- 3.85 dB of different RSSI level from -90° to +60° of tag rotation on the x-axis in practice. - 13.6 dB of different RSSI level from -60° to 0° of tag rotation on the y-axis, and false negative interrogation under ±75° or ±90° of rotation angle - 8.28 dB of different RSSI level by tag rotation on the z-axis.
Tag-to-Tag interference	Tag population	High	- 8.21 dB of maximal different RSSI level by existence of 4 adjacent tags
	Tag toTag distance	High	- 7.56 dB of maximal different RSSI level under various intervals
Multi Reader to Tag interference		High	- Over 63% of RSSI decrease and 96.94% decrease of interrogation rate
Operating Frequency		Low	- 2.59 dB of different RSSI level based upon frequencies

CHAPTER 4

INVESTIGATION OF TAG TO TAG INTERFERENCE AND USE FOR PASSIVE FAR-FIELD UHF RFID SYSTEM

In passive UHF RFID systems, tag-to-tag interferences affect to performance of passive RF tag. When two tags locate close each other, an adjacent tag influences other tags' IC impedance. And it causes excess increase or decrease of the backscattering communication budgets. According to our empirical results, compared with non-interfered backscattering signal strength in an anechoic chamber, tag-to-tag interference affects to the reader received signal strength, such as 5.8dB of excess decrease and 2.5dB of increase, depended on the distance between two tags. In this chapter, we present a new model of backscattered signal strength for passive UHF RFID system under tag-to-tag interference. The variation of excess power volume by the interference is depended on an interference coefficient. In order to analyze the impacts of tag-to-tag interference, we show empirical results in the anechoic chamber, then, we model the change of the backscattered signal strength using the second order under-damped system for different tag-to-tag distances and angles. Moreover, we propose a novel localization algorithm to estimate target object location using the presented Tag-to-tag Interference Model (LMTI). According to the empirical results, LMTI improves maximally 200% accuracy compared RSSI based KNN algorithm.

4.1 Introduction

Radio Frequency Identification (RFID) technologies system's primary function is automated identification and data capture. RFID technology has generated significant interest due to decrease in cost and size and increase of reliability and performance. An RFID system provides a cost efficient and simple method to identify objects. An RFID tag is attached to the

object and communicates with a reader for detection of the presence and identification of the tagged object. A passive RFID tag does not contain a power source itself and the tag communicates with a passive RIFD reader using passive communication such as backscattered communication.

In the passive RFID system, Tag-to-Tag interferences have rarely been researched contrary to Reader-to-Reader interference [40] and Readers-to-Tag interference [41]. In [42], the authors evaluated the decrease of interrogation range by multiple adjacent tags' interference. According to [43], the adjacent tag affects to change of IC impedance, and it brings substantial decrease of reader's interrogation range. In this chapter, we evaluate and normalize the tag-to-tag interferences for passive far-field UHF RFID system, such as changing tag antenna impedance and the backscattered signal strength.

In this chapter, we present a new useful model of backscattered signal strength for passive UHF RFID system under tag-to-tag interference. The variation of power volume by the interference is depended on the interference coefficient. In order to analyze the impacts of tag-to-tag interference, we show empirical results in ideal condition, such as anechoic chamber, then, we model the change of the backscattered signal strength using the second order under-damped system for different tag-to-tag distances and angles. Moreover, this chapter presents a novel localization algorithm using the model of tag-to-tag interference for smart shelf application.

The remainder of this chapter is organized as follows. In Section 4.2, we study mechanisms about backscattered signal strength for far-field passive UHF technologies under tag-to-tag interference. In Section 4.3, we present observed empirical results of impact of tag-to-tag interference. we model level of tag-to-tag interference in 2D space in Section 4.4, and analyze the proposed tag-to-tag interference model in Section 4.5. In Section 4.6, we apply the presented tag-to-tag model to localize object position, and we draw the relevant conclusions in Section 4.7.

Table 4.1 Notations

Notation	Description
P_{tag}^{RX}	Tag received power (dBm)
P_{reader}^{TX}	Power of the reader antenna transmission (dBm)
P_{reader}^{RX}	Reader antenna received power (dBm)
G_{reader}	Gain of the reader antenna (dBi)
G_{tag}	Gain of the tag antenna (dBi)
d	Reader antenna to tag distance (cm)
λ	RF wavelength of reader's operating frequency (cm)
σ	Radar Cross Section of the tag
ρ	Reflection coefficient
α	Interference coefficient
β	Variation of power volume by tag-to-tag interference (dB)
θ	Tag to tag angle in 2 dimensional space
Δ	Tag to tag distance (cm)
Δ_{min}	The minimum tag to tag distance (cm)
ζ	Damping factor
ω_0	The undamped natural oscillator frequency
ω_d	The damped oscillator frequency
ψ	Phase angle
Δ^{steady}	The minimum non-interfered tag-to-tag distance

4.2 Mechanism

Tag received power under an ideal condition is calculated by a modification of Friis transmission equation in the logarithmic scale [35]:

$$P_{tag}^{RX} = P_{reader}^{TX} + G_{reader} + G_{tag} - 20\,log_{10}(\frac{4\pi}{\lambda}) - 20\,log_{10}(d) \quad (4.1)$$

In Equation (4.1), we assume that there is not the cable loss and the reader and tag antennas have a polarization match. We further assume that there are not environmental

influences such as multipath, and background noise. For a single mono-static reader antenna system, the reader antenna received backscattering signal strength is written as

$$P_{reader}^{RX} = P_{reader}^{TX} + 2G_{reader} - 20\,log_{10}(\frac{4\pi}{\lambda}) - 40\,log_{10}(d) + 10\,log_{10}(\frac{\sigma}{4\pi}) \quad (4.2)$$

where σ denotes the radar cross section of passive RFID tag, and the radar cross section of tag can be written by following:

$$\sigma = \frac{G_{tag}^2 \lambda^2 |\rho|^2}{4\pi} \quad (4.3)$$

where ρ denotes the reflection coefficient, and the reader antenna received backscattering signal strength can be reformulated in the logarithmic scare as following [35]:

$$P_{reader}^{RX} =$$

$$P_{reader}^{TX} + 2G_{reader} + 2G_{tag} - 40\,log_{10}(\frac{4\pi}{\lambda}) - 40\,log_{10}(d) + 20\,log_{10}|\rho| \quad (4.4)$$

The backscattered signal strength can be influenced by a neighbor tag, because the adjacent tag affects tag's IC impedance. And the change of IC impedance brings out variation of the reflection coefficient, ρ. In this paper, we define α to an interference coefficient, and the interfered backscattering signal strength from the tag is rewritten by following:

$$P_{reader}^{RX} = P_{reader}^{TX} + 2G_{reader} + 2G_{tag} - 40\,log_{10}\left(\frac{4\pi}{\lambda}\right) - 40\,log_{10}(d) + 20\,log_{10}(\alpha \times |\rho|)$$

$$= P_{reader}^{TX} + 2G_{reader} + 2G_{tag} - 40\,log_{10}\left(\frac{4\pi}{\lambda}\right) - 40\,log_{10}(d) + 20\,log_{10}|\rho| + 20\,log_{10}(\alpha) \quad (4.5)$$

If α is greater than 0, but less than 1 (0<α<1), the reader antenna received signal strength is decreased due to the tag-to-tag interference. On the other hand, when α>1, the received backscattering signal strength is increased. If α is equal to 1, the backscattered signal strength is not affected by the adjacent tag. In Figure 4.1, we evaluate variation of power volume in dB, when α is between 0.001 and 3. The change of power variation shows logarithmic increase. When we define β to a power volume (or power variation) of interference in dB, β is expressed by following:

$$\beta = 8.6859 \times \ln(\alpha) \quad (4.6)$$

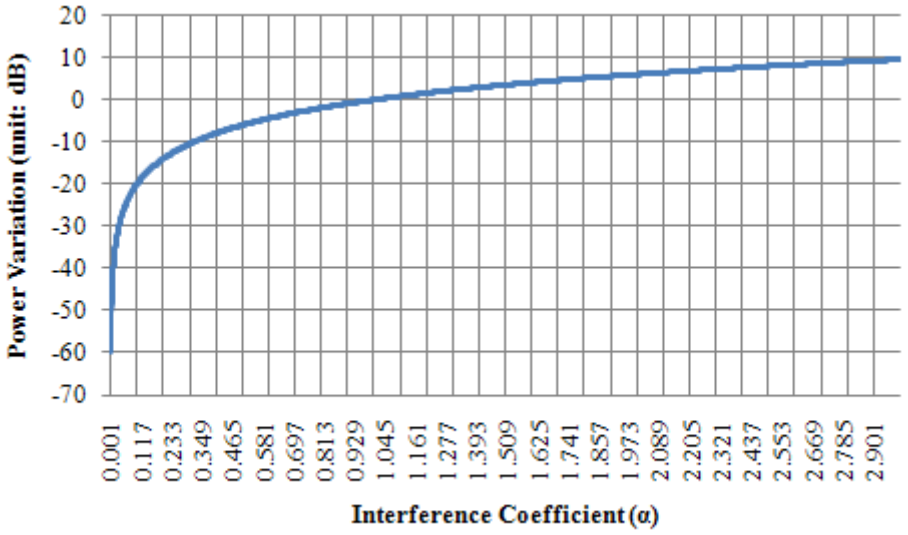

Figure 4.1 Power variation under various values of interference coefficient

The remained chapter focuses to how to achieve the interference coefficient, when a single tag is influenced by an adjacent tag, with detail empirical results.

4.3 Observation of Tag-to-Tag Interference

In this section, we evaluate the tag-to-tag interferences on the RSSI value with detail empirical results. An appearance of neighbor RFID tag employs the changing center of frequency on an existing tag. Figure 4.2 illustrates RSSI fluctuations of Tag of Interest (TOI) at the fixed position under interference of a neighbor tag, where the neighbor tag has various positions with small spacing of 5cm intervals. In this evaluation, we focus on the variation of TOI's backscattered signal strength against the interference from the neighbor tag. We analyze the relation between RSSI and a tag to tag distance on PVC test-frame in the ideal condition such as the anechoic chamber as shown in Figure 4.2 (a). We have also used the Alien GEN 2 Squiggle tag in the evaluation. The reader antenna and tag locate 1.2 meter height from the ground. The antenna's transmission power is 30dBm. For the accurate analysis of the tag-to-tag interference to compare with the non-interference case, we measure RSSI values of TOI only after each change of the tag to tag distance.

Figure 4.2 (b) illustrates the impact of tag-to-tag interference where the neighbor tag vertically locate above the TOI and the reader antenna's operating frequency is fixed to 915MHz. When the distance between the reader antenna and TOI is 100cm, RSSI of TOI is initially -47.66dBm without the neighbor tag's interference, and the volume of RSSI is substantially decreased to -52.83dBm by the existence of the neighbor tag with 5cm vertical interval. And the increase of the distance between the tags causes the variation of RSSI values from the TOI. The interesting observation in this evaluation is that the fluctuation of RSSI variation under the tag-to-tag interference shows a sine wave form with exponential decaying depending on the tag to tag distance. This pattern of impact is similarly observed in empirical results under various the antenna to tag distances. The increase of antenna to tag distance decrease RSSI of the tag of interest, but the influence of vertically located neighbor tag shows equal sine wave form with

exponential decaying. Moreover, depending on the antenna operating frequency, TOI backscatters different strength of signal to the reader antenna, but, the interference of existence of the neighbor tag is observed with same pattern of RSSI fluctuation as shown in Figure 4.3 (a).

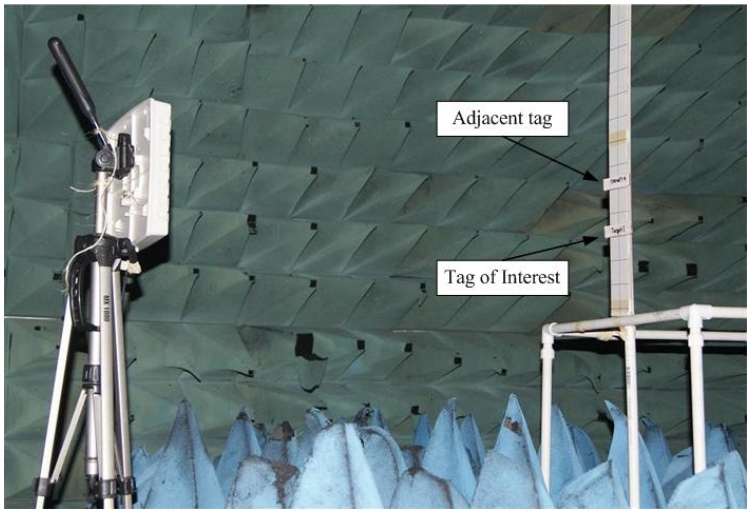

(a)

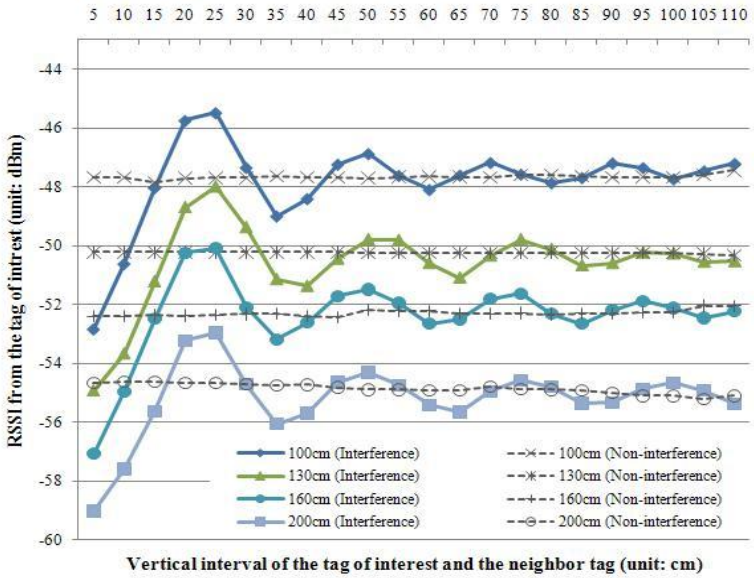

(b)

Figure 4.2 Interferences of adjacent tag with various tag distances in the anechoic chamber. (a) Snapshot of test in the chamber. (b) RSSI Fluctuations under tag-to-tag interference, where adjacent tag locates vertically from TOI.

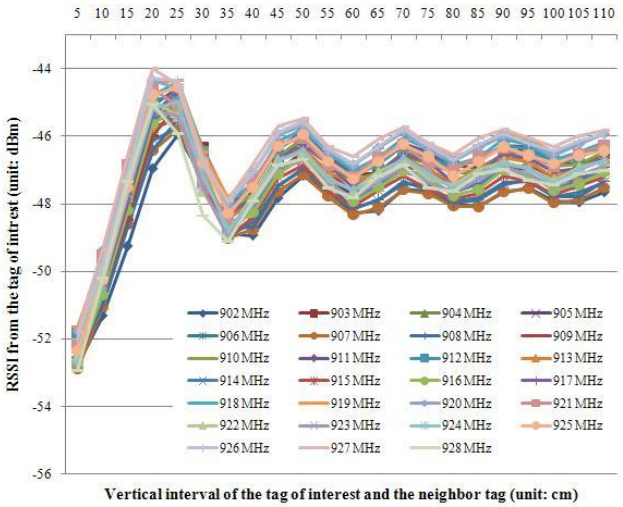

(a)

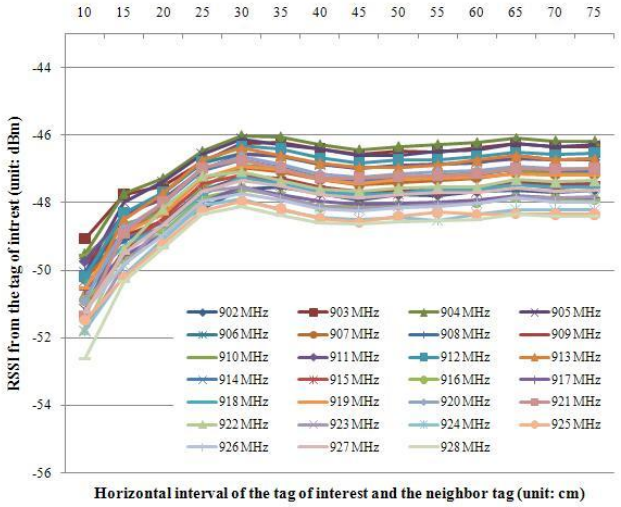

(b)

Figure 4.3 Impact of Tag-to-tag Interferences with various operating frequencies in the anechoic chamber. (a) RSSI fluctuations with various reader operating frequency, where adjacent tag locates vertically from TOI. (b) RSSI fluctuations with various reader operating frequencies, where adjacent tag locates horizontally from TOI.

Figure 4.3 (b) illustrates the impact of tag-to-tag interference where the neighbor tag horizontally locates next to TOI under various operating frequencies. When the reader antenna to tag distance is 100cm, and the neighbor tag places with 10cm of horizontal interval from the

TOI, the RSSI from TOI is sharply decrease similar to the vertical interval case. But, increase of tag-to-tag distance increase the RSSI of TOI until the distance is within 30cm. If the tag-to-tag distance is longer than 30cm, the fluctuation of RSSI is in the steady condition such as similar RSSI of TOI under non-interference case.

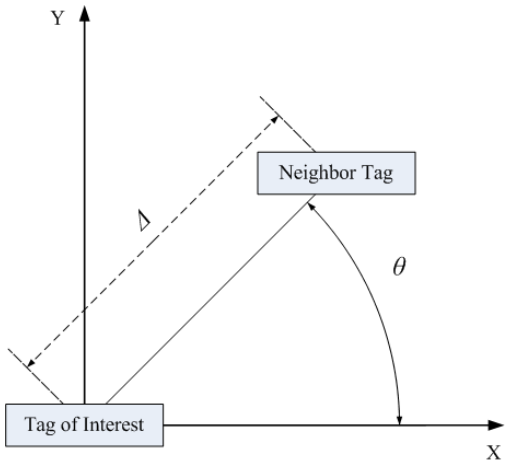

(a)

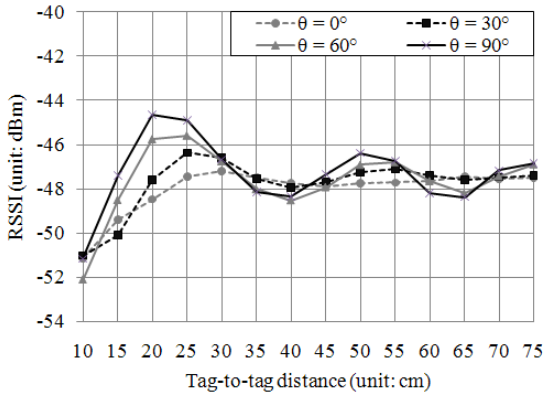

(b)

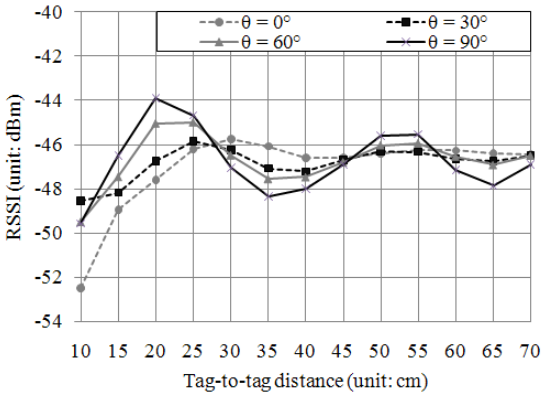

(c)

Figure 4.4 Interferences of adjacent tag under various tag to tag distances (Δ) and angles (θ) in an anechoic chamber, where 10cm ≤ Δ ≤ 75cm, and 0° ≤ θ ≤ 90°. (a) Results in the anechoic chamber. (b) Results in the hallway.

In Figure 4.4, we analyze the relation between a tag-to-tag distance and angle in 2-D condition under the tag-to-tag interference in the anechoic chamber and practical condition. As

shown in Figure 4.4 (a), TOI is fixed at a position with 100cm between the reader antenna and the tag, and the reader's operating frequency is 915MHz. Δ denotes a tag to tag distance and θ denotes an angle between two tags from the x axis. According to the empirical results as shown in Figure 4.4 (b), depending on the angle, the levels of tag-to-tag interference are varied. The mean of RSSI from TOI under non-interference case is -47.5285dBm and the standard deviation is 0.109dB. If the degree of angle is high, such as 90°, the fluctuation shows the highest sine wave form with shortest wave length. The decrease of degree of angle correlatively affects to the height and length of wave such as decrease of height of wave and increase of wave length. Moreover, Figure 4.4 (c) shows fluctuations of the observed interfered RSSI values in practical condition, such as a long, unobstructed hallway, with various tag-to-tag angles and distances. And, the observed impacts of tag-to-tag interference are very similar to the results in the chamber. Based on the observation, we can model the degree of tag-to-tag interference using the second order differential equation with under-damping in Section 4.4.

4.4 Modeling

According to the empirical data of the tag-to-tag interference observation, the fluctuation of RSSI appears periodic pattern as shown in Figure 4.4 (b). Therefore the interference of adjacent tag can be modeled as a homogeneous second order differential equation [58] as following:

$$\ddot{C}_{rssi}(\Delta) + 2\zeta\omega_0 \dot{C}_{rssi}(\Delta) + \omega_0^{\,2} C_{rssi}(\Delta) = 0 \tag{4.7}$$

where ζ is the damping factor, and ω0 denotes the undamped natural oscillator frequency. Due to the fluctuations of interfered RSSI values shows under-damped second order system, the damping factor, ζ, is greater than 0, but less than 1. When we define ω_d to the damped oscillator frequency, it can be calculate as follows:

$$\omega_d = \omega_0 \sqrt{1-\varsigma^2} \tag{4.8}$$

And, the general solution of the under-damped second order equation is defined as follows:

$$C_{rssi}(\Delta) = RSSI^{non-interfered} + A\frac{e^{-\zeta\omega_0(\Delta-\Delta_{\min})}}{\sqrt{1-\zeta^2}}\cos(\omega_d(\Delta-\Delta_{\min})-\psi) \tag{4.9}$$

where $RSSI^{non\text{-}interference}$ indicates the signal strength from the tag of interest without influence of adjacent tag, Δ_{min} denotes the minimum distance between two tags, A is the initial condition of the under-damped second order system, which is calculated as following:

$$A = RSSI^{interfered}(\Delta_{\min}) - RSSI^{non-interfered} \tag{4.10}$$

and ψ denotes the phase angle which is estimated by

$$\psi = \tan^{-1}\frac{\zeta}{\sqrt{1-\zeta^2}} \tag{4.11}$$

In Equation (4.9), the increase or decrease power volume of RSSI can be calculated by $A\,(e^{-\zeta\omega_0(\Delta-\Delta_{min})}/\sqrt{1-\zeta^2})cos\,(\omega_d(\Delta-\Delta_{min})-\psi)$, and it is represented by β in Equation (4.6), and the interference coefficient can be calculated by following:

$$8.6859\times\ln(\alpha) = A\frac{e^{-\zeta\omega_0(\Delta-\Delta_{\min})}}{\sqrt{1-\zeta^2}}\cos(\omega_d(\Delta-\Delta_{\min})-\psi) \tag{4.12}$$

and,

$$\alpha = e^{\left[A\frac{e^{-\zeta\omega_0(\Delta-\Delta_{\min})}}{\sqrt{1-\zeta^2}}\cos(\omega_d(\Delta-\Delta_{\min})-\psi)\right]\Big/ 8.6859} \tag{4.13}$$

Additionally, the minimum non-interfered tag-to-tag distance, Δ^{steady}, to avoid the interference is measured by following:

$$\Delta^{\text{steady}} = \frac{3}{\zeta\omega_0} + \Delta_{\min} \tag{4.14}$$

when the steady condition is defined that the variation of signal strength is less than and equal to ±5% of the non-interfered signal strength from the TOI.

4.5 Estimation of Tag-to-Tag Interference

The optimal of ζ and ω_0 are estimated by DSLM (Discrete Selection Levenberg-Marquardt) method which is developed for a numerical nonlinear optimization solution, extending Levenberg-Marquardt algorithm, which is a well-known local optimization solution, to a global optimization solution with efficient space searching strategy [59]. With N number of observation data, $\tilde{y}_v \in \Re$, DSLM performs to find the optimal value subject to minimize the sum of squares of the residuals, $R(x_v)$, between experiment data set $\tilde{y}_v$ and a model function $f(x_v)$, where x_v is a vector for the parameter and $f(x_v)$ is differentiable.

$$\arg\min_{x_v} F(x_v) = R(x_v)^{\mathrm{T}} R(x_v) \tag{4.15}$$

where,

$$R(x) = \tilde{y}_v - f(x_v) \tag{4.16}$$

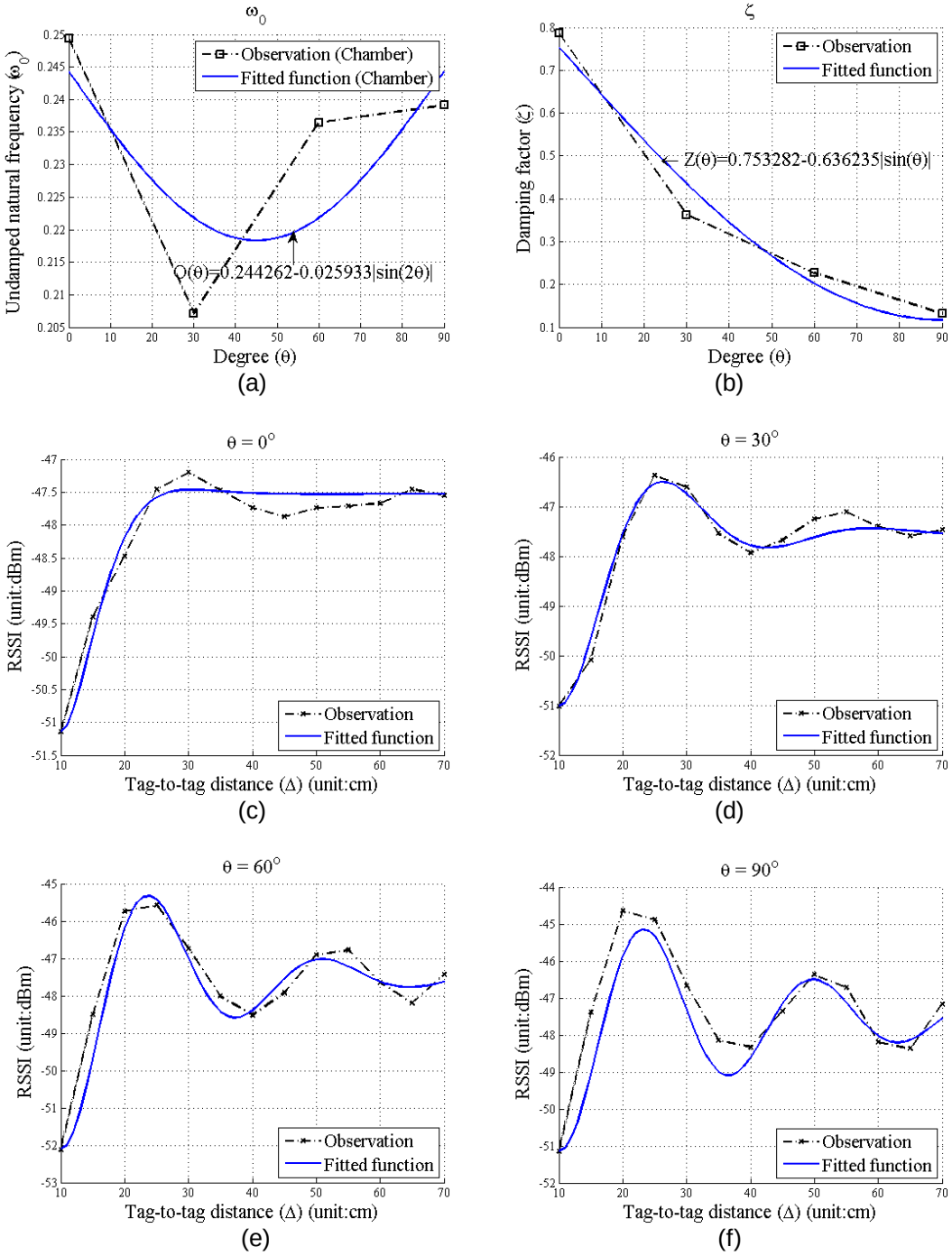

Figure 4.5 Comparison between Tag to Tag interference observations in the anechoic chamber and estimations. (a) The estimated optimal ω_0 values by DSLM. (b) The estimated optimal ζ values. (c) Case of θ=0°. (d) Case of θ=30°. (e) Case of θ=60°. (f) Case of θ=90°.

The experiment data are observed in two different environments such as the anechoic chamber and the hallway which is shown in Figure 4.4 (b) and (c). We simulate DSLM using MATLAB, and the optimally estimated parameter values ζ and ω_0 which are from two experiment data corresponding to each degree, θ, are listed in Table 4.2 and 4.3. The mean of non-interfered RSSI of TOI is -47.5285dBm and the standard deviation is 0.109dB when TOI has 100cm distance from the reader antenna in the chamber. In case of hallway, the mean of non-interfered RSSI of TOI is -46.6254dBm and the standard deviation is 0.1084 dB. Figure 4.5 (c) to (f) compare the observed RSSI and estimated tag-to-tag interference model per tag-to-tag angle. Figure 4.6 illustrates the modeled tag-to-tag interference system using the estimated damping factors and the nature oscillator frequencies for the practical condition such as the hallway.

In addition, ζ and ω_0 are also shown a certain pattern over the degrees, θ, which is depicted in Figure 4.5 (a) and (b), which is consequently defined with following functions:

$$Z(\theta) = 0.753282 - 0.636235|sin\ (\theta)| \tag{4.17}$$

and,

$$O(\theta) = 0.244262 - 0.025933|sin\ (2\theta)| \tag{4.18}$$

where $0° \leq \theta \leq 90°$. The model equations adopt sine function with an absolute value. The fittest parameters of the function lead an appropriate modeling system to estimate RFID signal interference between tags in term of distance and angle. Simulation of tag-to-tag interfered RSSI with the modeling system defined above is depicted in Figure 4.7.

Table 4.2 Estimated the Most Fitted Fucntion of Interfered Backscattering Signal Strength and The Minimum Non-Interfered Tag-to-Tag Distance in the case of Anechoic Chamber

Tag-to-Tag Angle (θ)	Chamber			
	ζ	ω_0	$F(x_v^*)$	Δ^{steady}
0°	0.786297	0.249428	0.529608	25.29cm
30°	0.36254	0.207169	0.574676	49.94cm
60°	0.226901	0.236437	2.482239	65.92cm
90°	0.132043	0.239096	6.285539	105.02cm

Table 4.3 Estimated the Most Fitted Fucntion of Interfered Backscattering Signal Strength and The Minimum Non-Interfered Tag-to-Tag Distance in the case of Hallway

Tag-to-Tag Angle (θ)	Hallway			
	ζ	ω_0	$F(x_v^*)$	Δ^{steady}
0°	0.798051	0.306978	1.954990	22.24cm
30°	0.294757	0.217992	0.794796	56.68cm
60°	0.166609	0.234919	0.822919	86.64cm
90°	0.084468	0.234498	4.591508	161.45cm

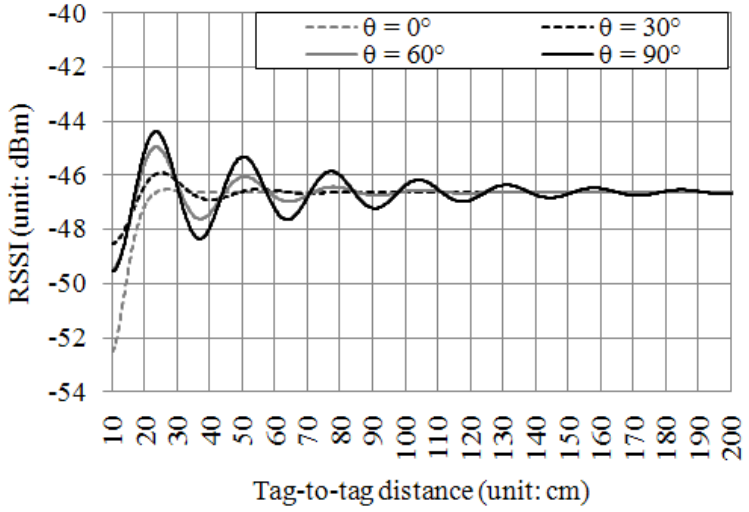

Figure 4.6 Estimations of Tag-to-tag interference using the proposed model

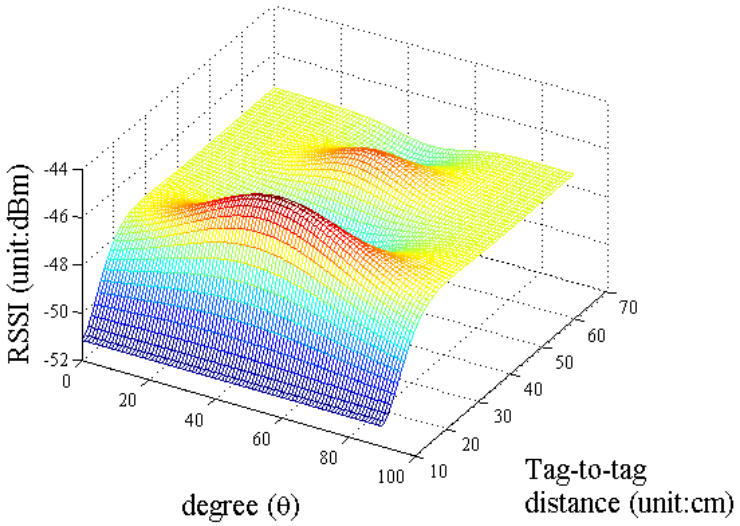

Figure 4.7 Interfered RSSI of a tag of interest by an adjacent tag, where the tag of interest locate 1m front of a reader antenna in the chamber

4.6 Localization using Model of Tag-to-Tag Interference

We propose a novel localization algorithm using observed level of tag-to-tag interference and its variation model. The proposed localization algorithm is applied to a smart shelf application, where the localization system estimates object locations in the shelving area.

4.6.1. System Model

Total *m* shelves are monitored by a single stationary mono-static reader antenna, and total *n* reference tags adhere to façades of shelves, and the localization system knows geographical 2D information of all of deployed reference tags. In this chapter, we assume there is a single carrier who causes target events such as target appearance, and disappearance within the interrogation range. we also assume there is no reference false positive interrogation. The localization system can recognize appearance and disappearance of the carrier using detection of a carrier introduced RF irregularity in the monitoring area. The carrier may bring out a single target per existence in the monitoring area.

Let R denote the set of unique IDs of deployed reference tags, C^i represent the set of IDs of read tags by i^{th} interrogation period. T represents the set of IDs of existing targets that have already had their locations estimated by previous positioning processes. Additionally, RS denotes the set of the means of measured RSSI values for each element of C. During the site-survey, the system estimates the damping factors, ζ and the undamped natural oscillator frequencies, ω_0, for expected tagged object' interference in the monitoring area.

4.6.2. Initial Stage

Initially, RS, C, and T are empty, and the ID of interrogation period, i, is initialized to 0. The localization system initiates the first interrogation cycle, and calculates rs_r^i for all identified tags. Each measured rs_r^i maps on each interrogated reference, *r*, where $r \in$ R. If there are false reference negative interrogations, the system assigns the minimum reader antenna sensitive power, P_{min}, to rs_r^i of the non-interrogated reference tags. The main reason of the use of P_{min}, is that the non-interrogation of the tags may cause by tag-to-tag interference of an incoming tagged target, and these tags should participate to the localization process. The minimum reader antenna sensitive power is estimated during the site-survey.

4.6.3. Localization Stage

After detection of the appearance and disappearance of carrier, the system triggers the location sensing process. The localization system operates the reader to detect newly incoming target ID. If the relative complement of the union set of R and T^{i-1} in C^i is empty, as non-detection of target ID, the system stores current RSSI information of references, RS^i, and, halts current localization process. If the system interrogates a new target ID, the system calculates possible target points using the modification of Equation (4.9). The variation of RSSI of a reference tag by the tag-to-tag interference is calculated as following:

$$V(\Delta,\theta) = A\frac{e^{-\zeta^\theta \omega_0^\theta(\Delta-\Delta_{min})}}{\sqrt{1-\zeta^{\theta^2}}}\cos\left(\omega_d^\theta(\Delta-\Delta_{min})-\psi^\theta\right) \qquad (4.19)$$

where θ denotes tag-to-tag angle ($0 \leq \theta < 360$), $\zeta^{\theta}$and $\omega_0^{\theta}$are the estimated damping factor and natural oscillator frequency by *Z(θ)*, and *O(θ)*, which are fitted functions of ζ and ω0, and estimated as Equation (4.17) and (4.18).

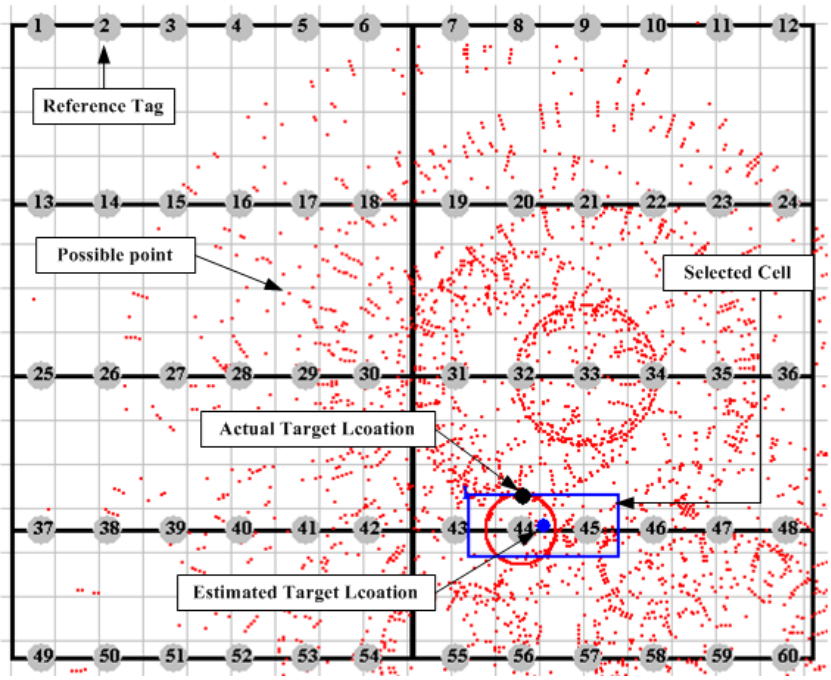

Figure 4.8 Example of estimation of target location using LMTI

In this section, we propose a novel Localization algorithm using Model of Tag-to-tag Interference (LMTI). Using Equation (4.19) and (4.14), and the observed RSSI variation, the system estimates the interference driven tag's 2D location. The tag-to-tag distance, *Δ*, is between $\Delta_{min}$and Δ_{steady}^{θ}, and if calculated *V(θ, Δ)* is greater than or equal to $rs_r^{i-1} - rs_r^{i,} - Th$, and less than or equal to $rs_r^{i-1} - rs_r^{i} + Th$, where Th denotes the threshold to decide interference of RSSI value and it is determined by the system, the expected 2D location, x_{exp} and y_{exp}, is estimated by follows:

$$x_{exp} = x_r \ + \Delta cos(\theta) \tag{4.20}$$

and,

$$y_{exp} = y_r \ + \Delta sin(\theta) \tag{4.21}$$

Figure 4.8 illustrates an example of estimation of target locations, when a single target enters into the 182cm × 152cm shelving area. Total 60 reference tags are deployed, and a target (as black spot in Figure 4.8) locates the shelving area. The system estimates total 4086 points (red spot) when θ interval is set 1°, and Δ interval is 1cm.

After the estimation of the expected target locations, the system finds the selected cell which is the most possible target area with a given cell width and height, such as the blue box in Figure 4.8. The selection of the most possible target cell is depended on the contained the number of expected target points, and the estimated target location (*ex*, *ey*) simply calculated by the coordination of the selected cell's center.

4.6.4. Evaluation of LMTI

In our experiment of Localization algorithm using Model of Tag-to-tag Interference (LMTI), two tiers of 91cm ×152cm wooden shelves are placed in an ordinary office environment, and a single circular polarized 6 dBi Poynting Patch-A0025 antenna covers the shelves, and its operating frequency is fixed to 915MHz and the RF transmission power is 30dBm as shown in Figure 4.9. And, the antenna is cabled to a SIRIT Infinity 510 RFID reader. Total 60 Alien Squiggle Gen 2 Passive tags are used for reference and 9 target objects attach the same type passive UHF RFID tag. Each of 60 reference tags is attached on each tier of the shelf. The target is 34cm × 14cm cardboard box, and each target tag is placed in the center of the front face of the box. The minimum antenna sensitive power, P_{min}, is given by -65.5dBm. In this evaluation, we compare the performance of LMTI with different types of target box contents, such as an empty box, and a printer cartridge within an aluminum foil bag. The selected cell

size in LMTI is set to 34cm × 14cm, which is the same size of target object, and we assume the initial condition of the under-damped second order system, *A*, is -6dB.

(a)

(b)

Figure 4.9 Setup of the object localization application. (a) The RFID reader and antenna (b) Actual target locations in the shelving area.

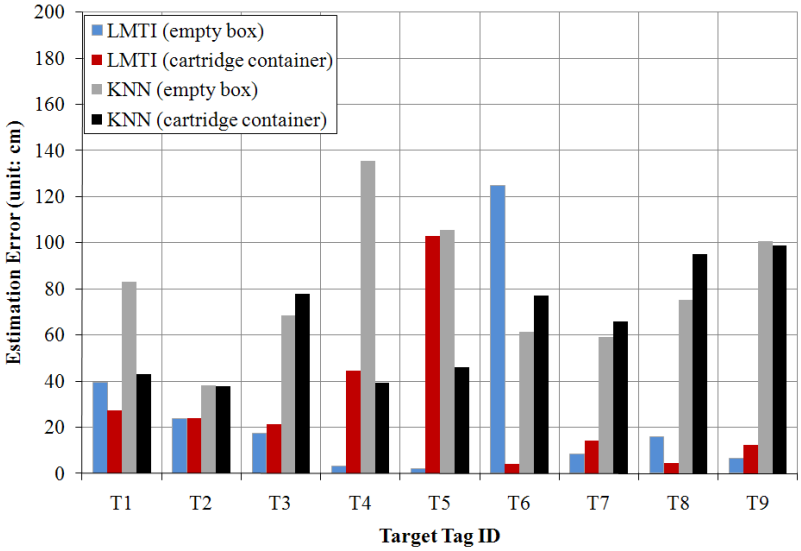

(a)

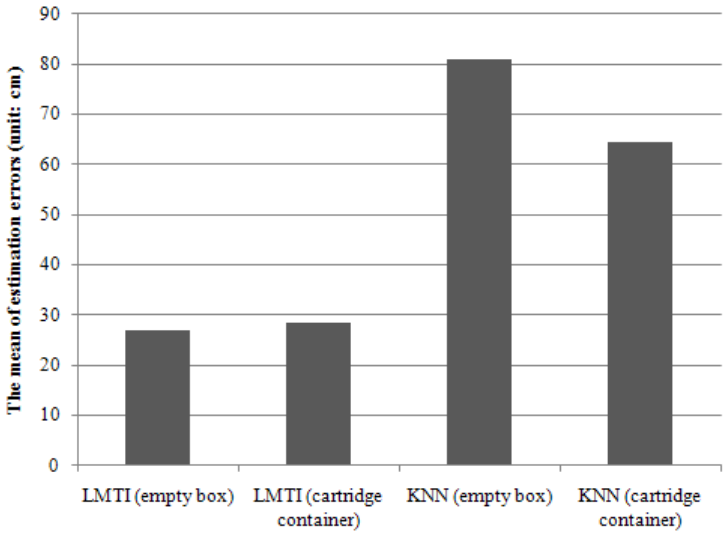

(b)

Figure 4.10 Performance of LMTI algorithm for static targets with comparison with the conventional KNN algorithm (k=5) under various contents of target. (a) Localization results of 9 targets within the shelving area (b) Means of 9 targets' estimation errors.

We carry a single target box per iteration, and a total of 9 targets are placed in the shelves as shown in Figure 4.9 (b). Figure 4.10 illustrates the estimation results of LMTI algorithm for the smart shelf application. In the case of empty target boxes, LMTI shows that the mean of

estimation errors for 9 targets is 26.86cm, and the standard deviation is 38.59cm. For a comparison, we estimate target locations using KNN algorithm [13], and k value is set to 5. According to the results, KNN shows an 80.81cm of mean estimation error and 29.32cm of standard deviation. The improvement of accuracy is over 200%. When each target contains a print cartridge within the metallic bag, the mean estimation error of LMTI is slightly increased to 28.33cm which is 127.7% accuracy improvement than KNN algorithm.

However, for better accurate localization, LMTI requires the analysis of degree of tag-to-tag interference for each expected tagged target object conditions, such as material and size. Because, the material of object and size can impact to the reference tag's performance, and eventually it can change the damping factor, the undamped natural oscillator frequency.

4.7 Conclusions

In passive UHF RFID systems, we presented of adjacent tag influences to another tag, and we defined the tag-to-tag interference problem. When two tags locate close each other, an adjacent tag influences other tags' IC impedance. And it causes excess increase or decrease of the backscattering communication budgets. According to our observation, tag-to-tag interference changes the reader received signal strength, such as 5.8dB of excess decrease and 2.5dB of increase, depended on the distance between two tags in the anechoic chamber compared with non-interfered RSSI. In this chapter, we presented a new model of backscattered signal strength for passive far-field UHF RFID system under tag-to-tag interference, and we presented a method to estimate variations of excess power volume by the interference depended on a tag-to-tag distance and angle using the second order under-damped system. We estimate the minimum non-interfered tag-to-tag distance. According to our results, the adjacent tag can influence the other tag within horizontally 22.24cm and vertically 161.45cm in the practical condition such as hallway. Additionally, we proposed a novel localization algorithm to estimate target object location using the presented Tag-to-tag Interference Model (LMTI). According to the empirical results, LMTI improves over 200% accuracy compared RSSI based KNN

algorithm when we implement with empty boxes, and 127% improvement with the print cartridge contained an aluminum foil bag.

CHAPTER 5

LOCALIZATION USING DETECTION OF TAG INTERFERENCE ON SMART SHELF

In this chapter, we present novel radio frequency identification (RFID) smart shelf that accurately locates tagged objects using standard passive UHF RFID tags. This standards based COTS approach provides significant advantages over custom HF RFID and other near-field RFID approaches including reduced tag costs, minimal infrastructure costs, and simple operation. In order to achieve accurate location sensing of objects sitting on the shelf, we utilize a novel localization algorithm that utilizes detected changes in a tag's readability to infer the presence of neighboring tags. According to our experimentation results, with a single RFID reader antenna for two wooden shelves of size 91cm ×152cm, our smart shelf system estimates 9 box-level object locations with an average error just 18.48cm, a 71% improvement in accuracy compared to the previously published KNN algorithm.

5.1 introduction

Automation of asset management is an important goal in many industries such as retail and pharmaceuticals [6], [19-21]. The major benefits of automated asset tracking and inventory control are reduction of labor, fast inventory counting and management, and high visibility of individual items. To improve automation, Radio Frequency Identification (RFID) technologies have been applied in several industries. Due to easy and fast identification of individual items of interest under non-line-of-sight conditions, RFID based asset management is being substituted for bar code technologies in factories, warehouses, and retail stores. In order to achieve higher performance of automating asset management, RFID smart shelves can be an essential part of streamlined supply chain operations to automatically identify and localize assets in the retail and storage spaces.

Near-field HF and near-field UHF RFID based smart shelf applications have been researched in [24], [60], [61]. In these applications, near-field antennas are placed inside each tier of the shelving typically covering the entire shelf area, RFID tagged objects within the tier can communicate using inductive coupling to the antenna located directly below the object. Inductive coupling communication is limited by physics and laws to a short range (typically less than 1 meter). Thus, multiple specially designed reader antennas are installed for a single shelf. Moreover, in the case of HF RFID based smart shelves [24], the typical communication range is less than 0.5 meter, and the tags are often significantly more expensive than the standard Electronic Product code (EPC) tags operating in the UHF frequency range [1]. The EPC tags are being used for a broad range of supply chain applications in many retail distribution operations.

In this paper, we present a far-field passive UHF EPC RFID smart shelf, shown in Figure 5.1, to maximize labor reduction and asset visibility in the supply chain. The following are the benefits of far-field passive UHF RFID based smart shelf, to overcome the drawbacks of the near-field RFID smart shelf.

1) **Simplicity**: Simple installation and maintenance of RFID smart shelf.
2) **Compatibility**: Can use an existing EPC based infrastructure.
3) **Scalability**: The smart shelf application can be easily expanded for large number of shelves of interest.
4) **Cost Efficiency**: Low cost for installation and maintenance to identify and localize objects on the shelf.

For implementation of the proposed far-field RFID smart shelf, a plurality of cheap passive UHF RFID tags are attached to an existing shelf and a single reader antenna monitors multiple shelves to identify and localize an inventory based on EPC infrastructures. Although the

far-field UHF RFID smart shelf application has latent advantages, few of far-field UHF RFID smart shelf applications have been researched due to a lack of accurate localization using passive UHF RFID tag. A precise and accurate localization of a tagged item can satisfy the requirement of item visibility, but, in practice, existing localization algorithms such as those proposed in [13] and, [62] for homogeneous passive UHF RFID systems potentially have problems with ambiguous mapping between geographical information and measured relative features such as the Received Signal Strength Indicator (RSSI) from deployed passive tag. Therefore, the accurate localization, which we focus on in this paper, is the main challenge of the far-field passive UHF RFID smart shelf application.

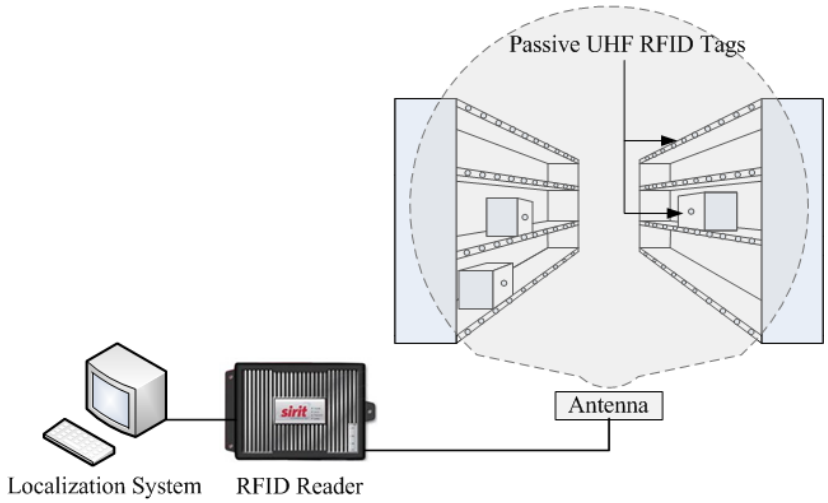

Figure 5.1 Smart Shelf system using far-field passive UHF RFID system

In this chapter, our contributions are: First, we present a novel Localization using Detection of Tag-Interference (LDTI) algorithm to achieve accurate estimation even if the monitoring space (as shelf) is covered by single reader antenna; Second, we implement and analyze an LDTI based far-field UHF RFID smart shelf with various target objects such as an empty box, a water contained box, and a metallic object contained box to show that our approach is realistic.

The remainder of this paper is organized as follows. We review related work in Section 5.2. In Section 5.3, we present our novel LDTI algorithm for location. We present our empirical evaluation of our LDTI algorithm in Section 5.4, and we draw the relevant conclusions in Section 5.5.

5.2 Related Work

In [24], the authors design an HF (13.56 MHz) RFID system based smart bookshelf with multi-loop antennas to interrogate items on the 90cm × 28cm tier and it achieves at least 95% identification rate. The HF RFID smart shelf provides highly reliable and accurate identification of tagged items that consist of metallic or liquid material. But, HF RFID smart shelves require high antenna density, have low read range, and are not compatible with UHF RFID tags. Thus, their use is limited to a narrow range of applications. In [60], and [61], the authors propose newly designed near-field reader and tag antennas for UHF item-level tagging systems. Like the HF RFID system, the near-field UHF RFID reader antenna must be placed in each tier of the shelf system, and it can cover only limited reading range. Under these circumstances, existing smart shelf schemes require a large number of RFID readers and reader antennas to cover a large monitoring space. However, the short interrogation range of the near-field HF and UHF reader antennas provides reasonably accurate and easy localization of items compared with basic far-field passive UHF RFID based smart shelf.

5.3 Localization using Detection of Tag Interference

We propose a novel deterministic localization algorithm using detection of tag interference to solve the major problem of far-field passive UHF RFID smart shelf, which is inaccurate object localization. The monitoring area is covered by a stationary monostatic single reader antenna. We assume there is a single carrier, such as a person, of a target object within a reader antenna's interrogation range. The going-in and out of the carrier is recognized by extra devices, such as IR sensors and Ultrasound sensors, which are placed on each end of possible path within the monitoring area. The carrier can bring a single object into the

monitoring area, and the carrier can generate a single event such as target appearance, disappearance or relocation per existence in the monitoring area. We assume there is no *reference false positive*. This means that a reference tag, which places out of the reader's monitoring area, would not be interrogated by irregular RF reflecting and scattering. In Figure 5.2, a flowchart represents the process of localization using detection of tag interference for far-field passive UHF RFID smart shelf.

5.3.1. Initial Stage

Consider a single RFID reader antenna that is able to read all tags on, or covers, a shelf of interest, and *n* reference tags deployed on a façade of the shelf (or shelves). An estimated target location by a localization system is constrained on a storage space on top of the shelf. Let R denote the set of unique IDs of known references within the antennas coverage area, C represent the set of IDs of read tags by the current interrogation cycle, and T represent the set of IDs of existing targets, that have already had their locations estimated by previous positioning processes. Additionally, RS denotes the set of the means of measured RSSI values for each element of C.

In an initial stage, RS, C, and T are empty. An initial interrogation cycle ID, *i*, is initialized to 0, and the ID is sequentially increased by each activation of the interrogation cycle. The localization system initiates the first interrogation cycle, and calculates rs_r^i for all interrogated tags.

During the initial stage, each measured rs_r^i maps on each interrogated reference, *r*, where $r \in R$. If the relative complement of C^i in R is not empty (as $R \setminus C^i \neq \emptyset$), there is a reference false negative as a reference tag, which is located in the monitoring area, is not interrogated. The reference false negative can happen frequently due to negligible backscattered strength from a susceptible passive RFID tag.

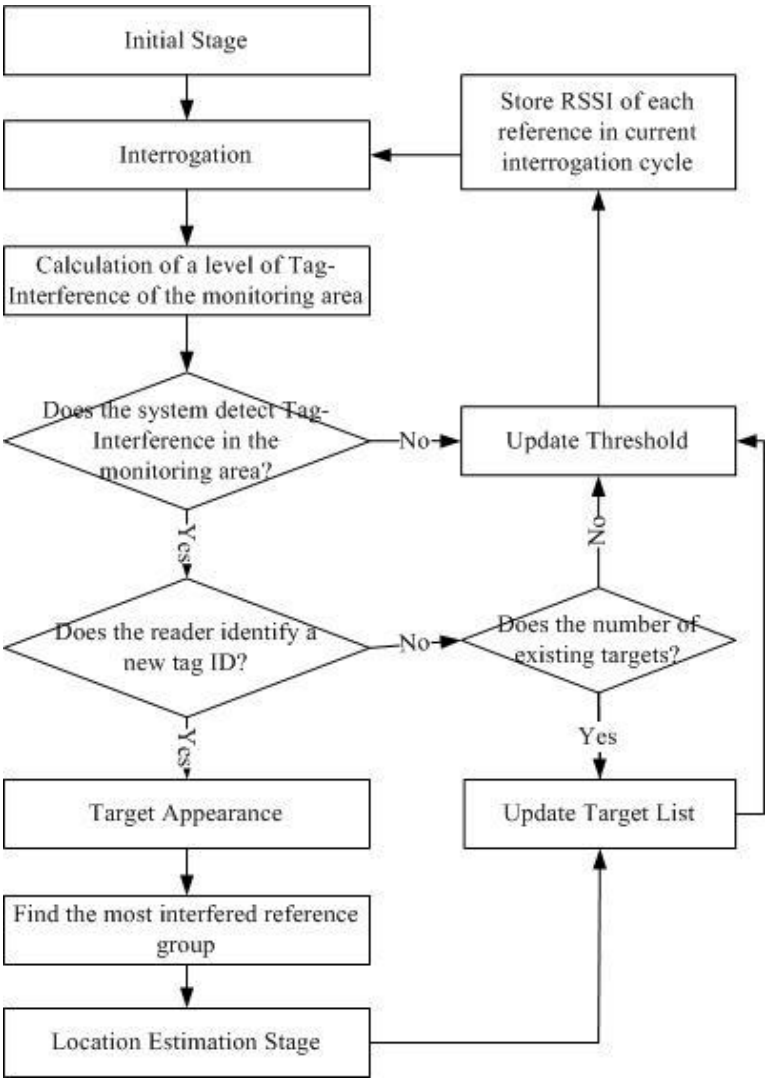

Figure 5.2 Flowchart of the localization using detection of tag interference for the far-field passive UHF RFID smart shelf application

In order to achieve accurate localization, the positioning system has to detect and handle the invisible reference tag, which might become visible due to interference of incoming target. Therefore, the system keeps maintaining the invisible reference information for target location sensing. Whenever the system detects an invisible reference, the system assigns the minimum reader antenna sensitive power, P_{min}, to rs^i for the invisible reference, where P_{min} is

measured during the site-survey. And then the ID of invisible reference is put in an invisible reference set, IR^i.

```
//C^i denotes the set of IDs of read tags by i^th interrogation cycle
//R the set of reference tags
//T^i denotes the set of IDs of existing targets in i^th interrogation cycle
//Th^i denotes the threshold
//E denotes RSSI differentiations between the current and previous
//interrogation cycles from a reference tag
//L^i denotes the level of Tag-Interference of the monitoring area in i^th
//interrogation cycle

IF (C^i \ (R∪T^i-1) ≠ ∅ and |C^i \ R| > |T^i-1| ) THEN
   IF (L^i > Th^i-1) THEN
   /* Detection of Target Appearance*/
      incomingTarget  =  C^i \ (R∪T^i-1)
      T^i = C^i \ R
      Th^i = Th^i-1
      Call ReferenceGrouping(incomingTarget )
   END IF
   ELSE IF (L^i ≤ Th^i-1 and IR^i = IR^i-1 ) THEN
   /* Target false positive */
      T^i = T^i-1
      Update Th^i
   END ELSE IF
ELSE IF (C^i \ (R∪T^i-1) = ∅ and C^i \ R = T^i-1 and L^i > Th^i-1) THEN
/* Detection of Target Relocation */
      relocatedTarget = Max (E_t^i: t∈ T^i-1)
      Disconnection(relocatedTarget's reference group, Reference Graph)
      Th^i = Th^i-1
      Call ReferenceGrouping(relocatedTarget )
END ELSE IF
ELSE IF(C^i \ (R∪T^i-1) = ∅ and |C^i \ R| < |T^i-1| and L^i > Th^i-1) THEN
/* Detection of Target Disappearance */
   T^i = C^i \ R
   Th^i = Th^i-1
END ELSE IF
```

Figure 5.3 Pseudocode of the detection of target driven events

5.3.2. Interference Detecting and Reference Grouping Stages

The localization system periodically triggers the interrogation process of the reader, and the reader identifies and collects tag IDs and RSSI values for the tags in a given interrogating duration. In order to avoid the RSSI influence by existence of the target carrier, the system

suspends the interrogation cycle until the carrier goes out. After an interrogation cycle, the system calculates each rs^i , and sets C^i with all of the identified tag IDs. For the reference false negative, RSSI information of the invisible reference tags is assigned to P_{min}.

As I discussed in Chapter 3 and 5, an appearance of new tag (incoming target tag) can influence the backscattered signal strength of existing tags (reference tags). Using this phenomenon, the system detects the tag interference on the map of reference tags, and selects useful reference tags, which might be the most interfered references by the target, to estimate target location. By contrast, the conventional RSSI based location systems [3], [15] select the reference tags using the minimum Euclidean distance between deployed reference and the target.

In an interference detecting stage, the positioning system monitors the interrogation area as the shelves, and it can perceive the target driven event from interfered reference tags. In Figure 5.3, pseudocode of decision of target driven events is described. For the detection of the tag-interference, the system restores RS^{i-1}, the sets of reference tag's RSSI in the previous interrogation cycle and calculates a level of Tag-Interference of the monitoring area, L, to compare with a threshold. L is calculated by the following:

$$L^i = \frac{1}{n}\sum_{r=1}^{n} E_r^i \tag{5.1}$$

where E is RSSI differentiations between the current *rs* and the previous *rs* for the reference and it is given by

$$E_r^i = \left| rs_r^i - rs_r^{i-1} \right| \tag{5.2}.$$

The threshold, *Th*, is maintained by the system. The threshold represents a typical RSSI variation from environmental factors such as temperature, humidity and background noise. The system updates the threshold after each interrogation cycle except the cycle with detection of tag-interference by targets.

$$Th^{i} = \begin{cases} L^{i} & \text{If } i=1 \\ ((1-\lambda)\times L^{i}) + (\lambda \times Th^{i-1}) & \text{If } i>1 \text{ and } L^{i} \le Th^{i-1} \\ Th^{i-1} & \text{If } L^{i} > Th^{i-1} \end{cases} \quad (5.3)$$

where $\lambda \in (0,1)$ is a forgetting factor for updating the threshold. The value of forgetting factor is determined in a site survey. In the site-survey, the system monitors the idle interrogation area during enough interrogation cycles. If there are frequent RSSI changes from the deployed reference tags, the system assigns lower λ, which is close to 0, to give more weight to the latest RSSI variation by the environmental factors.

5.3.2.1 Target Appearance

If the calculated level of current RSSI variation of the monitoring area is greater than the threshold (as $L^{i} > Th^{i-1}$), the system perceives the change of monitoring space as a target appearance. Otherwise, the system satisfies $L^{i} \le Th^{i-1}$ and the relative complement of the union set of R and T^{i-1} in C^{i} is empty, the system stores current RSSI information of references, RS^{i}, due to non-detection of changing, and updates the threshold value using Equation (5.3). However, it is possible that L^{i} is smaller than the threshold even if the reader identified a new target ID. This case can be related on target false positive (known as the ghost tag problem [63]), which the reader identifies erroneously as a non-existent tag within the monitoring area, and it can be detected, when the positioning system satisfies following conditions: non-empty of the relative complement of the union set of R and T^{i-1} in C^{i}, unchanged invisible reference set as

$IR^i = IR^{i-1}$, and $L^i \leq Th^{i-1}$, and If the system detects the newly identified tag is false positive case, then it ignores the fault target ID as $T^i = T^{i-1}$.

The system can recognize an appearance of a target, when the relative complement of the union set of R and T^{i-1} in C^i is not empty, and the number of interrogated targets is increased, and the $C^i \setminus R \neq T^{i-1}$, and the calculated L^i is grater the threshold. In the case of detecting target appearance, the system steps to a reference grouping stage.

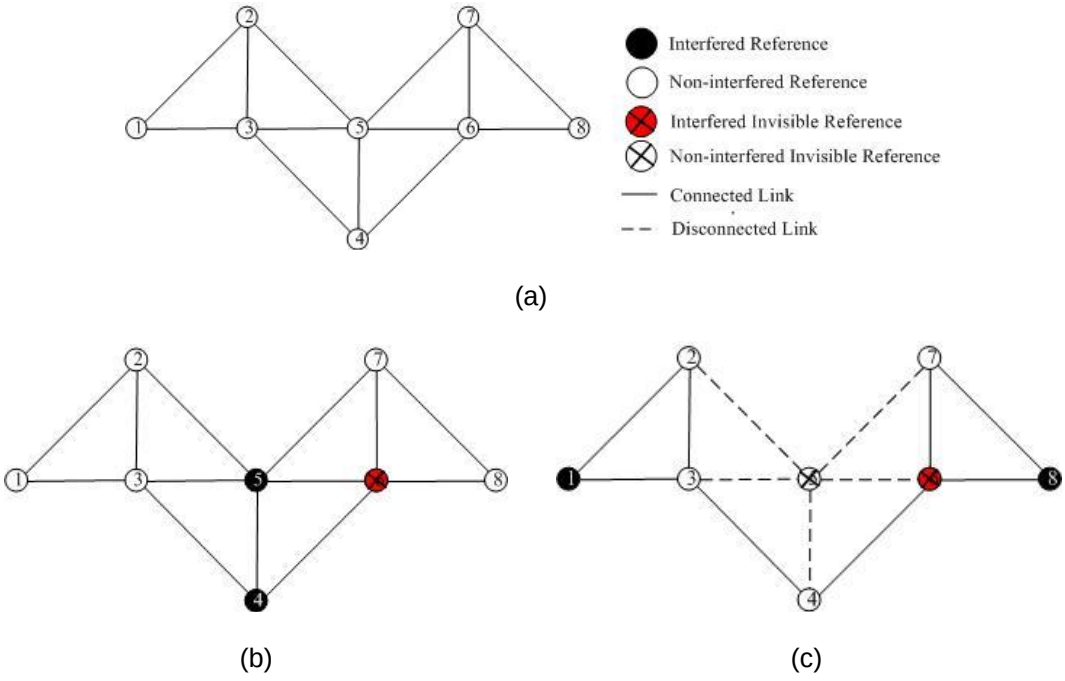

Figure 5.4 A reference graph with consideration of an invisible reference tag. (a) Initial graph. (b) Case of interfered invisible references. (c) Case of Non-interfered invisible references.

In the reference grouping stage, the system selects the most useful reference tags for location sensing of the incoming target. For the selection of reference tags for the target, the system compares E^i for each reference, and selects the most interfered references as $E_r^i >> Th^i$. However, reference selection using only E^i value potentially brings about significant localization error. For example, a typical positioning algorithm such as K-Nearest Neighbor (KNN) algorithm in RSSI based localization systems [8], [13] choose the k reference tags which have the most

similar RSSI values (as the minimum Euclidean distance) as the target, but there is high chance that the tags, which locate at a long distance, report similar RSSI in practice. If the system picks spatially non-adjacent tags for the nearest neighbors, the accuracy of localization is substantially decreased. In order to achieve accurate localization, we propose a reference selection gives consideration to spatial relations between each reference. The main idea of our proposed reference selection algorithm is that the system groups reference tags among the most interfered region by the target object. Instead of selection of an individual reference tag within the monitoring space in conventional positioning algorithm, the proposed algorithm selects a group of references and the group members are spatially close. Even if a singular reference experienced large degree of interference with non-interfered adjacent neighbor references, the reference cannot be accepted from a selected group.

```
//S denotes the seleteced group
//g denotes the size of group
/* Initiation*/
S=∅
MaxSumE=0
CurrentSumE = 0

/*Find the most interfered reference group */
FOR {r∈R: r has connected neighbor }
  Sort r's neighbor list by neighbor's E
  CurrentSumE = E_r + Summation of top (g-1) neighbors' E
  IF (MaxSumE<CurrentSumE) THEN
    S = r ∪ Top (g-1) neighbors of r
    MaxSumE = CurrentSumE
  END IF
END FOR
```

Figure 5.5 Pseudocode of the most interfered reference group finding algorithm

For selection of the most interfered group, I employ graph theory. A reference graph is generated in a reference grouping stage, and each reference tag (as node) is initially connected

to one hop distance tags in the graph as shown in Figure 5.4 (a). A selected group has to satisfy the following condition to keep the spatial relation between selected reference tags in the reference graph:

Condition 5.1: In a group, at least one node has to be connected to all of the other nodes in one hop distance in a given group size *g*, where g is greater than or equal to 1.

If a reference tag is in the invisible condition in the current i^{th} interrogation cycle, the system checks the invisible reference tag's E^i to decide a participation of the invisible reference in group selection. Because the system assigned P_{min} to rs^i of invisible reference, an interfered invisible reference tag, by the incoming target, satisfies $E^i > 0$, and it keeps the connections to its neighbors as shown in Figure 5.4 (b). If E^i of the invisible reference is zero, the system assumes that the invisible reference node is not influenced by the target, and it is disconnected from all of one hop distance neighbor nodes in the graph as shown in Figure 5.4 (c). Finally, as described in Figure 5.5, the system selects a single group, S_t where t represent the event driven target ID, which has the maximum sum of each group member's E^i, under satisfaction of the condition 1.

5.3.2.2 Target Relocation

If the system detects reference interference with the same interrogated target tags as the previous cycle, the system determines one of existing targets is relocated within the interrogation area. In the target relocation event, first, the system finds the relocated target ID using measured RSSIs of existing targets. The system compares each existing target's current and previous RSSI values, because the relocated target RSSI value can be affected by change of spatial conditions between the target and the RFID reader antenna. Among the existing targets, the system determines the possibly relocated target which has the largest altered RSSI.

When the target location is changed, the positioning system captures two major interfered sections where include the original target position and the relocated target position along the shelves. The each member of reference group of the selected target's original position does not participate in the reference grouping stage for the relocated target localization. The positioning system disconnects each group member of relocated target from the member's one hop distance neighbor tags in the reference graph. And then, the system triggers reference grouping stage for the relocated target to select the most interfered reference tag group.

5.3.2.3 Target Disappearance

The system determines the target is taken out from the monitoring area, when the system detects reference interference as $L^i > Th^{i-1}$ and the number of current interrogated target tags is decreased. In the case of target disappearance, the system updates T^i to count out the out-going target, and releases the target corresponding selected reference group information, S_t. And then, the system stores RS^i, but the threshold is not updated relative on Equation (5.3).

5.3.3 Location Estimation Stage

Using the selected references, s, where $s \in S_t^i$, which locate the spatially known positions, the system estimates the target's location on the shelf of interest. In the estimation process, priority of reference tag is dependent on the degree of encountered impact (as *E*) by the target tag. The priority, *p*, can be calculated as follows:

$$p_s^i = \frac{E_s^i}{\sum_{j=1}^{g} E_j^i} \tag{5.4}$$

And, similar to [3], the estimated target location (ex, ey) is calculated by

$$(ex, ey) = \sum_{s=1}^{g} p_s^i (x_s, y_s) \tag{5.5}$$

where x_s and y_s denotes the actual coordinated of the selected reference, s.

(a) (b) (c)

(d)

Figure 5.6 Setup of the smart shelf application. (a) Target tag position on 34cm × 14cm box level item. (b) Box contains a print cartridge, which wrapped by an aluminum foil bag. (c) Box contains10 water bottles. (d) Two of 91cm ×152cm wooden shelves which tagged 60 reference tags. A single reader antenna covers the shelves.

5.4 Practical Evaluations

5.4.1 System Setup

In our experiment of Localization using Detection of Tag-Interference (LDTI), two tiers of 91cm ×152cm wooden shelves are placed in an ordinary office environment, and a single reader antenna covers the shelves. I have used a SIRIT Infinity 510 RFID reader. Its operating

frequency is fixed to 915MHz and the RF transmission power is 30dBm. A single circular polarized 6 dBi Poynting Patch-A0025 antenna is cabled to the reader. Figure 5.6 (d) and 5.7 (a) illustrate the exact position of the single reader antenna. Alien Squiggle Gen 2 Passive tag is used for reference and target tags.

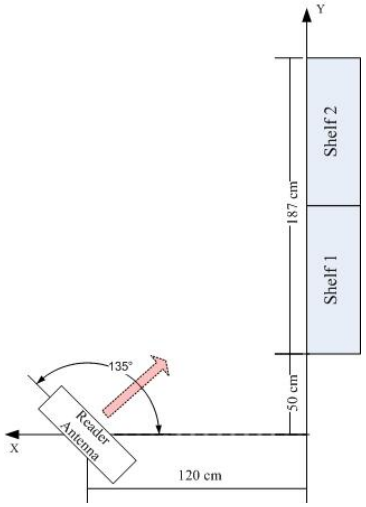

(a)

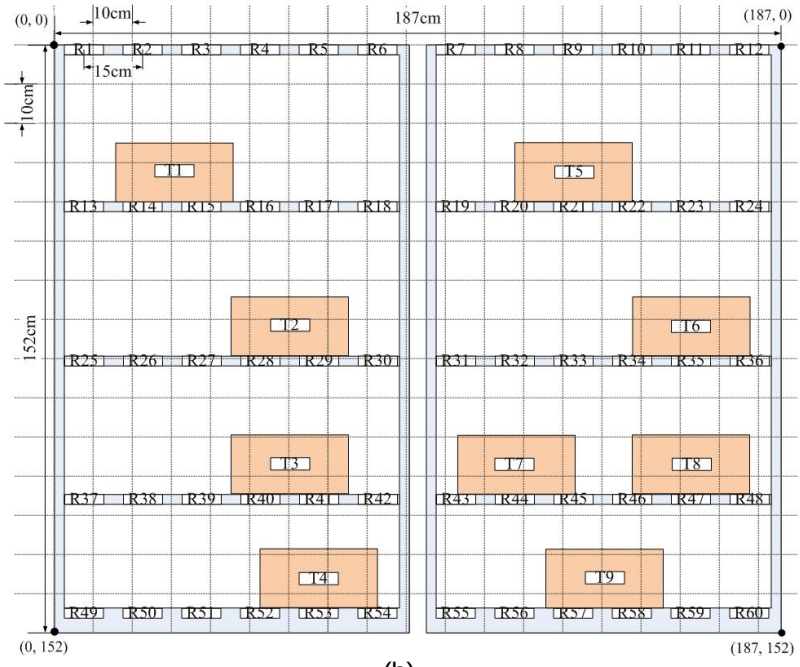

(b)

Figure 5.7 Reader antenna location and target object locations in the shelving area. (a) Reader antenna position. (f)Actual target locations in 2D space of the shelves.

Each of 60 reference tags is stuck on cardboard and is tagged on each tier of the shelf. The target is 34cm × 14cm cardboard box, and each target tag is placed in the center of the front face of the box as shown in Figure 5.6 (a). Depending on the evaluation case, the target boxes contain various contents such as print cartridge in an aluminum foil bag, and 10 water bottles as shown in Figure 5.6 (b) and (c). Duration of each interrogation cycle is 60 seconds to gather enough RSSI samples. Forgetting factor, λ, is set to 0.8, and the minimum antenna sensitive power, P_{min}, is given by -65.5dBm.

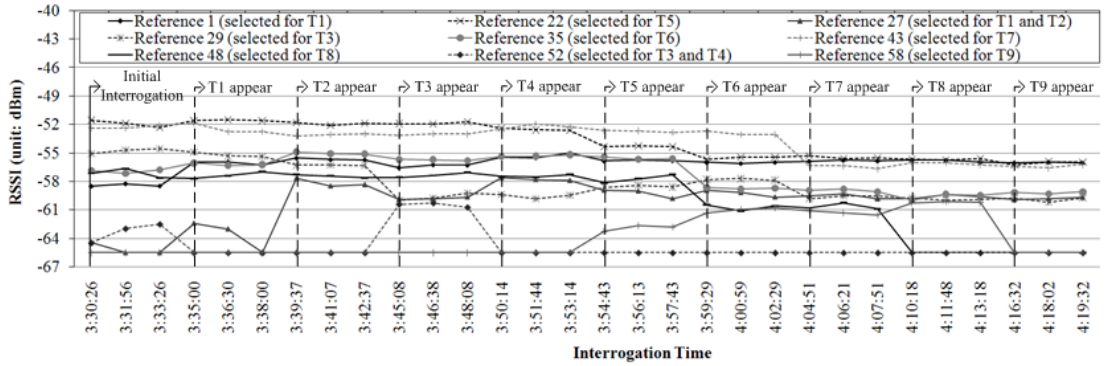

Figure 5.8 Example of fluctuations of RSSI values from remarkably interfered references among the deployed 60 reference tags

5.4.2 Detection of Tag-Interference

In the LDTI, the system detects tag-interference and selects the most interfered reference group using the fluctuation of RSSI of each reference tag to estimate RSSI differentiation between the current and the previous interrogations. Figure 5.8 illustrates fluctuations of RSSI values from remarkable references among the deployed 60 reference tags. During 50 minutes, we measure backscattered signal strengths for all references and a total of 9 targets that contain an ink cartridge wrapped in aluminum foil in a cardboard box and are located on the shelves as shown in Figure 5.7 (b). As shown in the fluctuation of reference 1, the appearance of target 1 (denoted as T1), its RSSI is increased from -58.24dBm to -55.93dBm due to interference from the target. When T2 arrives to the shelf, the reference 27,

which was an invisible tag in the previous interrogation cycle, turns into a visible tag with 7.84dB power increase from the given minimum antenna sensitive power, P_{min}. In the case of reference 52, T1 interferes to make it invisible, and the existence of T3 makes reference 52 visible. Then, reference 52 experiences power loss due to the appearance of T4. Additionally, with the forgetting factor 0.8, the threshold is calculated to be 0.2865dB after the last interrogation cycle.

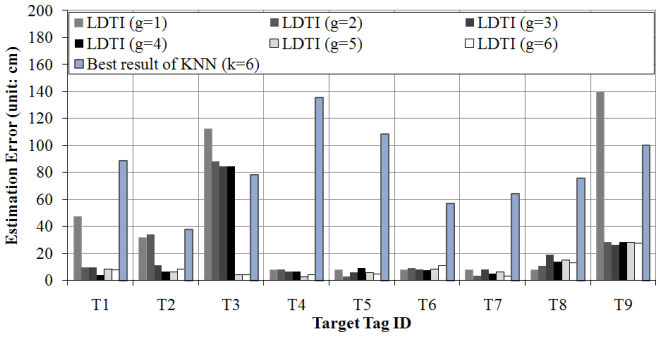

(a)

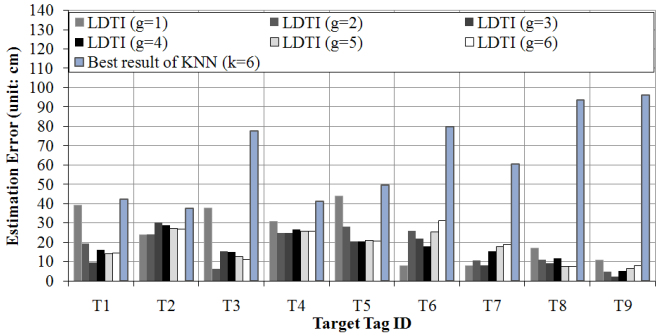

(b)

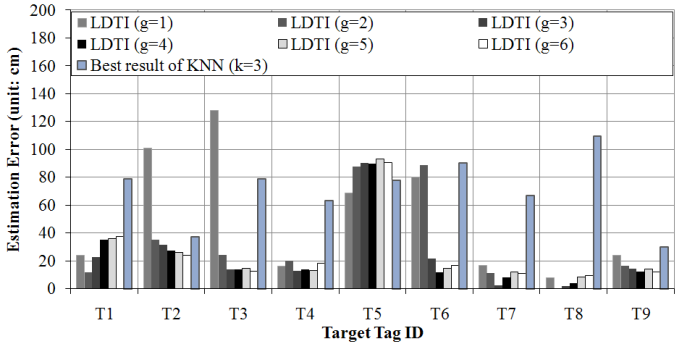

(c)

Figure 5.9 Localization results for static targets with comparison with the conventional KNN algorithm under various contents of target. (a) Case of empty box localization. (b) Case of print cartridge contained target boxes. (c) Case of water bottles contained target boxes.

5.4.3 Evaluation of LDTI

We carry a single target box per iteration, and a total of 9 targets are placed in the shelves as shown in Figure 5.7 (a). The localization system estimates target position whenever the system detects an incoming target. Figure 5.9 shows the empirical results of localization for 3 different contents of 9 targets under various group sizes. In the case of empty target boxes, LDTI shows that the mean of estimation errors for 9 targets is 9.48cm, and the standard deviation is 7.49cm when the group size g is 6. Comparatively, KNN (k=6) shows an 80.35cm of mean estimation error and 29.82cm of standard deviation. When each target contains a print cartridge, the minimum mean estimation error of LTDI for 9 targets is 15.81cm (standard deviation = 9.21cm) where g is 3. In the case of water container, the minimum mean estimation error of LTDI is 23.62cm (standard deviation =26.79cm) where g is 3. According to the results, the large group size improves the performance of localization as shown in Figure 5.10. On the contrary, k value of KNN algorithm does not affect the performance in practical conditions such as cartridge or water bottle contained targets.

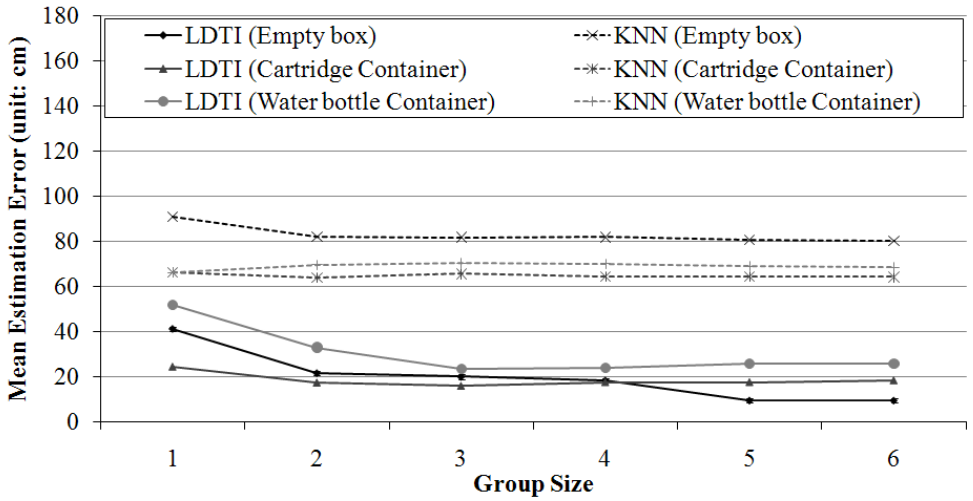

Figure 5.10 Means of 9 targets' estimation errors under various group sizes. For KNN, the group size represents k value.

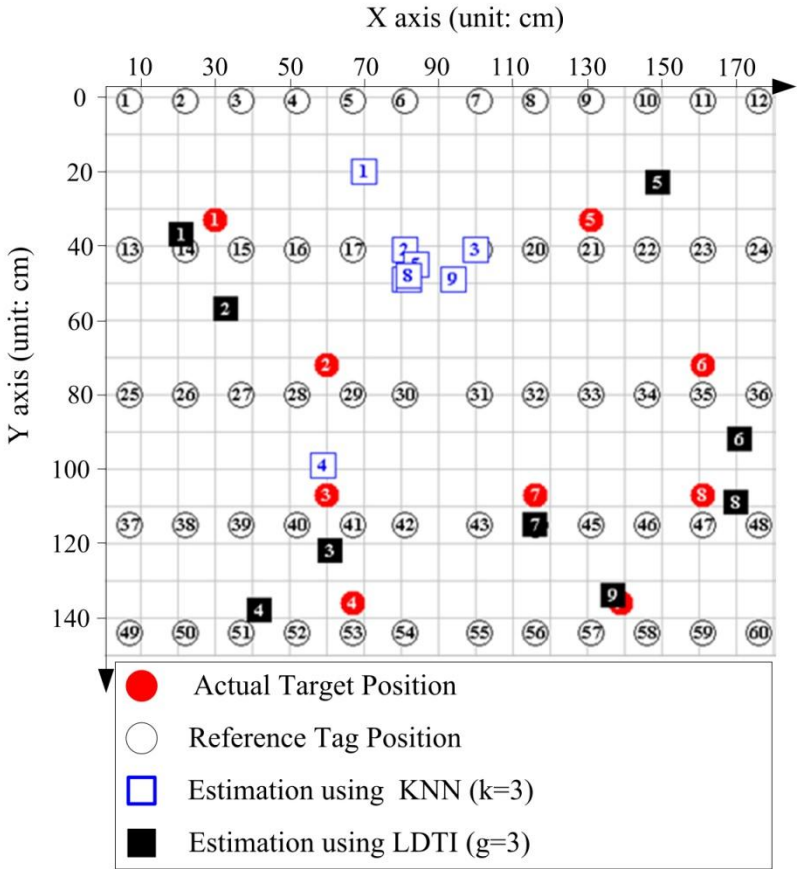

Figure 5.11 Estimation results of 9 targets using LDTI and KNN on 2D grid map of monitoring shelf space. g and k are 3, and the target box contains a print cartridge. Each grid size is uniformly 10cm × 10cm.

When the target box contains cartridge with the aluminum foil bag, the target tag backscatters stronger signal due to high volume of reflected power by the aluminum foil bag. According to the empirical results, the mean of 9 cartridge contained target RSSI values is -51.4224dBm (standard deviation = 2.48) and, comparatively, the means of empty box and water contained targets are -54.5654dBm (standard deviation = 4.26) and -55.4847dBm (standard deviation = 2.62). Since the increased RSSI from the cartridge contained target, KNN algorithm selects the nearest neighbors, which have strongest RSSI values as reference 18, 19, and 20, among the reference tags, and this selection brings inaccurate localization results as shown in Figure 5.11. When k is 3, the unrealistic estimation results position near the strongest reference

tags (as the reference 18 and 19). On the other hand, because LDTI selects reference tags, which mostly interfered by incoming target, the estimation results are highly accurate and robust as the maximum 30.33cm and the minimum 2.17cm errors.

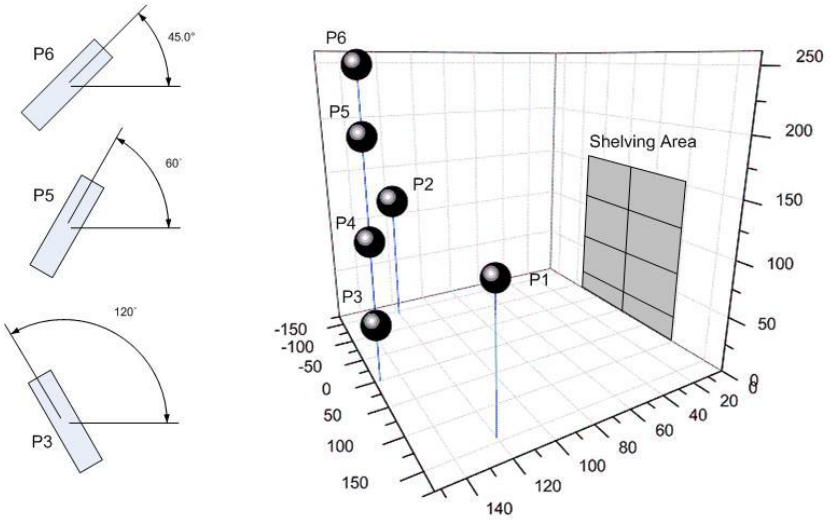

(a)

(b)

Figure 5.12 LDTI performances with 6 different reader antenna positions. (a) Position of the reader antenna. (b) The mean of estimation errors of 9 targets (cartridge container) per antenna position (g=3)

Moreover, Figure 5.12 shows the localization results with 6 different reader antenna locations as shown in Figure 5.12 (a). The localization system estimate the printer cartridge contained target locations Figure 5.12 (b). According to the empirical results, the LDTI localization system shows the best performance, where the reader antenna locates 1.5m from the shelving area with less RF reflection by the ground as the position 3.

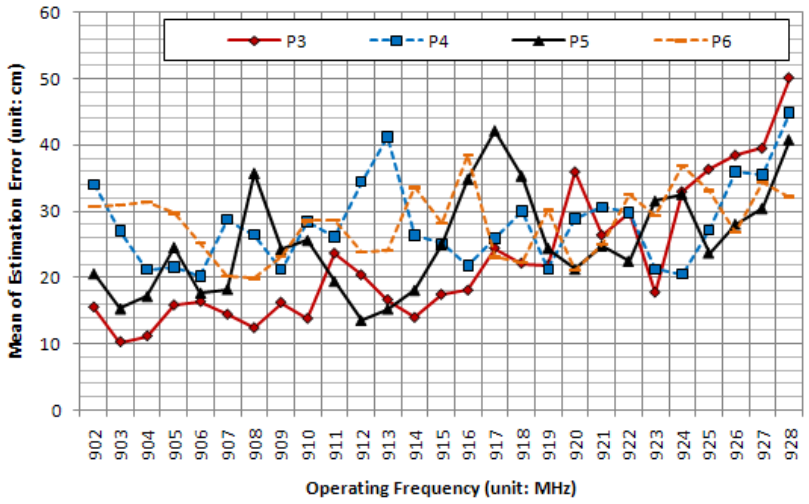

(a)

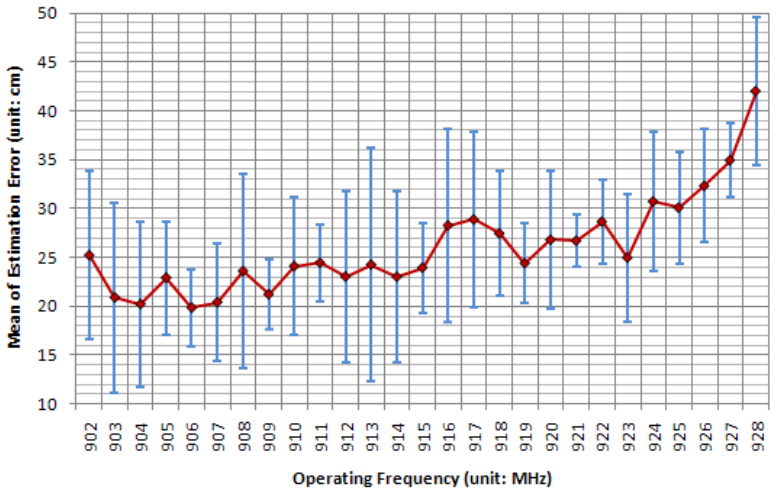

(b)

Figure 5.13 LDTI performances under various reader operating frequencies. (a) Localization results for P3, P4, P5, and P6 in Figure 5.12 (a) with various operating frequencies. (b) Mean of estimation errors and the standard deviations of the various antenna locations.

In Figure 5.13, we analyze LDTI performance under various reader operating frequencies between 902MHz and 928MHz. According to the results, the accuracy of localization is highly depended on the reader operating frequency. Moreover, when the system uses lower frequency such as 906MHz, the system provides more accurate location sensing for the targets. As shown in Figure 3.8 (Non-interfered case), the squiggle passive UHF RFID tag shows better performances under lower frequency range than higher range in the Federal Communications Commission (FCC) ISM band in Unite State, and this characteristic also affects to LDTI performance where the distributed reference tags and target tags are uniformly the squiggle passive UHF RFID tag.

Figure 5.14 shows the localization results of the relocated targets such as T1 and T2. T1's location is changed to the top of T3, and T2 is relocated to next to T6 as shown in Figure 7 (f). Using LDTI, the means of estimation errors for relocated T1 and T2 are 14.98cm and 16.541cm when the group size g is 6.

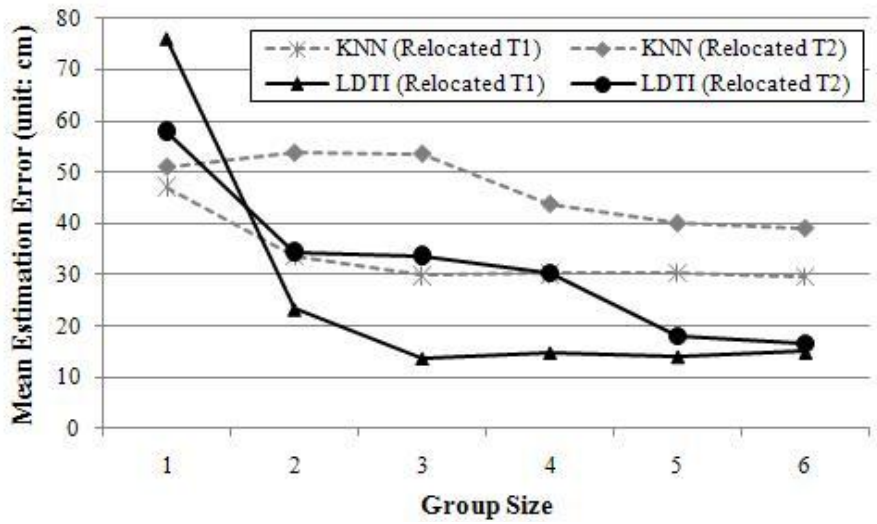

Figure 5.14 Localization results for relocated targets which contain the cartridge

5.5 Conclusions

In this chapter, we present a far-field passive UHF RFID smart shelf to achieve simplicity, compatibility, scalability, and cost efficiency for asset tracking and localization. To tackle the major challenge of lack of accurate localization in far-field passive UHF RFID systems, we present the Localization using Detection of Tag Interference (LDTI) algorithm. Table 5.1 summarizes the benefits of the LDTI algorithm compared to previously published approaches. The LDTI localization system detects the tag interference on the map of reference tags to estimate target location. To avoid selection of spatially non-adjacent reference tags, we also present the most interfered reference group finding algorithm, which considers spatial relations between reference tags. As summarized in Table 5.2, LDTI performs average 9.48cm estimation error for 9 empty cardboard boxes, and average 18.31cm estimation error for 9 print cartridge containers, which is a 71% accuracy improvement compared the KNN algorithm.

Table 5.1 Comparison of Smart Shelf Schemes

Smart Shelf Scheme	LDTI	Qing et al [11]	Choi et al [12]	Medeiros et al [13]
Frequency Band	UHF	HF	UHF	UHF
Communication Type	Far-field	Near-field	Near-field	Near-field
Number of installed Antennas per shelf	Single	Many	Many	Many
Location Sensing	Detection of tag interference	Interrogated zone	Interrogated zone	Interrogated zone
Reference Tag	Yes	No	No	No
Simplicity for Installation	High	Low	Low	Low
Compatibility for EPC infrastructure	High	Low	Medium	Medium

Table 5.2 Summary of Performance of LDTI

		Mean Esitimation Error	Max Esimtation Error	Min Estimation Error	Improvement by mean
KNN (k = 6, 9 targets, and 60 references)	Empty Box	80.35cm	135.65cm	37.94cm	
	Cartridge	64.29cm	96.23cm	37.72cm	
	Water bottle	68.45cm	104.47cm	36.54cm	
LDTI (g = 6, 9targets, and 60 references)	Empty Box	9.48cm	27.45cm	4.46cm	88.20%
	Cartridge	18.31cm	31.39cm	7.73cm	71.51%
	Water bottle	25.80cm	90.76cm	9.60cm	62.30%

CHAPTER 6

EFFICIENT AND ROBUST OBJECT LOCALIZATION USING PASSIVE RFID AND COMPUTER VISION INTEGRATION ON SMART SHELF

Location sensing of physical objects is critical in many applications. Passive UHF Radio Frequency Identification (RFID) technique provides an efficient solution because of its low cost for installation and easy identification of the tagged objects, and it has potential to localize the objects of interest. However, in practice, RFID based localization inherently involves ambiguous mapping between a physical location and a measured value such as RSSI, leading to significant decrease of accuracy of localization results. In order to achieve accurate and robust object localization, we suggest sensor fusion such as integration of passive far-field UHF RFID and computer vision to overcome the high false negative reference tag reading conditions. According to the experimentation results, maximally 620% increased accuracy compared with LDTI in high false negative reference reading condition, and 555% decreased computation time compared with homogeneous vision based localization in low false negative reference reading condition.

6.1 Introduction

In a smart environment, real time spatial information is fundamental and critical issue. It is preliminary requirement for extended functionality, and it provides efficient management of objects of interest. For example, in an asset management system, the system achieves maximized automation of inventory management using stored inventory real time spatial information. The major benefits of automated asset tracking and inventory control are reduction of labor, fast inventory management, and high visibility of individual items.

For the object localization, many technology based location sensing techniques such as using GPS [16], ultra-sound [17], WLAN [18], and UWB [18] utilize actual communication for

positioning after at long range. GPS is not suitable in an indoor situation because signals from satellites are blocked by building structure. For indoor environments, WLAN, and UWB based localization systems have been researched. However, for higher accuracy, these systems are expensive to implement in large scale object deployment such as inventory tracking in warehousing scenario. Moreover, if the signal transmitter and receiver run with built-in power sources, the maintenance costs are increased to replace the power source.

To improve automation in dense object deployments, passive UHF Radio Frequency Identification (RFID) technologies have been applied recently to these industries. Due to easy and fast identification of individual items of interest under non-line-of-sight conditions, RFID based asset management is being substituted for the bar code technology in factories, warehouse, and retailers.

In order to achieve higher performance of automating asset management, RFID smart shelves can be an essential part of streamlined supply chain operations to automatically identify and localize assets in the retail and storage spaces. However, because the passive far-field UHF RFID suffers easily influenced backscattering communication by circumstance factors, and differences between theoretical and practical performance of the passive UHF RFID systems, it is difficult to estimate accurate position of the tagged objects using the typical location sensing techniques with the use of stationary reader and its antenna in the smart shelf applications.

Computer vision based object localization [65], [66] provides higher accurate detection and estimation of object location than RF device based localization. But, homogeneous vision based localization system has to solve the identification of detected object. Additionally, the system suffers high computation overload and processing time, and requirements of huge storage space for the captured multimedia data.

In this chapter, we present a far-field passive UHF EPC RFID smart shelf with computer vision aid, as shown in Figure 6.1, to maximize labor reduction and asset visibility in the supply

chain. The following are the advantages of the passive UHF RFID and vision integrated smart shelf.

1) **Simplicity**: Simple installation and maintenance of RFID smart shelf.
2) **Compatibility**: The use of existing EPC based infrastructure.
3) **Scalability**: The smart shelf application can be easily expanded for large number of shelves of interest.
4) **Cost Efficiency**: Low cost for installation and maintenance to identify and localize objects on the shelf.
5) **Object Recognition**: Minimizing effort to identify uniform objects on the shelf.
6) **Accuracy**: Can estimate accurate object location on the shelf.
7) **Robustness**: Accurate localization results with less number of interrogated reference tags

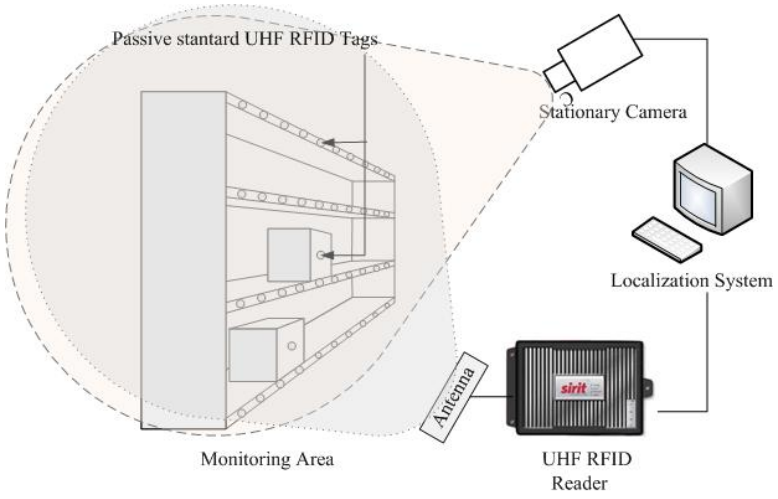

Figure 6.1 Smart Shelf system using far-field passive UHF RFID and Vision systems

In this chapter, our contribution is that we propose a novel and simple computer vision and passive UHF RFID integrated localization, and evaluate it with detail empirical results.

The rest of this chapter is organized as follows: In Section 6.2, we summarize the challenge of passive far-field UHF RFID smart shelf. In Section 6.3, we suggest robust heterogeneous localization technique as integration between passive UHF RFID and computer vision to overcome false negative reference tag reading problem. In Section 6.4, the performances of the proposed localization technique are described. we present our conclusions in Section 6.5.

6.2 Challenges on the Passive Far-Field UHF RIFD Smart Shelf

Passive far-field UHF RFID technologies have operated its primary goals such as interrogating and identifying tagged objects in many real applications. However, passive far-field UHF RFID system cannot localize the tagged objects accurately, because potential measured factors of RFID system, such as the received signal strength (RSSI), and direction of signal arrival (DOA), can be influenced by environmental conditions such as multipath fading, RF reflection by surrounding, the number of adjacent tags, the material of tagged object, and reader antenna location. Thus, the most of smart shelf applications adopt custom HF RFID and other near-field UHF RFID approaches. In these applications, multiple specially designed reader antennas are placed inside each tier of the shelves, and RFID tagged objects within the tier can communicate using inductive coupling to the antenna with very limited communication range. Moreover, in the case of HF RFID based smart shelves, cost of HF RFID tag is typically significantly higher than the standard Electronic Product code (EPC) tags operating in the UHF frequency range [1].

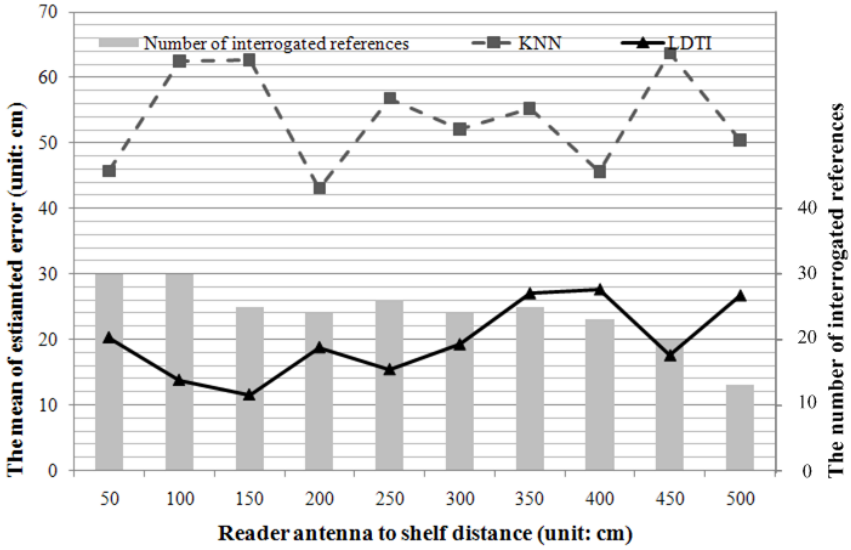

Figure 6.2 Performance evaluation of LDTI algorithms under various reader antenna to shelf distances and the number of interrogated reference tags. In case of KNN based localization, k value is set to 6.

In chapter 5 and 6, the homogeneous passive far-field UHF RFID based smart shows reliable and accurate object localizing results to compare RSSI based KNN algorithm as shown in Figure 6.2. However, depending on the physical condition of the stationary reader antenna, such as distance between the antenna and the shelf, the performance of LDTI based RFID smart shelf is various. For example, when a wooden 91cm × 152 cm single shelf is monitored by a single circular polarized 6 dBi Poynting Patch-A0025 antenna which is cabled to a SIRIT Infinity 510 RFID reader, and total 30 Alien Squiggle Gen 2 Passive tags adhere to façade of the shelf. The reader antenna locates at 90 degree and at a height of 100 cm from the ground in an ordinary office environment. And, the reader antenna to shelf distance is vary from 50cm to 500cm with 50cm interval. And total 8 tagged target objects are placed in the shelving area one by one. And, the system estimates the target location, when the target enters the monitoring area. According to the empirical results, the mean of estimated errors is 11.54cm with 83.3% of false negative reference interrogation (FNR) rate, when the antenna to shelf distance is 150cm. But if the distance is increased, FNR rate is increased as less number of references are

identified, and the estimation error also increased. In the worst case (antenna to shelf distance=500cm), FNR rate is 43.33% and the mean of estimation error is 26.68cm.

6.3 Vision and Passive UHF RFID Integrated Localization

In this section, we present a novel integrated Vision and passive UHF RFID Localization (VRL) algorithm for the smart shelf application. High probability of false negative tag reading is an inherent problem of the passive RFID, when RFID reader antenna places with further distance from tag. Under high false negative reference reading environments, the localization system experiences non-identification of a large number of reference tags, and it might substantially decrease accuracy of localization results. In this section, given single UHF RFID reader, its antenna, and single camera, a localization system estimates an accurate location of object of interest to overcome high false negative reference readings within a given monitoring area, instead of increase the number of reader and antennas.

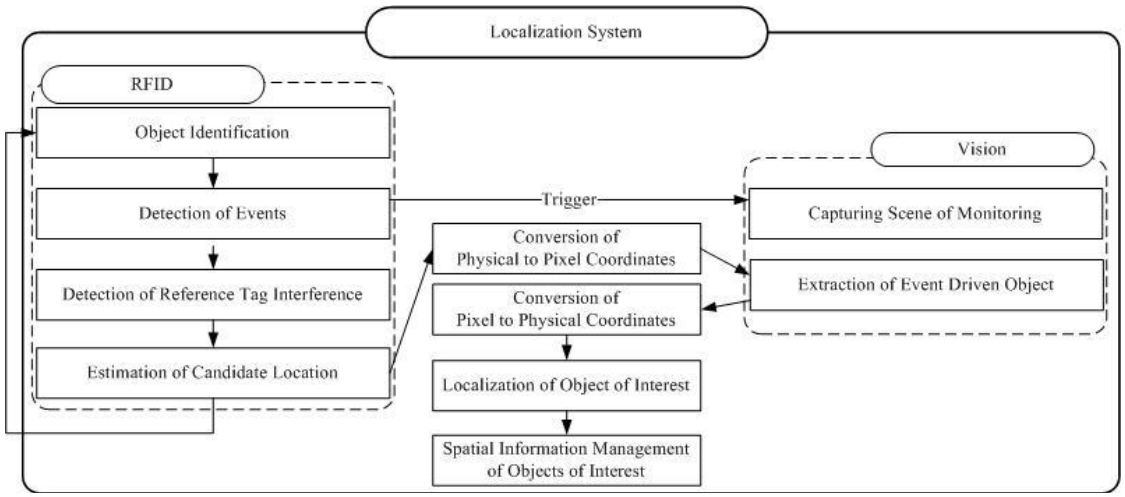

Figure 6.3 Main processes of each component in the proposed VRL system

6.3.1. System Design

single stationary RFID reader, reader antenna, and camera in a monitoring space. The main components of the proposed localization system consist of RFID, vision, and localization system as shown in Figure 6.3. Using an RFID reader, the system detects object appearance. Then the system estimates probable target locations, as we called candidate area, using detection of reference tag interference. The candidate area is represented by the Minimum Boundary Rectangle (MBR) which covers a number of adjacent interfered reference tags within given a physical 2D monitoring map. Simultaneously, when RFID system detects any event driven object, it triggers to capture monitoring scene. Then the localization system extracts the object within the estimated MBRs which are converted to pixel coordinates for comparison of previously and currently captured scenes, I^{prev} and $I^{current}$, for minimized computation overhead and processing time. A pixel coordinate of each image is represented by $px=(x', y')$, and the value of px is $I(px)$. The initially captured image is set to I^{prev}.

Total m shelves are monitored by a single stationary mono-static reader antenna, and total n reference tags adhere to façades of shelves, and the localization system knows geographical 2D information of all of deployed reference tags. A single stationary camera is connected to the localization system, and it also covers the monitoring area. In this section, we assume there is a single carrier who causes target events such as target appearance, and disappearance within the interrogation range. The localization system can recognize appearance and disappearance of the carrier using detection of a carrier introduced RF irregularity in the monitoring area. The carrier may bring out a single target per existence in the monitoring area. Let R denote the set of unique IDs of deployed reference tags, C^i represent the set of IDs of read tags by i^{th} interrogation period. T represents the set of IDs of existing targets that have already had their locations estimated by previous positioning processes. Additionally, RS denotes the set of the means of measured RSSI values for each element of C^i.

6.3.2. Estimation of Candidate Area by Passive Far-Filed UHF RFID System

The localization system periodically operates RFID system to builds the latest RSSI map for the deployed reference tags. In the RSSI map, the false negative interrogated reference tag's RSSI value is assigned to the minimum reader antenna sensitive power, P_{min}, which is measured during the site-survey.

After detection of the appearance and disappearance of carrier, the system triggers the location sensing process which is based on modification of LDTI algorithm. If C^i does not contains any newly identified tag ID, the system halts current localization. If the system detects newly incoming target tag's ID, the current RSSI map, RS^i, is compared to the previous interrogation period's RSSI map, RS^{i-1}. For each reference tag, the system calculates the absolute value of difference, $E_r^i = \left| rs_r^{i-1} - rs_r^{i,} \right|$, and if the difference of a certain reference is greater than a given threshold, the system regards the reference is interfered with E_r^i degree.

Then, the system ties references to estimate the most interfered area by the target tag, and the estimated given size of group is called candidate area. The each group member is geographically adjacent by satisfaction of the following condition:

Condition 6.1: In a group, at least one node has to be connected to all of the other nodes in $[\sqrt{g}]$-2 hop distance in a given group size g, where g is greater than 4.

Some reference tag's E^i is less than the threshold, the reference are participated the grouping process, because a backscattered signal strength from a reference tag may be slightly interfered, even though the target places closely as shown in Figure 4.4 (b) and (c). When the system estimates candidate area, the reference group size, g, is depended on dense of false negative reference reading. Initially, the system estimate the candidate area using the initial group size, g^{init}, and then, the system aggregates reading rates of each initial group member, and updates the group size, g, using the following:

$$g = g^{init} + \lfloor g^{init} \times (1 - FNR) \rfloor \quad (6.1)$$

The proposed heterogeneous localization system estimates total q candidate areas. Each estimated candidate area has different rank depended on the sum of degree of encountered impact of each member as $\sum E_r^i$. The candidate area is represented by Minimum Boundary Rectangle (MBR) of the selected reference group, and each MBR does not make overlap, but two MBRs can share a single edge. Finally, the system calculates MBR of each reference group, and stores its 2D information in a queue, CQ.

6.3.3. Vision based Object Localization

To estimate the target location, we apply the image difference detection algorithm [65]. By comparison of currently captured and previous inventory space scenes, the system detects a change of pixel intensity as following rule:

$$C'(px) = \begin{cases} 1 & If\ |I(px^{prev}) - I(px^{current})| > Th' \\ 0 & Otherwise \end{cases} \quad (6.2)$$

where *Th'* denotes a pre-specified threshold. If Euclidean distance of pixel intensity between I^{prev} and $I^{current}$ is over the threshold, the system considers the pixel indicates a part of the target in the current image.

When the captured image has *w* × *h* size of pixels, where w denotes the width and h is the height, the system requires processing time to compare *w*× *h* pixels of each image. In order to reduce the processing time and computational load, the system minimizes comparable image block within the captured monitoring area scene using the geometrical information of candidate locations.

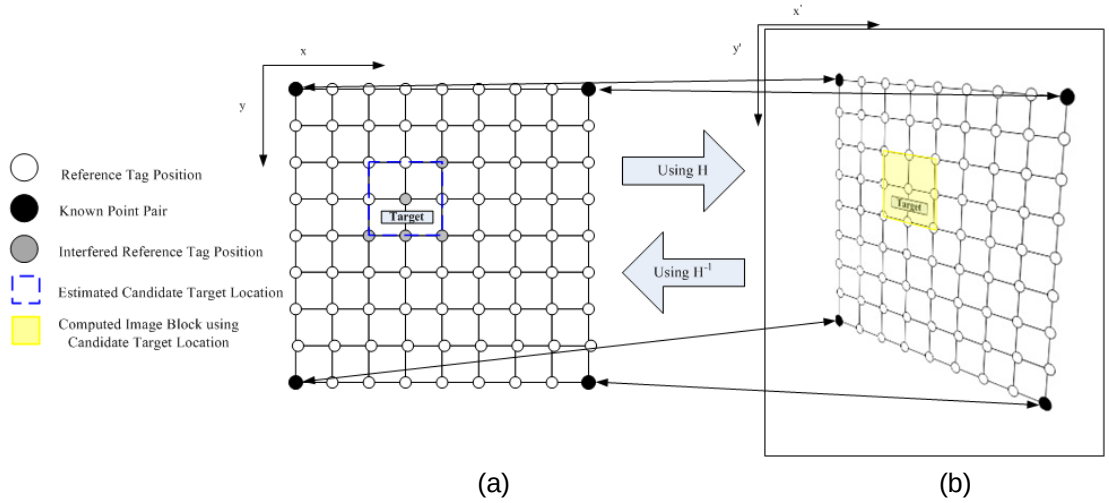

Figure 6.4 Example of conversion of spatial information between a physical position and a pixel coordinate in the captured image. (a) Map of physical 2D monitoring area. (b) Captured Image of the monitoring area by a fixed camera

Given a captured image of the monitored area (Figure 6.4 (b)) and the physical 2D monitoring map (Figure 6.4 (a)), the system needs to convert physical position information to the captured image pixel coordinates. To solve the spatial information mapping problem, we apply the 2D Image planar homography algorithm [64] for image transformation between world plane (as physical position) and its corresponding image (as captured scene). A point in the world plane p =(x, y) corresponds a pixel coordinate, p'=(x', y'), in the captured image, and these two points satisfied by a non-singular 3×3 matrix, H, as following:

$$p' = H \times p \tag{6.3}$$

and Equation (6.3) can be rewritten as:

$$p' \times Hp = 0 \tag{6.4}$$

or,

$$\begin{bmatrix} wx' \\ wy' \\ w \end{bmatrix} \times \begin{bmatrix} h1 & h2 & h3 \\ h4 & h5 & h6 \\ h7 & h8 & h9 \end{bmatrix} \begin{bmatrix} x \\ y \\ 1 \end{bmatrix} = 0 \tag{6.5}$$

When we assume the system knows at least N corresponding point pairs, where N≥4, between the physical positions and the pixel coordinate, Equation (6.5) can be rewritten as following [64]:

$$\begin{bmatrix} x_1 & y_1 & 1 & 0 & 0 & 0 & -x'_1 x_1 & -x'_1 y_1 & -x'_1 \\ 0 & 0 & 0 & x_1 & y_1 & 1 & -y'_1 x_1 & -y'_1 y_1 & -y'_1 \\ : & : & : & : & : & : & : & : & : \\ x_N & y_n & 1 & 0 & 0 & 0 & -x'_N x_N & -x'_N y_N & -x'_N \\ 0 & 0 & 0 & x_N & y_n & 1 & -y'_N x_N & -y'_N y_N & -y'_N \end{bmatrix} \begin{bmatrix} h1 \\ h2 \\ h3 \\ h4 \\ h5 \\ h6 \\ h7 \\ h8 \\ h9 \end{bmatrix} = \begin{bmatrix} 0 \\ 0 \\ : \\ 0 \\ 0 \end{bmatrix} \tag{6.6}$$

Using the calculated H, any of physical position (x, y) can convert to the pixel coordinate (x', y') in the image as following:

$$(x', y') = \left(\frac{(x \times h1) + (y \times h2) + h3}{(x \times h7) + (y \times h8) + h9}, \frac{(x \times h4) + (y \times h5) + h6}{(x \times h7) + (y \times h8) + h9}) \right) \tag{6.7}$$

Then, first, the system pops the first rank MBR from CQ, then the system maps the estimated MBR as candidate location to an image block within $I^{current}$ using Equation (6.7), then compares the pixel intensity with same pixel coordinate in I^{prev} by Equation (6.2). Then, if the selected image block contains changed pixels as $C(px_h)=1$, where $1 \le h \le w \times h$, the system

calculates a MBR of changed pixel coordinates. And then, the system transforms each coordinate of convex to the physical point using the inversed H (as H^{-1}).

Eventually, the target location, tpest, is estimated by the centroid of 4 degree polygon which is transformed MBR. Where the positions of the polygon convexes is denoted by CP={(cx1, cy1),.., (cx4, cy4)}, tp^{est} is calculated as following:

$$tp^{est}.x = \frac{\left(\sum_{i=1}^{3}(cx_i + cy_{i+1})(cx_i \times cy_{i+1} - cx_{i+1} \times cy_i)\right) + (cx_4 + cy_1)(cx_4 \times cy_1 - cx_1 \times cy_4)}{6A} \quad (6.8)$$

and,

$$tp^{est}.y = \frac{\left(\sum_{i=1}^{3}(cy_i + cy_{i+1})(cx_i \times cy_{i+1} - cx_{i+1} \times cy_i)\right) + (cy_4 + cy_1)(cx_4 \times cy_1 - cx_1 \times cy_4)}{6A} \quad (6.9)$$

where *A* denotes the area of 4 degreed MBP, which is given by:

$$A = \frac{\left(\sum_{i=1}^{3}(cx_i \times cy_{i+1} - cx_{i+1} \times cy_i)\right) + (cx_4 \times cy_1 - cx_1 \times cy_4)}{2} \quad (6.10)$$

In practice, because there is high chance that the captured image contains noise pixels, MBP, which may contain the target, only covers the largest set of adjacent changed pixels to increase the accuracy of localization. If the localization system could not detect any pixel change among the first ranked transformed candidate area, the system pops next highest ranked candidate area from CQ, and repeats transforming and image change detecting procedures until the system estimates the target location.

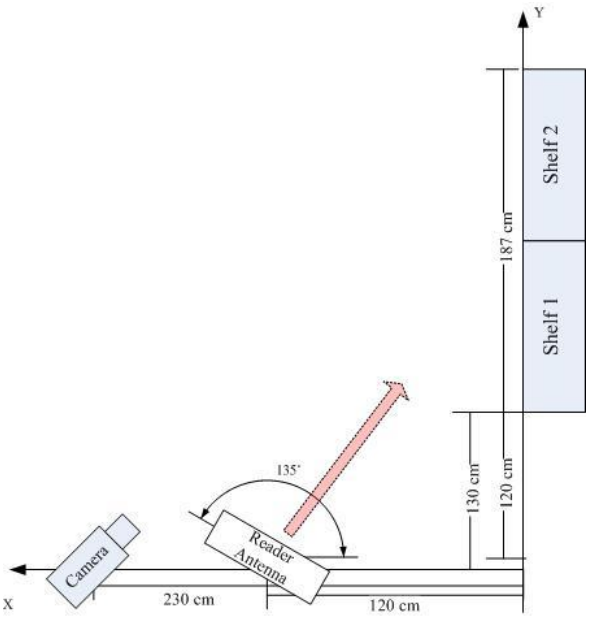

(a)

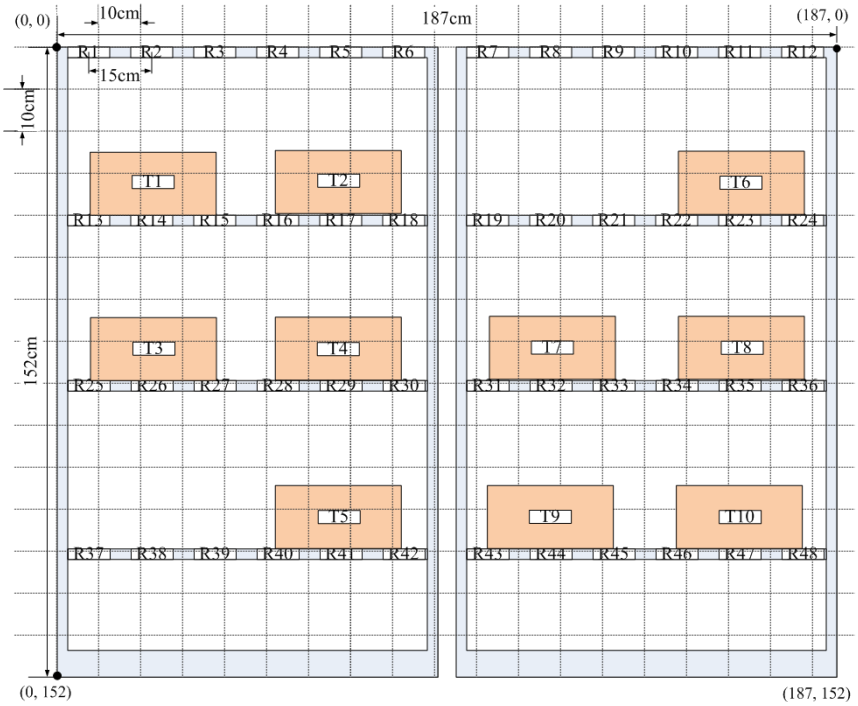

(b)

Figure 6.5 Setup of the smart shelf application using VRL. (a) Two of 91cm ×152cm wooden shelves. A single reader antenna and PC camera cover the shelving area. (b) Actual 10 target locations in 2D space of the shelves.

6.4 Experimental Results

6.4.1. Smart Shelf set-up

In our experiment of the integrated Vision and passive UHF RFID smart shelf, two tiers of 91cm ×152cm wooden shelves are placed in an ordinary office environment, and a single reader antenna and a single PC camera, at the fixed position, cover the shelving area as shown in Figure 6.5. As summarized in Table 6.1, the SIRIT Infinity 510 RFID reader and Poynting Patch-A0025 antenna are used, and the reader's operating frequency is 915MHz and the reader antenna's transmission power is set to 30dBm. The heights of reader antenna and the camera are 120cm and 180cm from the ground. 48 Alien Squiggle Gen 2 Passive tags are adhered to the façade of each shelf, and total 10 of 34cm × 14cm cardboard boxes also attach the squiggle tag at the center of front side. Each box contains a print cartridge within an aluminum foil bag. Duration of interrogation period is set to 30 seconds. The threshold for detection of interfered RSSI is fixed to 0.3dB. Moreover, the minimum antenna sensitive power, P_{min}, is set to -65.5dBm. And the initial group size for the candidate area is set to 4. The localization system is developed and run by Microsoft Visual Studio C# 2008 on Dell Optiplex 3300 computer system with Intel core2 CPU and 2GB of RAM.

Table 6.1 Specification of System Setup

Specification	Details
Reader	SIRIT INFINITY 510
Antenna	Poynting Patch-A0025 with 6 dBi of gain
Reference tag	Alien Squiggle Gen 2 Passive tag × 48
Target tag	Alien Squiggle Gen 2 Passive tag
Frequency	915 MHz
TX power	30 dBm (1 Watt)
Monitoring area	91cm ×152 cm Wooden Book shelf × 2
Camera	Philips PC Camera SIC4700/37

6.4.2. Evaluation of VRL System

RFID components detect any event driven target among the monitoring area, the localization system triggers capturing of the monitoring space. When the system stores 4 of corresponding point pairs between the physical map and the captured image, the 3 × 3 non-singular homography matrix is calculated in this experimentation as following:

$$H = \begin{bmatrix} 0.86124572 & 0.031643213 & 65.0451778 \\ 0.058518426 & 1.46038226 & 2.4773457 \\ -0.00141782 & 0.000479442 & 1 \end{bmatrix}$$

As shown in Figure 6.6, the estimated candidate area is transformed to image pixel coordinate using Equation (6.7). The black circle denotes actual target position in the physical map, and the red circle denotes the estimated target location. And the numbered dark-red rectangle represents MBR with its ranking. In the current captured image, the red area represents the detected changed pixels.

For the analysis of the proposed VRL system, we compare its performance with KNN based, LDTI, and Vision only localization algorithms. In the vision based localization, since, the system cannot identify the incoming target ID, we assume the system has pre-defined ID for the target objects. The k value of KNN algorithm and the size of group, g, in LDTI are set to 6.

Under low false negative reference interrogation (FNR) rate, the integrated localization system provides 61.3% and 847.2% increased the mean of accuracy of 10 targets' localization compared to LDTI and KNN as shown in Figure 6.7 (a) and (b). The mean of computation times of VRL (33.88 ms) is improved 555% compared to the homogeneous vision based localization system (222.14 ms) as shown in Figure 6.8 (a) and (b).

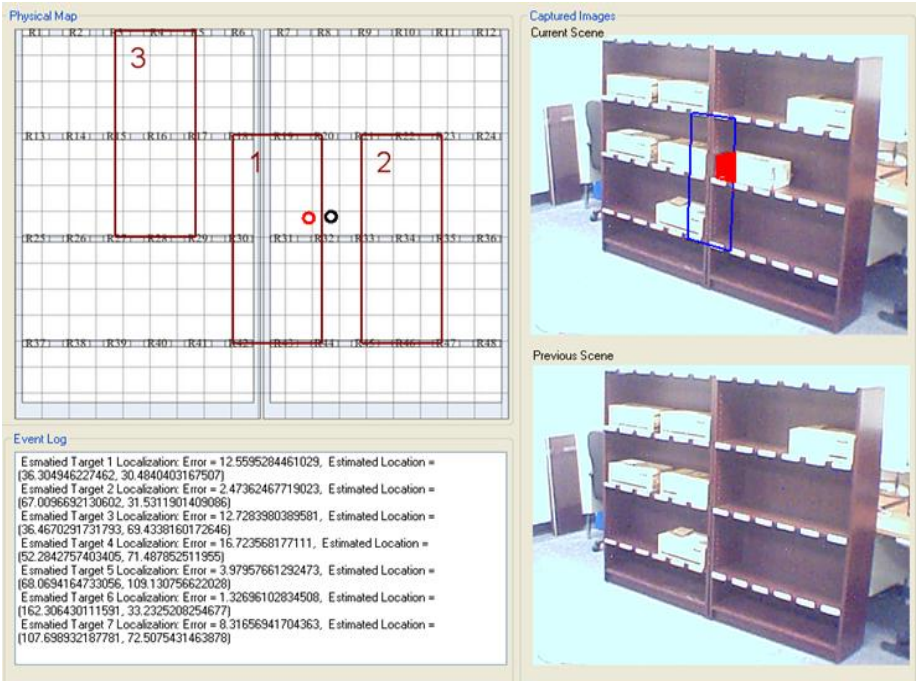

(a)

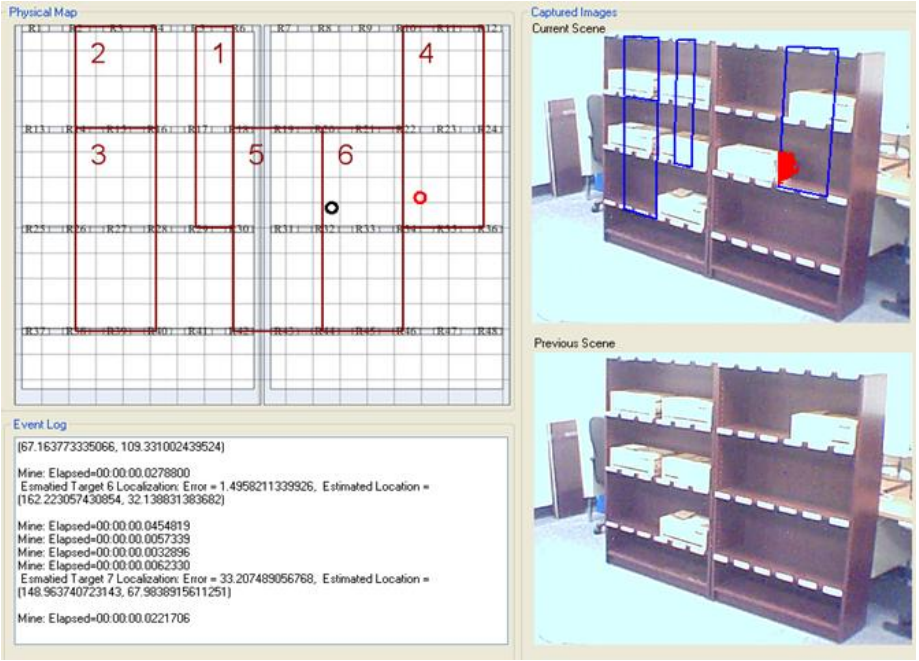

(b)

Figure 6.6 Examples of VRL system. The black circle is the actual target position, and the red circle is the estimated target location. (a) Case of low FNR. (b) Case of high FNR.

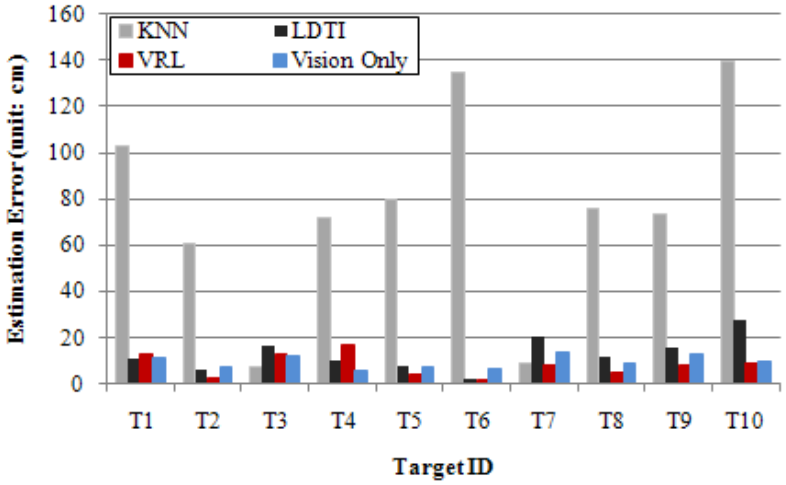

(a)

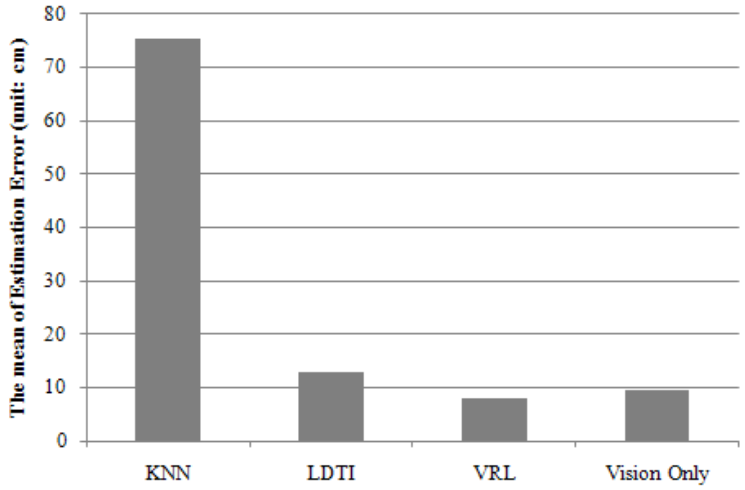

(b)

Figure 6.7 Evaluation of Estimation error of VRL system under low false negative reference interrogation rate (6.25%). (a) Estimation errors of 10 targets. (b) The mean of estimation errors.

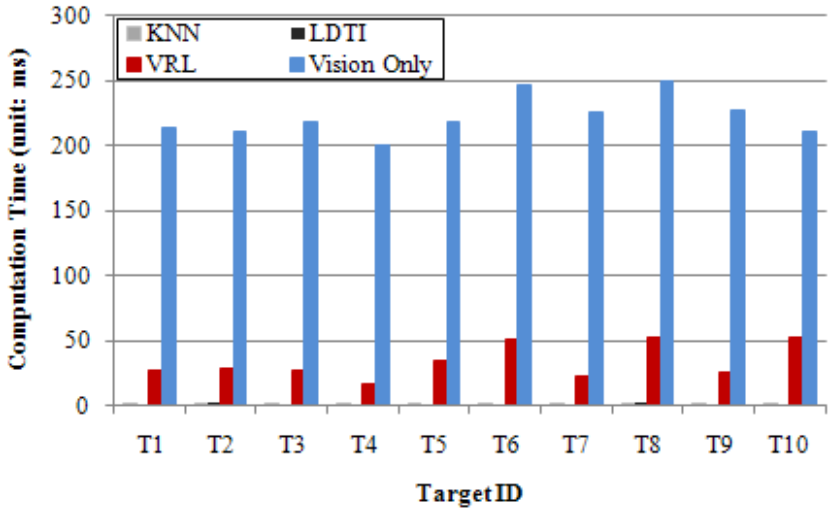

(a)

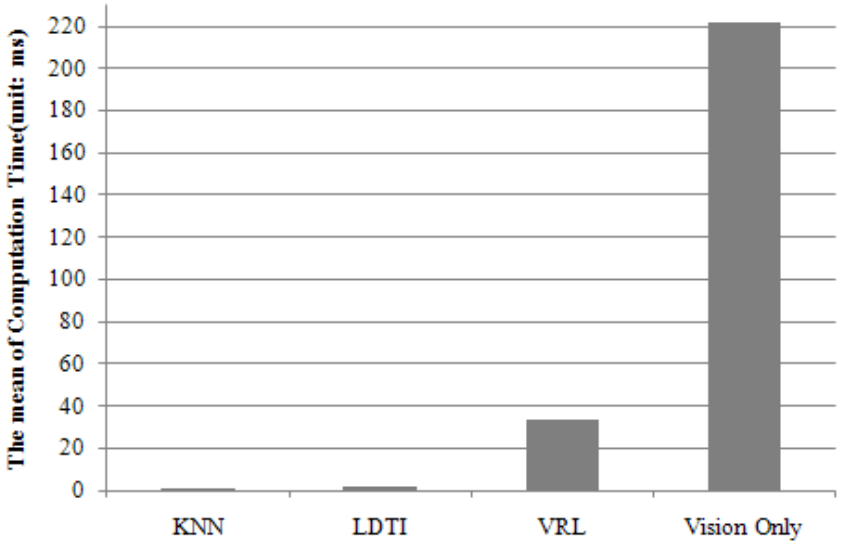

(b)

Figure 6.8 Evaluation of computation time of VRL system under low false negative reference interrogation rate (6.25%). (a) Computation times of 10 targets. (b) The mean of computation times.

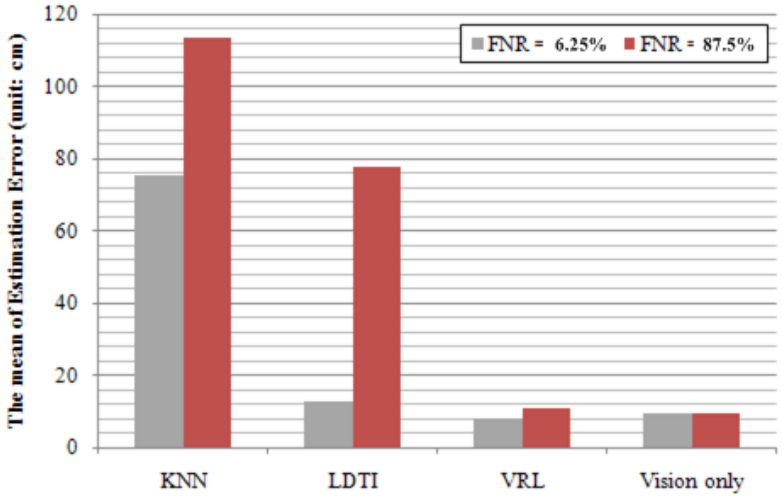

(a)

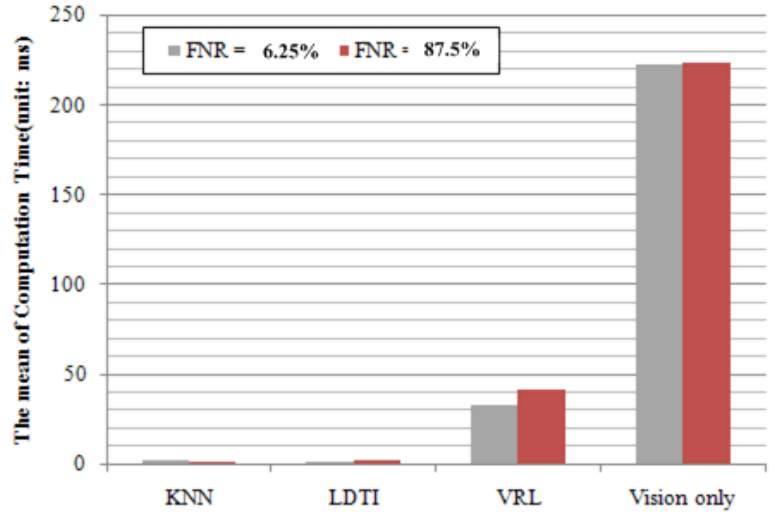

(b)

Figure 6.9 Comparison of VRL system performances under various false negative reference interrogation rates. (a) The mean of estimation errors. (b) The mean of computation times.

Figure 6.9 (a) and (b) illustrates the performance evaluation of the proposed VRL under different rates of false negative reference reading condition. For high FNR condition, we set the reader antenna's transmission power to 23.5dBm and FNR is increased to 87.5% (6 interrogated references out of 48). Moreover, with the weak transmission power, the False

Negative Target interrogation (FNT) rate is measured 30%, as 7 out of 10 targets are identified. Thus, Figure 6.9 shows the results for the interrogated 7 targets. Under 87.5% FNR rate, the group size of candidate area is increased to 8. On the other hand, for low FNR condition, the reader transmits 30dBm of power and total 45 references are identified as 6.25% of FNR and 0% of FNT. Where LDTI shows substantially increased error in the high FNR, VRL and vision based localization system show very robust and accurate localization results both high and low FNR conditions. But, if we compare the computation time, the proposed VRL estimates target locations 437.8% faster than the vision based localization in high FNR condition.

Table 6.2 Summary of Performance of VRL

	VRL (g^{int} = 4)		LDTI (g = 6)		Vision only	
	Low FNR	High FNR	Low FNR	High FNR	Low FNR	High FNR
Mean Esitimation Error	7.96cm	10.78cm	12.85cn	77.72cm	9.53cm	9.55cm
Standard Deviation of Esitimation Error	4.95cm	10.30cm	7.32cm	48.94cm	2.80cm	2.65cm
Computation time	33.88ms	41.50ms	1.39ms	1.79ms	222.14ms	223.23ms
Standard Deviation of Computation time	13.37ms	18.39ms	0.54ms	0.41ms	15.65ms	15.87ms
Improvement of VRL by the mean of estimation errors			61.43%	620.96%	19.72%	-11.41%
Improvement of VRL by the mean of computation times			-95.90%	-95.69%	555.67%	437.90%

6.5 Conclusion

In this chapter, we present an integrated smart shelf system using a far-field passive UHF RFID and computer vision to achieve simplicity, compatibility, scalability, cost efficiency, accuracy and robustness for asset tracking and localization. We present the challenges of passive far-field UHF RFID system based smart shelf with detail empirical results. we propose a novel integrated Vision and passive UHF RFID Localization (VRL) with minimized RFID components and image

sensor. As summarized in Table 6.2, under low False Negative Reference (FNR) interrogation condition (FNR=6.25%), VRL performs average 7.96cm estimation error for 10 print cartridge containers, which is a 61% accuracy improvement compared the LDTI algorithm, which is our previous work, an 555% computation overhead reduction compared the homogeneous vision system. Moreover, The proposed VRL achieves over 620% increased accuracy compared to LDTI, and 437% reduced computation time compared to Vision based localization system under high FNR (FNR = 87.5%).

CHAPTER 7

CONCLUSIONS

In conclusion, we proposed achievement of accurate localization with low cost using passive far-field UHF RFID system. First, we studied the causes of problems of passive UHF RFID based localization with detail empirical results. The variation of uniform tags, tag posture, and the material of tagged object, the strong-weak tag problem and the tag-to-tag interference brings out ambiguous mapping between a physical location and a measured RSSI value in practice. Moreover, we presented the impacts of the causes on the existing localization technique such as KNN in the real world.

Second, we presented a new model of backscattered signal strength for passive far-field UHF RFID system under tag-to-tag interference, and proposed a method to estimate variations of excess power volume by the interference depended on a tag-to-tag distance and angle using the second order under-damped system. Additionally, we presented a novel localization algorithm to estimate target object location using the presented Tag-to-tag Interference Model (LMTI). According to the empirical results, LMTI improves over 200% accuracy compared RSSI based KNN algorithm when I implement with empty boxes, and 127% improvement with the print cartridge contained an aluminum foil bag.

Third, we presented another approach to achieve accurate localization. The presented Localization using Detection of Tag Interference (LDTI) algorithm detects the tag interference on the map of reference tags to estimate target location. To avoid selection of spatially non-adjacent reference tags, we also present the most interfered reference group finding algorithm, which considers spatial relations between reference tags. Using LDTI system with reference grouping algorithm, we presented a far-field passive UHF RFID smart shelf to achieve simplicity, compatibility, scalability, and cost efficiency for asset tracking and localization. LDTI based

smart shelf performs average 9.48cm estimation error for 9 empty cardboard boxes, and average 18.31cm estimation error for 9 print cartridge containers, which is a 71% accuracy improvement compared the KNN algorithm.

Finally, we presented an integrated smart shelf system using a far-field passive UHF RFID and computer vision. The proposed novel integrated Vision and passive UHF RFID Localization (VRL) with minimized RFID components and image sensors performs average 7.96cm estimation error for 10 print cartridge containers, which is a 61% accuracy improvement compared the LDTI algorithm under low False Negative Reference (FNR) interrogation condition. Moreover, it shows 555% computation overhead reduction compared the homogeneous vision system. In high FNR condition, VRL system achieves over 620% increased accuracy compared to LDTI, and 437% reduced computation time compared to Vision based localization system.

REFERENCES

[1] EPCglobal GEN2 [ONLINE], http://www.epcglobalinc.org/standards/uhfc1g2

[2] D.M. Dobkin, The RF in rfid: Passive UHF rfid in Practice, Newnes Press, 2007.

[3] RFID Journal, Chicago Fire Dept. Tests ZigBee-based RFID System , http://www.rfidjournal.com/article/articleview/2717/1/1/

[4] Chieh-Ling Huang, Pau-Choo Chung, Ming-Hua Tsai, Yen-Kuang Yang and Yu-Chia Hsu, “Reliability Improvement for an RFID-based Psychiatric Patient Localization System ”, Computer Communications, Vol. 31, Issue 10, pp. 2039- 2048, 2008

[5] Balch, Tucker and Feldman, Adam and Wilson, Wesley P., “Assessment of an RFID System for Animal Tracking,” Technical Report, Georgia Institute of Technology, 2004.

[6] D'Mello, S., Mathews, E., McCauley, L., and Markham, J. 2008. Impact of position and orientation of RFID tags on real time asset tracking in a supply chain. *J. Theor. Appl. Electron. Commer. Res.* 3, 1 (Apr. 2008), 1-12.

[7] Hightower, J. and Vakili, C. and Borriello, G. and Want, R, “Design and Calibration of the SpotON Ad-Hoc Location Sensing System,” unpublished, August 2001.

[8] Ni, L.M.; Yunhao Liu; Yiu Cho Lau; Patil, A.P., "LANDMARC: indoor location sensing using active RFID," *Pervasive Computing and Communications, 2003. (PerCom 2003). Proceedings of the First IEEE International Conference on* , vol., no., pp. 407-415, 23-26 March 2003

[9] Kuen-Liang Sue, Chung-Hsien Tsai, Ming-Hua Lin: FLEXOR: A Flexible Localization Scheme Based on RFID. ICOIN 2006, Sendai, Japan, January 16-19, 2006

[10] Guang-yao Jin; Xiao-yi Lu; Myong-Soon Park, "An Indoor Localization Mechanism Using Active RFID Tag," *Sensor Networks, Ubiquitous, and Trustworthy Computing, 2006. IEEE International Conference on* , vol.1, no., pp. 40-43, 05-07 June 2006

[11] Zhao, Yiyang; Liu, Yunhao; Ni, Lionel M., "VIRE: Active RFID-based Localization Using Virtual Reference Elimination," *Parallel Processing, 2007. ICPP 2007. International Conference on* , vol., no., pp.56-56, 10-14 Sept. 2007

[12] Hahnel, D.; Burgard, W.; Fox, D.; Fishkin, K.; Philipose, M., "Mapping and localization with RFID technology," *Robotics and Automation, 2004. Proceedings. ICRA '04. 2004 IEEE International Conference on* , vol.1, no., pp. 1015-1020 Vol.1, 26 April-1 May 2004

[13] Chattopadhyay, A.; Harish, A.R., "Analysis of low range Indoor Location Tracking techniques using Passive UHF RFID tags," *Radio and Wireless Symposium, 2008 IEEE* , vol., no., pp.351-354, 22-24 Jan. 2008

[14] X. Liu, M. Corner, and P. Shenoy. *"Ferret: Rfid localization for pervasive multimedia."* In *Ubicomp 2006*, pages 422–440, 2006.

[15] ISO/IEC FDIS 19762-5 Information technology AIDC techniques - Harmonized vocabulary, Part 5 – Locating systems, October, 2007.

[16] What is GPS [ONLINE], http://www8.garmin.com/aboutGPS/

[17] N.B. Priyantha, A. Chakraborty and H. Balakrishnan, "The Cricket location-support system", In *Proceedings of MOBICOM 2000*, Boston, MA , pp. 32–43., 2000.

[18] D. Seetharam and R. Fletcher. "Battery-Powered RFID", SenseID 2007 1st ACM Workshop on Convergence of RFID and Wireless Sensor Networks and their Applications. November 2007

[19] Dianmin Yue; Xiaodan Wu; Junbo Bai; , "RFID Application Framework for pharmaceutical supply chain," *Service Operations and Logistics, and Informatics, 2008. IEEE/SOLI 2008. IEEE International Conference on* , vol.1, no., pp.1125-1130, 12-15 Oct. 2008

[20] Lehto, A.; Nummela, J.; Ukkonen, L.; Sydanheimo, L.; Kivikoski, M.; , "Passive UHF RFID in Paper Industry: Challenges, Benefits and the Application Environment," Automation Science and Engineering, IEEE Transactions on , vol.6, no.1, pp.66-79, Jan. 2009

[21] Ming-Ling Chuang, M.-L.; Shaw, W.H.; , "RFID: Integration Stages in Supply Chain Management," Engineering Management Review, IEEE , vol.35, no.2, pp.80-87, Second Quarter 2007

[22] Raty, T.D.; , "Survey on Contemporary Remote Surveillance Systems for Public Safety," Systems, Man, and Cybernetics, Part C: Applications and Reviews, IEEE Transactions on , vol.40, no.5, pp.493-515, Sept. 2010

[23] Aittola, M., Ryhänen, T. & Ojala, T. SmartLibrary: Location-aware mobile library service. Proc Fifth International Symposium on Human Computer Interaction with Mobile Devices and Services (2003), vol. Udine, Ita, pp. 411-416.

[24] Xianming Qing; Zhi Ning Chen; Ailian Cai; , "Multi-loop antenna for high frequency RFID smart shelf application," Antennas and Propagation Society International Symposium, 2007 IEEE , vol., no., pp.5467-5470, 9-15 June 2007

[25] Hightower, J.; Borriello, G.; , "Location systems for ubiquitous computing," Computer , vol.34, no.8, pp.57-66, Aug 2001

[26] Patwari, N.; Ash, J.N.; Kyperountas, S.; Hero, A.O., III; Moses, R.L.; Correal, N.S.; , "Locating the nodes: cooperative localization in wireless sensor networks," Signal Processing Magazine, IEEE , vol.22, no.4, pp. 54- 69, July 2005

[27] T. Rappaport. Wireless Communications: Principles and Practice. Prentice Hall PTR, Upper Saddle River, NJ, USA, 2001

[28] Varshavsky, A., LaMarca, A., Hightower, J., and de Lara, E. 2007. The SkyLoc Floor Localization System. In Proceedings of the Fifth IEEE international Conference on Pervasive Computing and Communications 2007, Washington, DC, 2007

[29] Yunye Jin; Wee-Seng Soh; Wai-Choong Wong; , "Indoor localization with channel impulse response based fingerprint and nonparametric regression," Wireless Communications, IEEE Transactions on , vol.9, no.3, pp.1120-1127, March 2010

[30] Aditya Nemmaluri, Mark D. Corner and Prashant Shenoy, "*Sherlock: Automatically* Locating Objects for Humans", MobiSys' 08, Breckenridge, Colorado, USA, June 2008.

[31] Kamol, P.; Nikolaidis, S.; Ueda, R.; Arai, T., "RFID Based Object Localization System Using Ceiling Cameras with Particle Filter," Future generation communication and networking (fgcn 2007) , vol.2, no., pp.37-42, 6-8 Dec. 2007

[32] Song, J., Haas, C. T., and Caldas, C. H. 2007. A proximity-based method for locating RFID tagged objects. Adv. Eng. Inform. 21, 4 (Oct. 2007), 367-376.

[33] F. Brannstrom, "Positioning Techniques Alternative to GPS," Master's Thesis, Univ. Lund, 2002.

[34] Guerrieri, J.R.; Francis, M.H.; Wilson, P.F.; Kos, T.; Miller, L.E.; Bryner, N.P.; Stroup, D.W.; Klein-Berndt, L., "RFID-assisted indoor localization and communication for first responders," Antennas and Propagation, 2006. EuCAP 2006. First European Conference on , vol., no., pp.1-6, 6-10 Nov. 2006

[35] Griffin, J.D.; Durgin, G.D.; Haldi, A.; Kippelen, B.; , "RF Tag Antenna Performance on Various Materials Using Radio Link Budgets," Antennas and Wireless Propagation Letters, IEEE , vol.5, no.1, pp.247-250, Dec. 2006

[36] Hong gang Wang; Chang xing Pei; Qiao Pan; , "Test and Analysis of Passive UHF RFID Readability in Multipath Environments," Wireless Communications, Networking and Mobile Computing, 2009. WiCom '09. 5th International Conference on , vol., no., pp.1-5, 24-26 Sept. 2009

[37] ALIEN TECH, ALN 9640 Squiggle UHF RFID tag [ONLINE], http://www.alientechnology.com/docs/products/DS_ALN_9640.pdf

[38] SIRIT Reader [ONLINE], http://www.sirit.com/Fixed_RFID_Readers.asp

[39] Poynting Patch-A0025 [ONLINE], http://www.poynting.co.za

[40] Waldrop, J., Engels, D.W., Sarma, S.E., "Colorwave: an anticollision algorithm for the reader collision problem," Communications, 2003. ICC '03. IEEE International Conference on , vol.2, no., pp. 1206-1210 vol.2, 11-15 May 2003

[41] D. Y. Kim, J.G. Yook, H.G Yoon, and B.J. Jang, “Interference analysis of UHF RFID systems,” Progress In Electromagnetics Research B, Vol. 4, 115–126, 2008.

[42] D. Dobkin, S. Weigand, “UHF RFID and tag antenna scattering.Part I: experimental results”, Microwave Journal, vol. 47, no. 5, pp. 170-190 May 2006,

[43] D. Dobkin, S. Weigand, “UHF RFID and tag antenna scattering.Part II: Theory”, Microwave Journal, vol. 49, no. 5, pp. 86-96, June 2006.

[44] J. Banks, D. Hanny, M.A. Pachano, and L.G. Thompson, RFID Applied, John Wiley & Sons, Inc., Hoboken, NJ, 2007.

[45] D. Shih, P. L. Sun, D. C. Yen and S. M. Huang, “Taxonomy and survey of RFID anti-collision protocols”, Proc. Computer and Communications, vol 29, pp 2150-2166, 2006.

[46] J. Myung and W. Lee, “An Adaptive Memoryless Tag Anti-Collision Protocol for RFID Networks” Proc. IEEE INFOCOM, Miami, FL, 2005.

[47] N. Abramson, “The Aloha System-Another Alternative for Computer Communications”, Proc. Fall Joint Computer Conference, Am. Federation of Information Processing Soc. Conf., vol. 37, pp. 281-285, Nov. 1970.

[48] S. Lee, S. Joo, and C. Lee, “An Enhanced Dynamic Framed Slotted ALOHA Algorithm for RFID Tag Identification”, Proc. the Second Annual international Conference on Mobile and Ubiquitous Systems: Networking and Services, IEEE Computer Society, Washington, DC, pp. 166-174, Jul. 2005.

[49] J. Cha and J. Kim, “Dynamic framed slotted ALOHA algorithms using fast tag estimation method for RFID system”, Proc. IEEE Consumer Communications and Networking Conference, vol 2, pp 768-772, 2006.

[50] H. Vogt, “Multiple object identification with passive RFID tags”, Proc. IEEE International Conference on Systems, Man and Cybernetics, Hammamet, Tunisia, vol 3, pp 6-9, Oct. 2002.

[51] H. Vogt, “Efficient object identification with passive RFID tags”, Proc. International Conference on Pervasive Computing, pp 98-113, Apr. 2002.

[52] D. R. Hush and C. Wood, “Analysis of tree algorithms for RFID arbitration”, Proc. IEEE International Symposium on Information Theory, pp 107-116, Aug. 1998.

[53] C. Law, K. Lee, and K.Y. Siu, “Efficient memoryless protocol for tag identification (extended abstract)”, Proc. the 4th international Workshop on Discrete Algorithms and Methods For Mobile Computing and Communications, ACM Press, Boston, MA, pp. 75-84, Aug. 2000.

[54] Technical Report 860 MHz-930 MHz Class 1 Radio Frequency Identification Tag Radio Frequency & Logical Communication Interface Specification Candidate Recommendation, Version 1.0.1, MIT AUTO-ID Center, Nov.2002.

[55] J. Kim, B. Kang, J. Jwa and D. Yang, “Bin-slotted Hybrid Search Algorithm for Multiple RFID Arbitration”, Proc. International Conference on Wireless Networks, pp 164-172, Jun. 2006.

[56] H. S. Choi and J. H. Kim, “Anti-Collision algorithm using Bin Slot in RFID system”, Proc. IEEE TENCON, Melbourne, Australia, pp 71-76, Nov.2005

[57] J. Myung, W. Lee, J. Srivastava, and T.K. Shih, “Tag-Splitting: Adaptive Collision Arbitration Protocols for RFID Tag Identification”, Proc. IEEE Transactions on Parallel and Distributed Systems, vol 18, no 6, pp. 763-775, Jun. 2007

[58] Review of First- and Second-Order System Response [online], http://web.mit.edu/2.151/www/Handouts/FirstSecondOrder.pdf

[59] Mingon Kang, Jean X. Gao, Liping Tang: Computational modeling of phagocyte transmigration during biomaterial-mediated foreign body responses. BIBM 2010: 609-612

[60] Medeiros, C.R.; Costa, J.R.; Fernandes, C.A.; , "RFID Smart Shelf With Confined Detection Volume at UHF," Antennas and Wireless Propagation Letters, IEEE , vol.7, no., pp.773-776, 2008

[61] Wonkyu Choi; Jeong-Seok Kim; Ji-Hoon Bae; Gilyoung Choi; Jong-Suk Chae; , "Near-field antenna for RFID smart shelf in UHF," Antennas and Propagation Society International Symposium, 2009. APSURSI '09. IEEE , vol., no., pp.1-4, 1-5 June 2009

[62] Erin-Ee-Lin Lau; Wan-Young Chung;, "Enhanced RSSI-Based Real-Time User Location Tracking System for Indoor and Outdoor Environments," Convergence Information Technology, 2007. International Conference on , vol., no., pp.1213-1218, 21-23 Nov. 2007

[63] K. Ramakrishnan and D. Deavours, “Performance benchmarks for passive uhf rfid tags,” In Proceedings of the 13th GI/ITG Conference on Measurement, Modeling, and Evaluation of Computer and Communications Systems, pages 137–154, 2006

[64] Sukthankar, R.; Stockton, R.G.; Mullin, M.D.;, "Smarter presentations: exploiting homography in camera-projector systems," Computer Vision, 2001. ICCV 2001. Proceedings. Eighth IEEE International Conference on , vol.1, no., pp.247-253 vol.1, 2001

[65] Radke, R.J.; Andra, S.; Al-Kofahi, O.; Roysam, B.; , "Image change detection algorithms: a systematic survey," Image Processing, IEEE Transactions on , vol.14, no.3, pp.294-307, March 2005

[66] Jusoh, R.M.; , "Application of Vision Target Localization for Mobile Robot," Research and Development, 2006. SCOReD 2006. 4th Student Conference on , vol., no., pp.144-146, 27-28 June 2006

[67] Yuen, D.C.K.; MacDonald, B.A.; , "Vision-based localization algorithm based on landmark matching, triangulation, reconstruction, and comparison," Robotics, IEEE Transactions on , vol.21, no.2, pp. 217- 226, April 2005

BIOGRAPHICAL INFORMATION

Jae Sung Choi received the B.A. degree in Computer Engineering in 2003 from Kyungsung University, Busan, South Korea. He also received his M.S degree in Computer Science and Engineering in 2006, and Ph.D degree in Computer Science in 2011 from University of Texas at Arlington, Arlington, Texas. His research interests include performance analysis of RFID system and passive UHF RFID based object location sensing.